Iceland Liechtenstein Norway grants

Norway grants

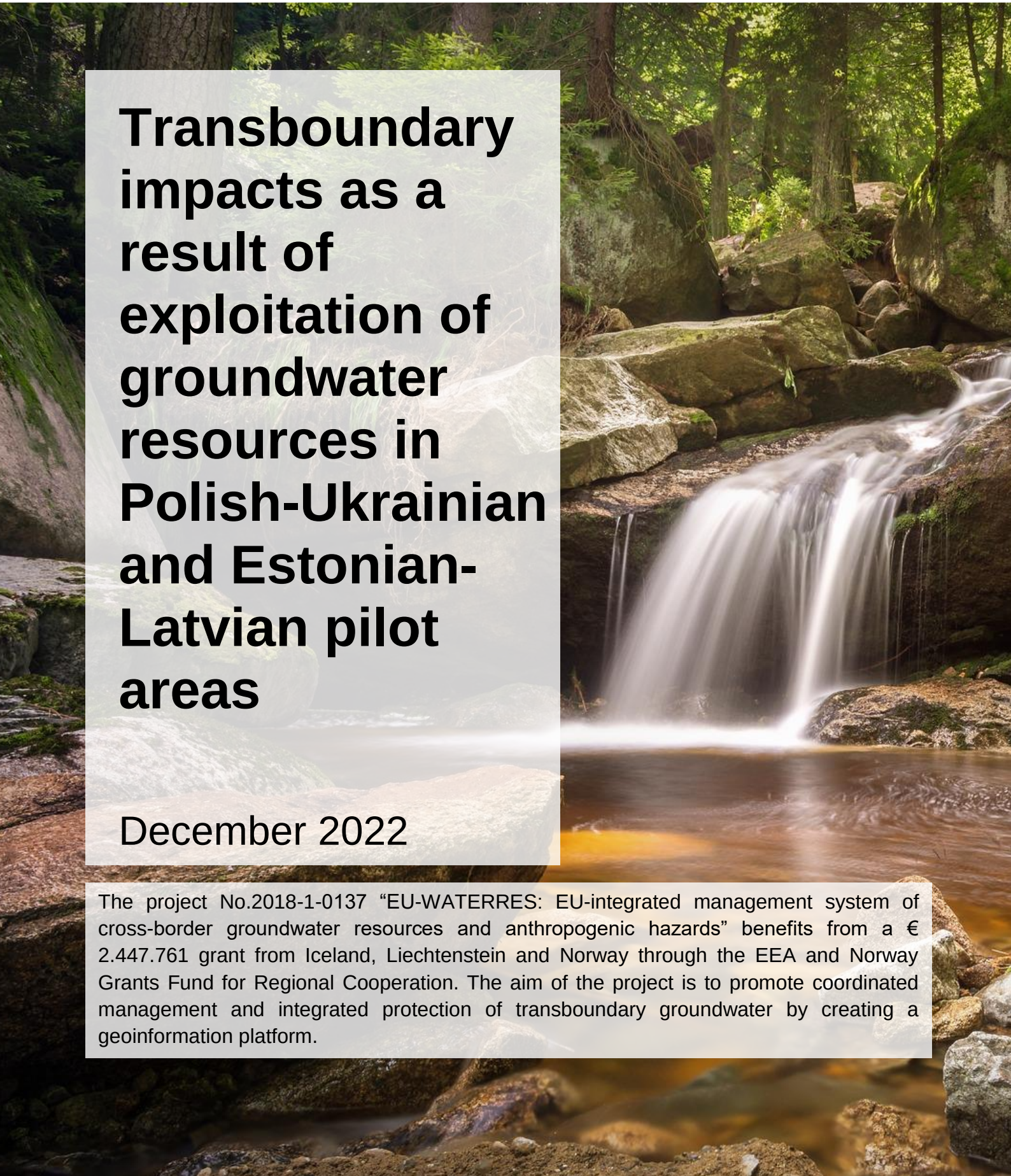

Transboundary impacts as a result of exploitation of groundwater resources in Polish-Ukrainian and Estonian-Latvian pilot areas

December 2022

The project No.2018-1-0137 “EU-WATERRES: EU-integrated management system of cross-border groundwater resources and anthropogenic hazards” benefits from a € 2.447.761 grant from Iceland, Liechtenstein and Norway through the EEA and Norway Grants Fund for Regional Cooperation. The aim of the project is to promote coordinated management and integrated protection of transboundary groundwater by creating a geoinformation platform.

Technical information	
Document code:	WP5 – Transboundary impacts as a result of exploitation of groundwater resources in Polish-Ukrainian and Estonian-Latvian pilot areas
Title of document:	Transboundary impacts as a result of exploitation of groundwater resources in Polish-Ukrainian and Estonian-Latvian pilot areas
Reference activity:	Output 5. The elaboration of solutions for coordinated use and integrated protection of transboundary groundwater
Dissemination level:	Public
Version	1
Date	30.12.2022
Scientific Editor	Tatiana Solovey (*Polish Geological Institute - National Research Institute*)
Authors (*Polish Geological Institute –NRI*):	Tatiana Solovey, Rafał Janica, Małgorzata Przychodzka, Hanna Kolos, Tomasz Gruszczyński, Tatiana Melnychenko, Rafał Łusiak, Anna Krysa, Aneta Starościak
Authors *(Zahidukrgeologiya)*:	Dmytro Panov, Natalia Pavliuk, Svitlana Sokorenko, Liubov Yanush, Halyna Medvid
Authors (*Ukrainian Geological Company*):	Volodymyr Klos, Hanna Kolos, Yurii Kharchyshin
Authors (*Latvian Environment, Geology and Meteorology Centre*)	Jekaterina Demidko, Dāvis Borozdins, Krišjānis Valters
Authors (*Geological Survey of Estonia*)	Andres Marandi, Magdaleena Männik, Marlen Hunt
Authors (*University of Latvia*)	Jānis Bikše, Inga Retike
Authors (*Norvegian Geological Survey*)	Belinda Flem
Authors (Norwegian Water Resources and Energy Directorate)	Lars Stalsberg
Project coordinator	PGI-NRI
Document summary	

The project No.2018-1-0137 “EU-WATERRES: EU-integrated management system of cross-border groundwater resources and anthropogenic hazards” benefits from a € 2.447.761 grant from Iceland, Liechtenstein and Norway through the EEA and Norway Grants Fund for Regional Cooperation.

Scientific work published as part of an international project co-financed by the program of the Minister of Science and Higher Education entitled "PMW" in the years 2020-2023; agreement No. 5152 / RF-COOPERATION / 2020/2.

Table of Contents

List of Figures

1. Norway's requirements, priorities, and restrictions on groundwater use

1.1. Norwegian legislation and requirements

The responsibility for water resources management in Norway is divided between the national, regional, and local levels. The water management is based on the Water Framework Directive (WFD) which was implemented into Norwegian law in 2007. The aim is to ensure a holistic and sustainable usage of the water resources.

In the law proposal to the parliament number 97 L, 2016-2017 (OED, 2017), amendments for groundwater are proposed for the Watercourses and Groundwater Act (Water Resources Act) (KLD, 2000) with focus on the duty of care. Following the recommendations from the low proposal 97 L a new paragraph, § 43 a, was added to the Norwegian Water Resources Act. The paragraph introduces a duty of care for influence of groundwater following the pattern as for impact on waterways. The paragraph is formulated and designed in the same way as the corresponding provision for watercourses, cf. Section 5 of the Water Resources Act. The provision regulates basic requirements for behaviour that can influence groundwater, and it is therefore appropriate that all requirements for care and fiduciary responsibility at questions about groundwater measures and the impact of groundwater is collected in one paragraph. Duty of care in the case of groundwater drilling is regulated by § 46. Proposition 97 L explains thoroughly the reasons for this extending the law to protect groundwater (OED, 2017). It points to the importance of the interconnection between groundwater and surface water, and the importance for surface water ecological systems. In average the groundwater contribution to the average total runoff is 46 %, and in some areas up to 85 % during wintertime. The law proposal 97 L points to a fact that is often forgotten; where does the water in the rivers come from when it does not rain and during winter? It points to the need for protecting the groundwater resource when extracting groundwater, activities that can affect the groundwater, the risk for structural damage, landslides etc. (OED, 2017). The proposal was taken into law 16 June 2017 (OED, 2000).

In addition to this the Water Resources Act there are other laws and regulations on technical requirements, impact assessments and such as the Act on Protection against Pollution and on Waste (Pollution Act) (KLD, 1981). The regulations and impact assessments take care of the practical implementation of the laws. The Environment Agency is responsible for the Pollution Act, which regulates any polluting activity which may have a negative impact on e.g., groundwater. Activities with release of harmful substances to the ground, or groundwater needs an application for license (KLD, 1981).

On the national level there are several ministries with a responsibility for groundwater. The Ministry of Climate and Environment (KLD), as the coordinating ministry for The Norwegian Water Regulation Act (KLD, 2006), heads a ministry group which is responsible for the implementation of the WFD in Norway. The other ministries in this group are the Ministry of Petroleum and Energy (OED), the Ministry of Trade, Industry and Fisheries (NFD), the Ministry of Health and Care Services (HOD), the Ministry of Agriculture and Food (LMD), the Ministry of Transport (SD), the Ministry of Finance (FIN), and the Ministry of Local Government and Regional Development (KMD). The underlaying directorates of these ministries coordinate the WFD-work and are responsible for subgroups created for specific implementation tasks.

The Water Regulation Act is founded in the Pollution Act (KLD, 1981), the Planning and Building Act (KMD, 2022), and the Water Resources Act (KLD 2000). The Ministry of Local Government and Regional Development (KMD) is the central competent authority under the WFD, with responsibility for water quality and biodiversity. The national authority for the implementation of the WFD is the Norwegian Environment Agency (NEA). The Ministry of Petroleum and Energy (OED) is responsible for the Water Resources Act, the management of watercourses and quantitative usage of water. Drinking water management is the responsibility of the Ministry of Health and Care services (HOD). Regional basin management plans (RBMP) developed by the County Authorities, which are responsible for the WFD river basin districts (RBD), are adopted as regional plans according to the Planning and Building Act §8-4 (KMD, 2022) with the special rules that follow from the Water Regulation Act. The ministries are responsible for defining the administrative, legal, and financial framework for the water management work. Additionally, they are to ensuring that the necessary instruments for the implementation of the planning processes and action programs are made available to the RBD competent authorities to be able to meet the environmental targets.

The County Governors are the responsible authority for the characterisation and classification for the water bodies. Groundwater data from NEA, The Water Resources and Energy Directorate (NVE), and The Geological Survey of Norway (NGU) is used for the management of the groundwater bodies. Of the 1400 groundwater bodies registered in Norway, only 13 is monitored by NVE (quantitatively) and NGU (qualitatively). In addition to monitoring data from NVE and NGU the County Governors use hydrogeological consultants in the work on groundwater classification. At the local level, the municipalities are responsible for the area and land use planning, where the control of groundwater usage is included. The Norwegian Water Resources Act (KLD, 2006) states that the landowner is the main owner of the water courses and groundwater on his/her property. The landowner can extract groundwater, as long as it does not have a negative impact on the groundwater resources or other public or private interests. This is described in more detail in the next chapter.

1.2. Priorities and groundwater use in Norway

The local self-government has a strong presence in the Norwegian population and there is broad political agreement that framework management should be the main principle for the state's management of the 11 counties and 356 municipalities. In principle, the municipalities are responsible for areal planning, the priority for land usage and exploitation of groundwater (KMD, 2022).

According to the Norwegian Water Resources Act the landowner owns the groundwater at the property. However, there are limitation on the beneficial rights. In principle, the landowner can take out groundwater for household use and livestock on the property without a licence, but not to an extent which will cause the runoff in nearby waterways to be less than the general low water discharge, or other negative impacts. Landowners cannot extract more water than what is regenerated. In such cases, the water abstraction is subject to a licence, cf. section 44 second paragraph and section 45 first paragraph in the Norwegian Water Resources Act.

Extraction of groundwater that exceed 100 m^3/day, must be reported to NVE for assessment of licensing obligations (Water Resources Act § 45). Drilling for groundwater, both by private households and public institutions, must be reported to the NGU within three months of completion of drilling (Water Resources Act § 46). Regulations and frameworks describe the obligations on the reporting of well drilling and groundwater investigations in connection with the drilling. Water supply from groundwater in Norway stands for about 15% (Kløve et al.,

2017). The limited use of groundwater is due to the abundance of surface water of good chemical quality suitable for drinking water. According to Statistics Norway, 193 of Norway's municipalities distribute groundwater to their inhabitants as drinking water through the public pipeline system. Sixty-six of these, deliver groundwater to less than 500 inhabitants. Only 10 municipalities provide groundwater to more than 10 000 people. Of these, Ringerike municipality, north of Oslo, is the largest actor providing almost its entire population, 29 000 inhabitants, with groundwater as pipelined water supply.

Geothermal heating utilize heat stored in bedrock, soil or groundwater and is a short-distance and environmentally friendly energy alternative (Fig. 1). In open systems, the energy from groundwater is extracted with the help of heat pumps to warm up buildings or to provide hot water. The stable groundwater temperature throughout the year provides good operating conditions and high efficiency for heat pumps. An estimated 70% of the heat distributed in the building comes from the ground, while the remaining 30% comes from the electricity supply necessary to run the heat pump.
The drilling company or the developer have to report all preliminary hydrogeological investigations and energy drilling carried out in connection with the establishment of a geothermal heating facility by decree cf. Water Resources Act §46 and associated regulations to the NGU (https://www.ngu.no/grunnvanninorge/registrering-bronner-rapporter).
Norway experiences an increasing use of groundwater as a heat source both for singe households and larger communities e.g., such as Melhus, Trøndelag County (Fig. 2), and Elverum, Innlandet County. Oslo is another example on extended usage of groundwater as energy as since oil furnaces were prohibited after 2020. At moment there are no regulations limiting the use of groundwater as a geothermal heating source as long as the water is transported back into the ground and the use do not exceed 10 million m^3 /year.

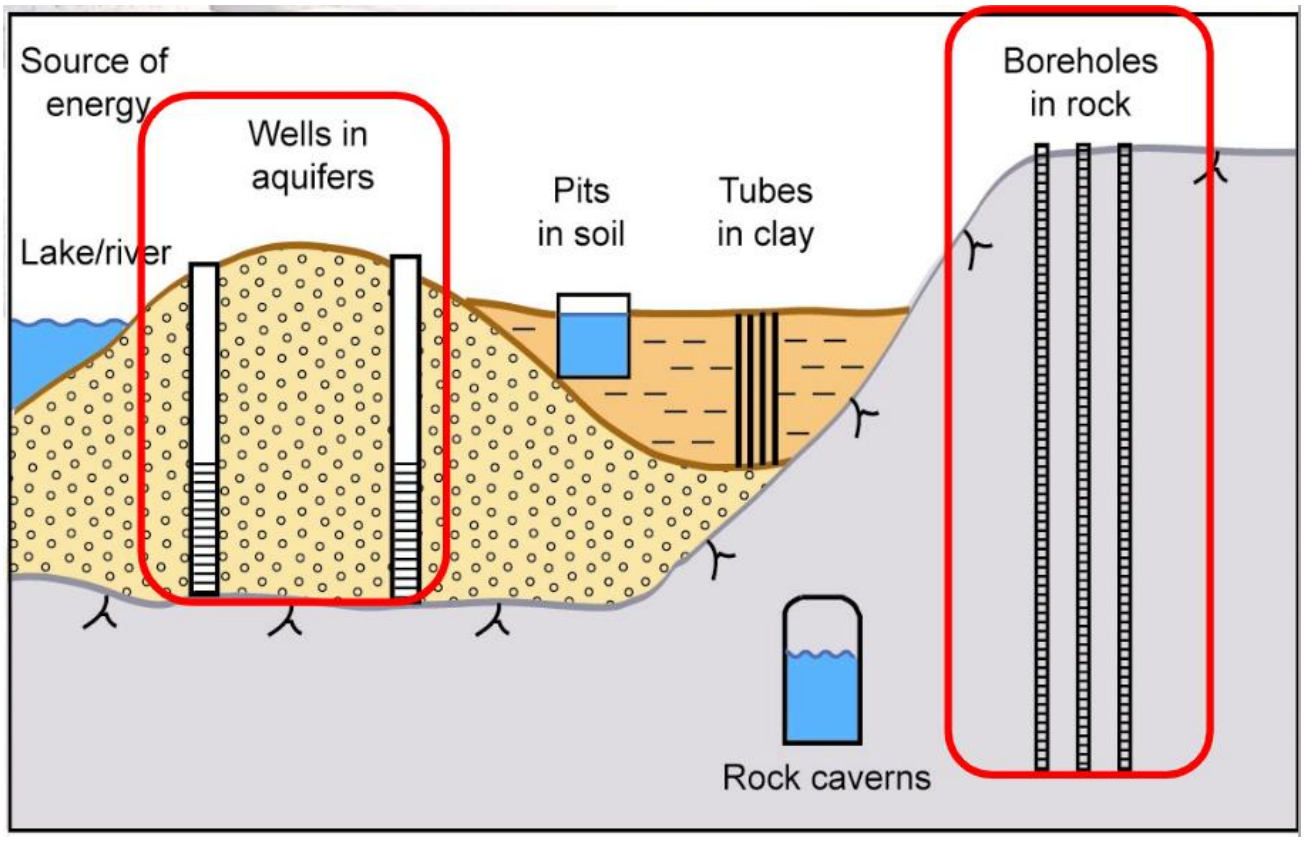

Figure 1. Different options for underground thermal energy storage (UTES) systems. (Figure from Andersson et al., 2003)

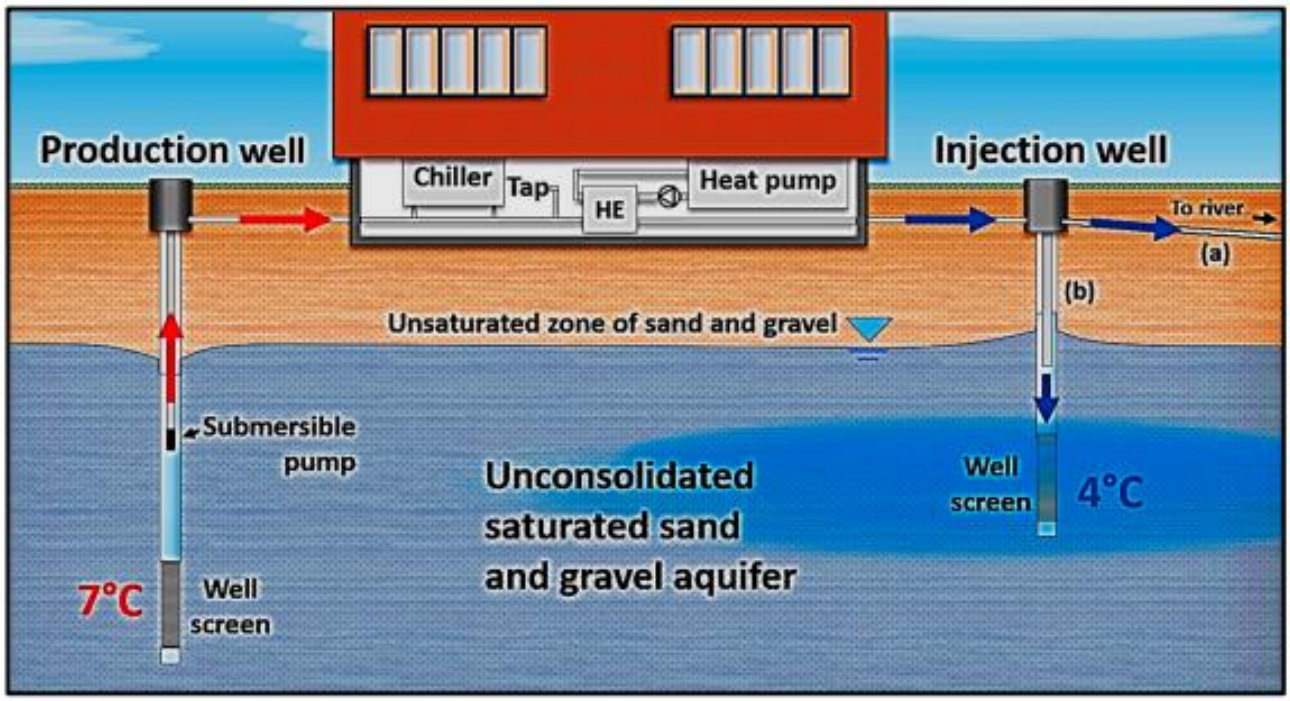

Figure 2. Types of groundwater heat pump (GWHP) systems in Melhus. (a) Design solution with run-off to nearby river through the local drainage system. (b) Most common design with re-injection of groundwater. (After: Gjengedal et al., 2019)

A serious challenge connected to groundwater in Norway is its effect on quick clay. Quick clay is found in countries close to the north pole e.g., in Russia, Canada, Norway, Sweden, and Finland, and in Alaska, United States, which were glaciated during the Pleistocene epoch. Quick clay, and other types of sensitive clay, were formed in Norway in areas where clay was deposited in a saline marine environment, and subsequently lifted near or above sea level due to post-glacial uplift. Quick clay has been the underlying cause of many landslides in Norway, both historical e.g., the Borregaard landslide in 1702, where 15 people perished (Klemsdal, 2003), and the Verdal landslide in 1893, where 116 people perished (Walberg 1993) and in recent years e.g., the Gjerdrum landslide in 2020, where 10 people perished. However, the majority of the landslides occurs without loss of lives e.g., the Alta landslide in 2020 which were larger than the Gjerdrum landslide. The triggering factor for the Alta landslide was major snowmelt and thus increased groundwater pressure in the days before the landslide.

Mapping of Quaternary geology in Norway has thus been an important basis for hazard and risk assessment for landslides in these highly sensitive clays (quick clay). The marine limit (ML) defines a natural upper limit to these deposits. Issues concerning marine clays can be disregarded above the ML. Below ML, a filtering of the Quaternary map information is needed to identify areas where clays are potentially present. Groundwater that flows through the marine clay will gradually wash out the electrically charged particles from the sediment pore water which have stabilized the loose grain structure, this leaching leads to instability and the clay becomes “quick”. Quick clay develops in pockets or layers in marine clay, preferably where there is or has been large groundwater flow. This can happen, for example, where the clay is above or near fractured bedrock, or where there are aquifers in or near the clay, for example a sand layer. Leaching can also occur near the soil surface, where the

groundwater has a high pressure or large gradients. Leaching can even occur below sea level if fresh groundwater flows upwards. In some cases, quick clay has been found in the seabed, 100 m from shore. In many places clay is not leached and is therefore stable (https://www.ngu.no/en/topic/quick-clay-and-quick-clay-landslides). As a consequence of the Gjerdrum landslide in 2020, the OED appointed a committee by royal decree to provide recommendations regarding measures and changes that can contribute to preventing destructive quick clay disasters in the future (OED, 2022).

As stated previously, an increased number groundwater and energy wells are established. Awareness has to be taken when these are drilled in areas with marine clay. The drilling can affect pore pressure conditions and groundwater flow, and lead to subsidence problems and slope failure. One of the committee's recommendations is that for areas mapped as "possible area with marine clay" (MML) or areas below marine limit (BML) drilling should require an application for drilling license. Data from well drilling can be combined with other data via the national database for land investigations, NADAG (NGU, 2022). The database NADAG shall ensure free sharing and reuse of important data from land surveys in Norway (NGU, 2022). The database contains geotechnical data, in addition, results from other land surveys such as geophysical investigations and groundwater wells, as well as various geological maps (Figure 3).

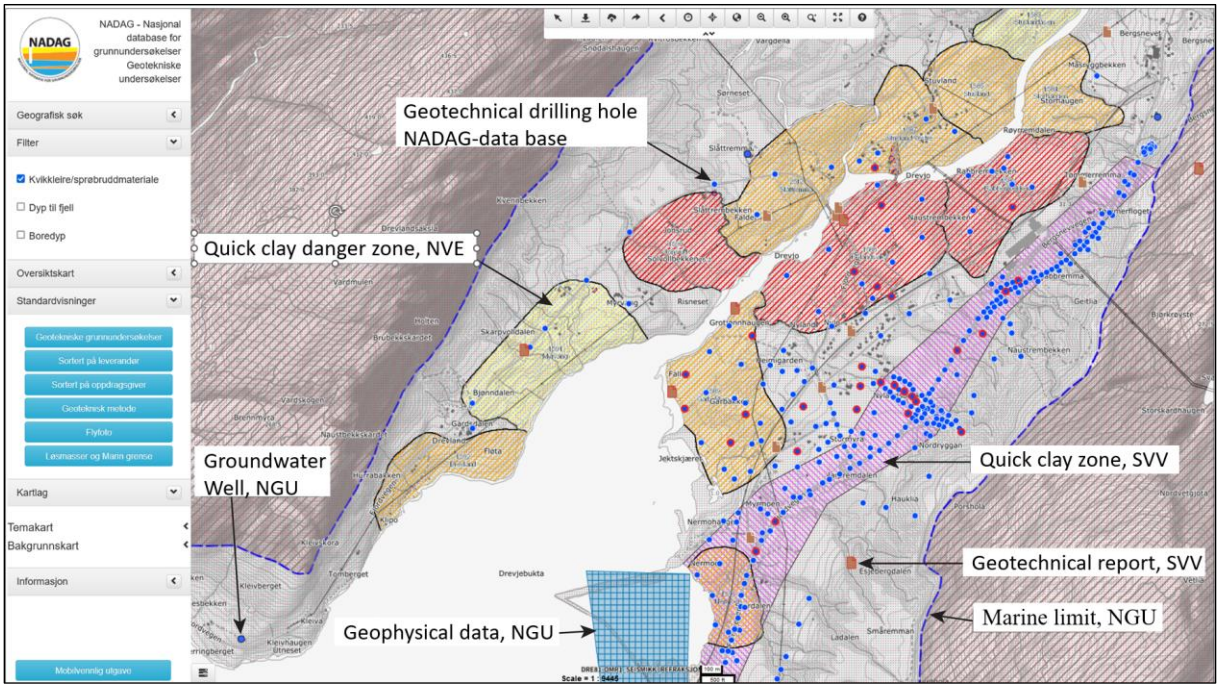

Figure 3. Example from NADAG's map view (NGU, 2022). Only the geotechnical boreholes are in NADAG, all the other map layers are taken from map services at NGU, NVE and the Norwegian Public Roads Administration (SVV). (After: OED, 2022)

Norway is a country with deep fjords, high mountains, and numerous islands, where tunnelling is an essential measure to ensure effective transportation connecting the different parts of the country. As of 2021 Norway have more than 1900 tunnels. If no measures are performed to reduce water inflow into tunnels, they will work as very efficient drains of the groundwater. Lowering of the groundwater table has many adverse consequences, such as damage on infrastructure and buildings due to ground surface settlement, drainage of lakes and desiccation of vegetation (Strømsvik, 2019). Analyses aiming at identifying the vulnerability and sensitivity of the surroundings in the area of planned tunnel constructions

was introduced in the late 1990s and are now mandatory. These analyses must also focus on local biotypes in combination with water balance studies (Grepstad, 2001; Kveldsvik et al., 2001). It is important to closely monitor

the leakage from the surrounding rock mass into the tunnel during and after construction, as well as the pore pressure and water levels in lakes and aquifers above the tunnel prior to and during the tunnel construction (Grepstad, 2021). The authorities have made these analyses mandatory to avoid incidents such as the one occurring during the construction of the Gardermobanen railway tunnel where a lake, Nordre Puttjern in Østmarka outside Oslo, was drained due to the tunnelling (1997). In addition, the groundwater leakage resulted in the bog surface sinking up to 5 meters, local subsidence, peat landslides, peat cracking and dry bog holes.

Figure 4. Lake, Nordre Puttjern in Nordmarka, dissapared into Romeriksporten in 1997. In the newspapers, the incident was referred to as: the plug has been taken out of the bathtub (Foto: Steinar Saghaug).

All the major cities in Norway are located on the coast. The coastline is stretching all the way from the Oslo fjord down to Kristiansand, around the land of the western fjords with the cities Stavanger, Haugesund, Bergen, Ålesund, Molde, before it is stretching out a long way north passing the cities Trondheim, Bodø, and Tromsø before bending around the top of the Scandinavian peninsular to the city Kirkenes to meet with Russia. All these cities are consolidated on land that is below the old marine limit (ML). In most of these cities the surfaces are dominated by impervious asphalt and concrete which reduce the shallow and deep infiltration and maintenance of the groundwater level and pressure, this is well demonstrated by FISRWG, 1998 (Figure 5).

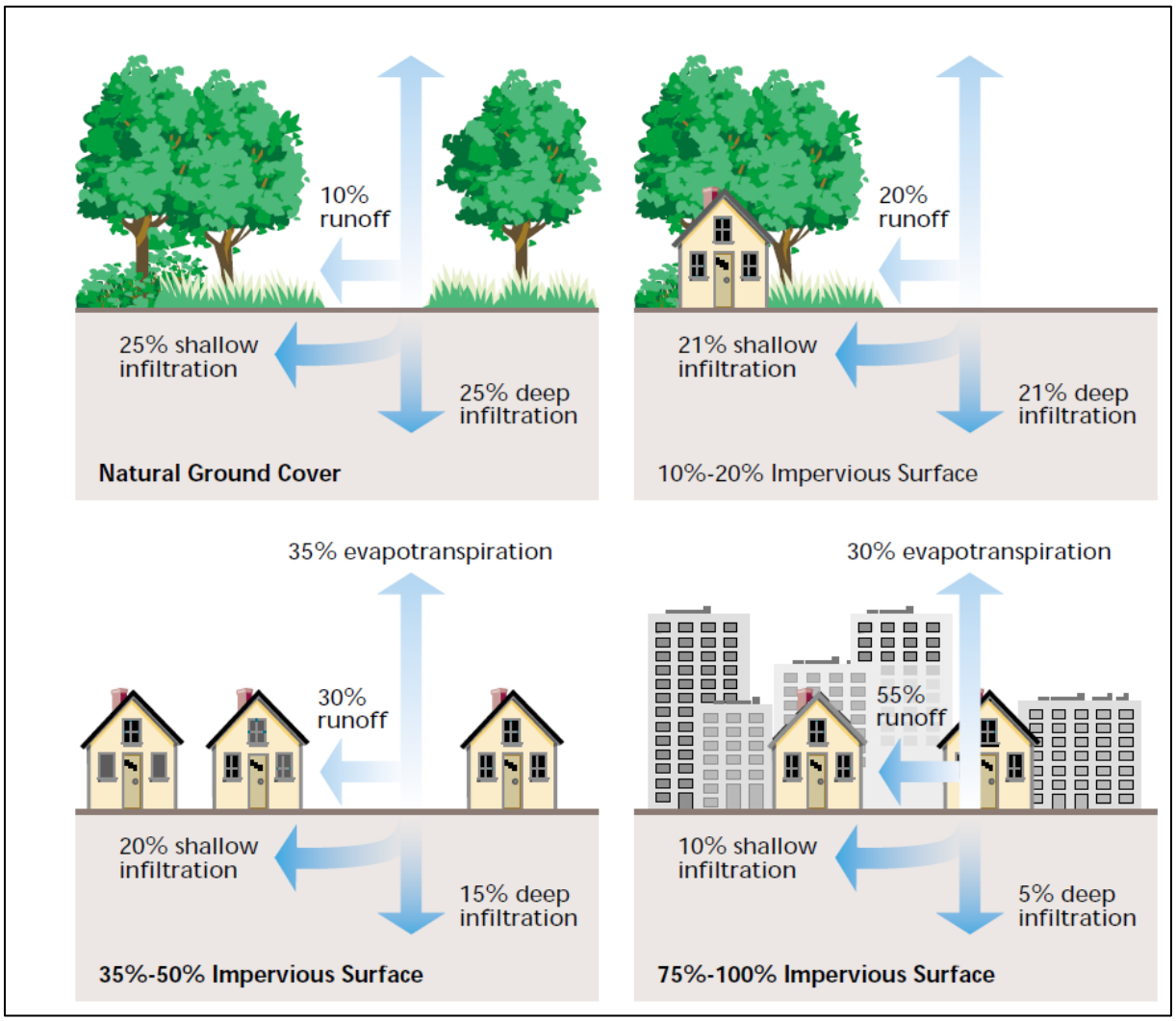

Figure 5. Relationship between impervious cover and surface runoff. Impervious cover in a watershed result in increased surface runoff. As little as 10 percent impervious cover in a watershed can result in stream degradation. (Figure and text from FISRWG, 1998)

Norway's capital Oslo is settled on old seabed sediments characterized by thick layers of unstable and sensitive marine clays. In many areas in Oslo, city developers have gradually replaced naturally occurring geological material with industrial aggregate. A major challenge in Oslo is subsidence caused by changes in groundwater pressure (e.g., Venvik et al., 2018). With the help of radar measurements from satellites, the InSAR (Synthetic Aperture Radar Interferometry), the magnitude of the movements can be estimated with an accuracy down to a few millimetres. Over time, radar images can be compared, to monitor variations in movement and subsidence (Figure 6).

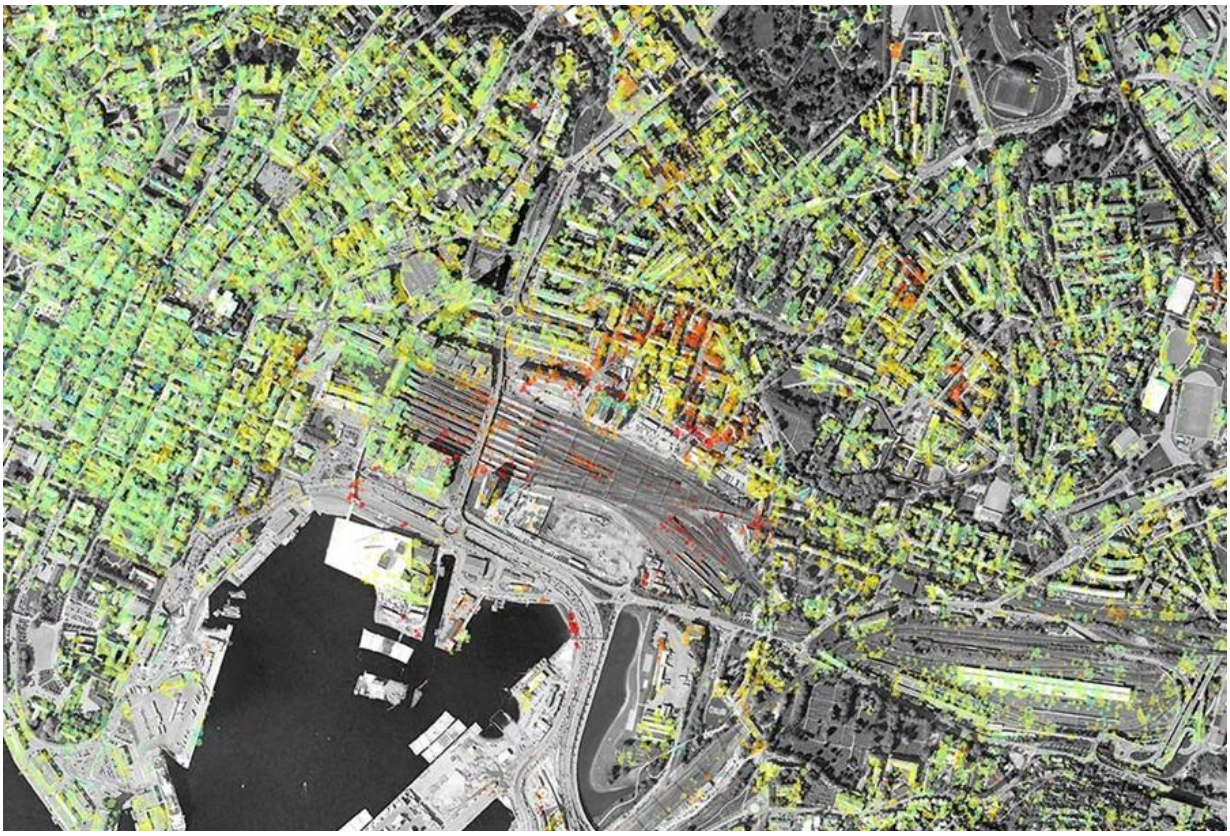

Figure 6. Oslo city centre, analysis of InSAR images between 2009 and today reveals more than one centimetre per year of subsidence in the Bjørvika area

Bryggen, in the city of Bergen, western Norway, was added to the World Heritage list based on the selection criterion “to bear a unique or at least exceptional testimony to a cultural tradition or to a civilization which is living, or which has disappeared” (Unesco, 2008). Throughout the centuries Bryggen has been ruined by at least seven large fires. Each time Bryggen was rebuilt on top of its old foundations and refuse, creating a more than 10-meter-thick archaeological deposit layer. The major negative consequence of lowered groundwater levels at this site is oxidation of these organic deposits and loss of archaeological information. By the turn of the 21st century it was observed that the old wooden buildings suffered from severe subsidence by damaging settling rates caused by deterioration of underlying cultural deposits caused by the lowered groundwater level (De Beer and Matthiesen, 2008). Repairing the sheet pile wall would only be part of the cure for Bryggen. More important, the levels of groundwater had to be raised and re-established. For this, new methods had to be established to secure a sustainable supply of water to the ground beneath Bryggen (Rytter and Schonhowd, 2015). One of the solutions was to raise the groundwater level in the area by a construction of “rainwater gardens” to compensate for reduced infiltration due to impervious surfaces (Fig. 5).

2. Summary

The Norwegian legislation reflects the priorities regarding groundwater use and the importance of groundwater in the Norwegian society. The legal framework is established by the parliament and government authorities, but it is mainly the local authorities who administer the legislation in their area through local development plans for land use e.g.,

water supply, sewage, garbage collection, gas and electricity supply, roads, and tramways. When an extraction of groundwater may have an impact on the groundwater resource, or harm other interests, an application for license has to delivered to NVE for assessment. When an activity may have an impact on the groundwater resource due to release of polluting substances, an application has to be handled by the NEA. The groundwater is owned by the landowner, but there are limitations on how to use this resource, as it may have a serious impact on both future usage of the resource, surface water, surface water ecology, landslides and harm on property by land subsidence. The use of groundwater for water supply is low, less than 15%, however there is a growing awareness both at the governmental and local administrative level that there is a need for increased knowledge of the whole hydrological cycle, and the administration of this. Knowledge on the water balance is crucial to avoid subsidence in in cities which e.g., can cause large damages on buildings and underground infrastructure such as pipelines and historical heritage sites. In addition, knowledge on water flow and groundwater system is getting increased attention in all infrastructure projects to avoid e.g., landslides after formation of quick clay, subsidence and change in groundwater level.

References:

Andersson, O., Hellström, G., Nordell, B., 2003. Heating and cooling with UTES in Sweden - Current situation and potential market development. FUTURESTOCK'2003, 1-4 September 2003, Warsaw Poland.

De Beer, J., Matthiesen, H., 2008. Groundwater monitoring and modelling from an archaeological perspective: Possibilities and challenges. NGU Special Publication, 11, pp. 67–81.

FISRWG, 1998. Revised August 2001. Stream Corridor Restoration: Principles, Processes, and Practices. By the Federal Interagency Stream Restoration Working Group (FISRWG) (15 Federal agencies of the US gov't). GPO Item No. 0120-A; SuDocs No. A 57.6/2:EN 3/PT.653. ISBN-0-934213-59-3

Flem, B., Stalsberg, L., Seither, A., 2022. Groundwater governance in international river basins - An analysis of the Norwegian-Swedish transborder area. J. Hydrol. Reg. Stud, 44, 2022, 101216. https://doi.org/10.1016/j.ejrh.2022.101216

Gjengedal, S., Stenvik, L.A., Storli, P.T.S., Ramstad, R.K., Hilmo, B.O., Frengstad, B.S., 2019. Design of groundwater heat pump systems. Principles, tools, and strategies for controlling gas and precipitation problems. Energies 12. https://doi.org/10.3390/en12193657

Grepstad, G. K., 2001. Water balance – definition and monitoring. NFF Publication No. 12. https://nff.no/wp-content/uploads/sites/2/2020/04/Publication-12.pdf

Halleraker, J.H., Sorby, L., Keto, A., Guðmundsdóttir, H., (eds.) 2013. Nordic collaboration on implementation of the Water Framework Directive – Status and further challenges. A report for the Nordic Council of Ministers, Umhverfisstofnun, Reykjavík, 2013, 37 pp. ISBN 978-9979-9818-1-7

Kitterød, N. O., Colleuille, H., Pedersen, T. S., Langsholt E., Dimakis, P., 1998. Vanntransport i oppsprukket fjell. Numeriske simuleringer av vannlekkasjer i Romeriksporten (Water transport in cracked mountains. Numerical simulations of water leaks in Romeriksporten) *In Norwegian.* NVE 11-98.

KLD, 1981. *Lov om vern mot forurensninger og om avfall* (Forurensningsloven). LOV-1981-03-13-6. (Act on Protection against Pollution and on Waste (Pollution Act)) *In Norwegian.* Lovdata. https://lovdata.no/dokument/NL/lov/1981-03-13-6

KLD, 2006. The Water Regulation Act; FOR-2006-12-15-1446; Ministry of Climate and Environment: Oslo, Norway, https://lovdata.no/dokument/SF/forskrift/2006-12-15-1446 (Accessed November 2022)

KMD, 2022. Reguleringsplanveileder. Kommunal og moderniserings departementet (Regulation plan supervisor. Ministry of Municipal Affairs and Modernization). *In Norwegian.* https://www.regjeringen.no/no/dokumenter/reguleringsplanveileder/id2609532/?ch=9

Klemsdal, T., 2003. Borregaardraset, natten mellom den 14. og 15. februar 1702. (Borregaardraset, the night between 14 and 15 February 1702). University of Oslo, Department of Geosciences Department of Geography. *In Norwegian*

Kløve, B., Kvitsand, H.M.L., Pitkänen, T., Gunnarsdottir, M.J., Gaut, S., Gardarsson, S.M., Rossi, P.M., Miettinen, I., 2017. Overview of groundwater sources and watersupply systems, and associated microbial pollution, in Finland, Norway and Iceland. Hydrogeol. J. 25, 1033–1044. https://doi.org/10.1007/s10040-017-1552-x.

Kveldsvik, V., Holm, T., Erikstad, L., Enander, L., 2001. Planning of a 25 km long water supply tunnel in an environmentally sensitive area. NFF Publication No. 12. https://nff.no/wp-content/uploads/sites/2/2020/04/Publication-12.pdf

NGU, 2022. NADAG, Map view, Geological Survey of Norway. Obtained from: https://geo.ngu.no/kart/nadag/og Informasjon: https://www.ngu.no/emne/nadag.

OED, 2017. Endringer i vannressursloven og jordlova (konsesjonsplikt for grunnvannstiltak og unntak fra omdisponeringsforbudet) (Prop. 97 L 2016-2017). (Amendments to the Water Resources Act and the Land Act (licence obligation for groundwater measures and exemptions from the redeployment ban). *In Norwegian.* https://www.regjeringen.no/no/dokumenter/prop.-97-l-20162017/id2547890/

OED, 2000. *Lov om vassdrag og grunnvann* (Vannressursloven). LOV-2000-11-24-82. (Watercourses and Groundwater Act (Water Resources Act)). *In Norwegian* Lovdata. https://lovdata.no/dokument/NL/lov/2000-11-24-82

OED, 2022. På trygg grunn. Bedre håndtering av kvikkleirerisiko. Utredning fra et utvalg oppnevnt ved kongelig resolusjon 5. februar 2021. (On safe ground. Better management of quick clay risk. Investigation by a committee appointed by royal decree 5 February 2021). *In Norwegian*. NOU, 2022:3. The Ministry of Petroleum and Energy.

Solli, G. S., 2020. Ute av syne, ute av sinn - om rettigheter til og forvaltning av grunnvann i norsk rett. (Out of sight, out of mind - about rights to and management of groundwater in Norwegian law). *In Norwegian*. PhD thesis, University of Oslo, Norway, 2020, pp. 470

Strømsvik, H., 2019. Assessment of High Pressure Pre-Excavation Rock Mass Grouting in Norwegian Tunnelling, Thesis for the Degree of Philosophiae Doctor, Trondheim, October 2019. Norwegian University of Science and Technology Faculty of Engineering Department of Geoscience and Petroleum.

Rytter, J., Schonhow, I., (eds.), 2015. Monitoring, Mitigation, Management, The Groundwater Project – Safeguarding the World Heritage Site of Bryggen in Bergen. A7 Print, Riksantikvaren, www.ra.no, http://hdl.handle.net/11250/300104

Venvik, G., Liinamaa-Dehls, A., Bjerke, C., et al., 2018. Pathways & Pitfalls to Better Sub-Urban Planning. Geological Survey of Norway, 2018. ISBN: 978-82-7385-201-4

Walberg, Ø., 1993. Verdalsboka. En bygdebok om Verdal. Ras i Verdal. Bind. B. Verdal kommune. (The Verdals book. A village book about Verdal. Landslide in Verdal. Volume. B. Verdal municipality). *In Norwegian.* ISBN 82-990950-7-7.

Table of contents

List of Figures

List of Tables

Transboundary aquifers (TBAs) of the Polish-Ukrainian borderland are considered important in shaping the strategic groundwater resources of both countries (Kamzist & Shevchenko, 2009; Kowalski, 2007). The Upper Cretaceous (K2) aquifer plays the main role here. This aquifer is associated with the extensive geological structure - Lublin Basin in Poland and Lviv Foredeep in Ukraine and is the main source of drinking water for both large urban agglomerations. In addition, the global list of TBAs published by UNESCO in 2015 included a transboundary groundwater reservoir within the catchment area of the Bug River (IGRAC, 2021).

Transboundary groundwater resources between Poland and Ukraine are largely uncharacterized due to the lack of data to date, differences in approaches to TBAs identification and stratigraphic classification methodologies, and limited institutional cooperation in TBA management between countries. Filling the existing gaps was possible thanks to cooperation on cross-border groundwater between Polish and Ukrainian geological surveys as part of the implementation of the international EU-WATERRES project “EU-integrated management system of cross-border groundwater resources and anthropogenic hazards” (www.eu-waterres.eu) –funded by Iceland, Liechtenstein and Norway through the EEA and Norway Grants Fund for Regional Cooperation. The main goal of the project is to develop the concept of coordinated management and harmonized monitoring of TBAs. The starting point was the harmonization of data for the development of a common conceptual and numerical model identifying TBAs. Of particular importance is the development of numerical models, which are not a requirement of the Water Framework Directive, but should nevertheless be taken into account when identifying groundwater bodies and developing water management plans.

The aim of this work is to simulate the abstraction of groundwater using a numerical hydrodynamic model with different variants of the pressure on the transboundary aquifer system within the Polish-Ukrainian borderland. The work focused on four main thematic areas:

- development of a new numerical model of the investigated aquifer system;
- development of a methodology allowing for the inclusion of unregistered abstractions in the calculations;
- carrying out an assessment of the impact of groundwater abstraction on the hydrodynamic condition of the system, in particular on transboundary flows;
- providing scientific support in developing practices for joint management and protection of identified TBAs.

1. Polish-Ukrainian pilot area characterization

1.1 Geographical settings

The pilot area is near the Polish-Ukrainian border in the south-eastern part of Poland and the north-western part of Ukraine (Figure 1). According to the geographical division, the study area is located on the border of two megaregions: the East European Plain and the Carpathian Region (Solon et al., 2018). The above-mentioned section of the border line is 203 km long and runs through the Eastern Beskids, Northern Podkarpacie, the Lublin-Lviv Upland and the Volhynia-Podolska Upland.

Figure 1. Location of the pilot area

In the hydrographic system, the study area covers fragments of the left bank catchment of the Bug River and the right bank catchment of the San River. The boundaries were drawn along surface watercourses and morphological watersheds. In the north-east, the boundary of the model was drawn along the Bug bed. To the south of the village of Ruda, the boundary line was drawn along the watershed line closing the catchment area of the Rata River. Then, the boundary of the model runs along the watershed line separating the Dniester basin from the Vistula basin. This border closes the model research area from the south-east and south. From the south-west, the border was drawn along the watershed line to the San riverbed near the town of Olszany. Further north, the border is marked by the channels of the San, Lubaczówka, Sołotów and Świdnica. From the north-west, the border of the area is marked by watersheds closing the catchments of the left tributaries of the Bug - Rata, Sołokija and Warężanka. From the north, the boundary of the research area is marked by the bed of the

Bukowa River. The total area of the land designated for model tests is 7023.5 km^2, of which 2065.25 km^2 is located in Poland and 4958.25 km^2 in Ukraine. Among the most important towns on the Polish side of the border Przemyśl, Tomaszów Lubelski and Lubaczów are worth mentioning and on the Ukrainian side - Czerwonograd, Żowkwa, Rawa Ruska, Chliwczany, Jaworiw and Sudowa Wysznia (Figure 2).

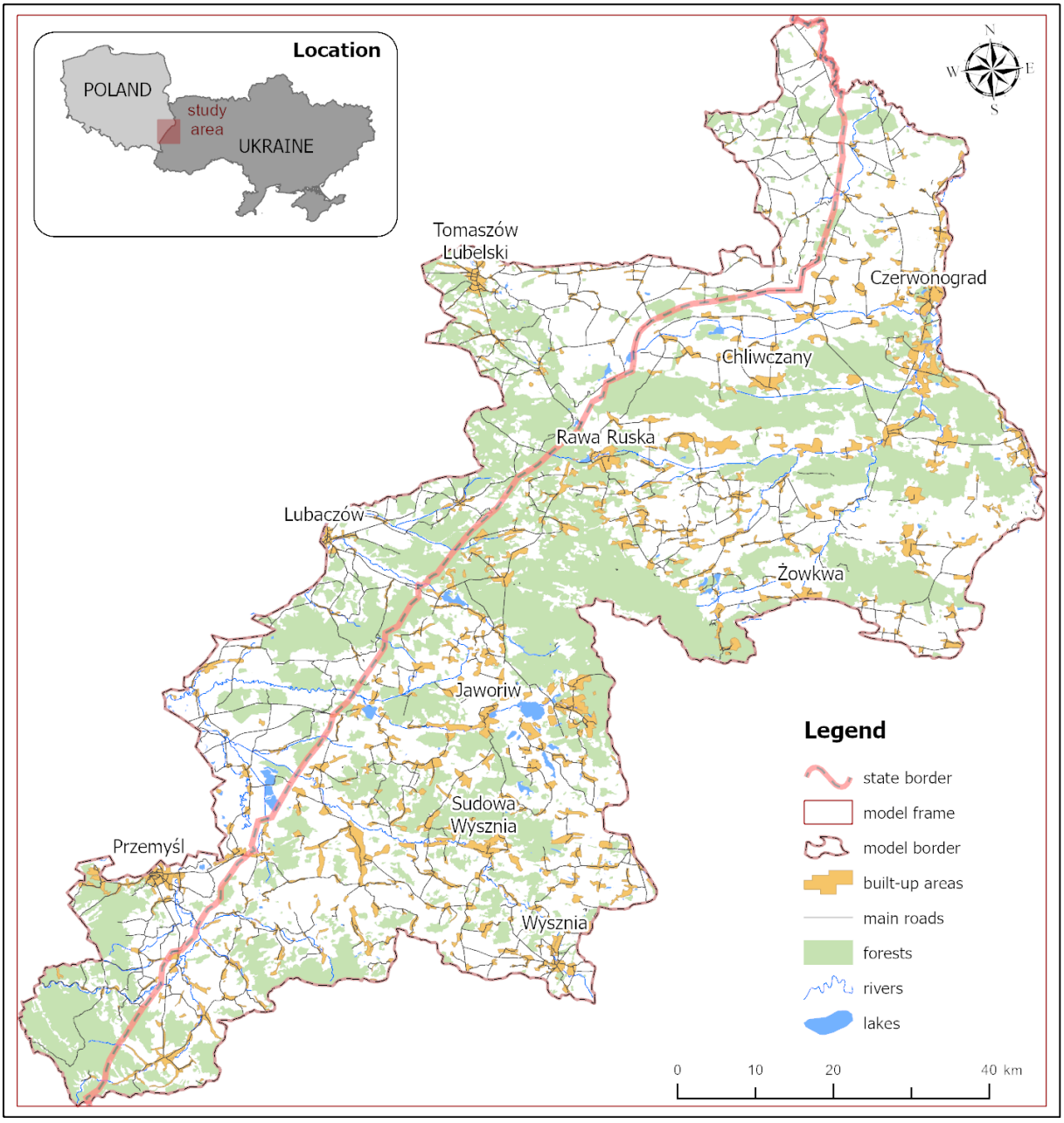

Figure 2. Environmental conditions of the model research area

Most of the area (91%) is below 300 m above the sea level (a.s.l.), highlands (4%) - Roztochia and Podilla Upland - reach a maximum of 400 m a.s.l., mountains (5%) - Outer Carpathians with the highest peaks reaching 610 m a.s.l. The humid temperate climate has evolved at the junction of two climatic regions: dry continental and humid mountain. The average air temperature ranges from -3.5°C to 5°C in January and from 16°C to 18°C in July (Lorenc, 2005). Average annual rainfall varies from 500 mm in the northeast to over 1,200

mm in the southwest (Outer Carpathians), influenced by orographic effects, while evaporation amounts to 450 and 520 mm/year, respectively (Lorenc, 2005).

The northern part of the study area – the Polesie mesoregion – is flat with a predominance of wetlands, a poorly developed network of rivers, and dense drainage canals and lakes, including the famous Shatské lake complex, belonging to the Ramsar protected area. The central part of the study area is in the Volyn Upland and Roztocze. Its characteristic feature is alternating hills and vast depressions and valleys. In the south of the study area, in the San and Dniester catchments, the highlands transform into the Outer Carpathian flysch. The name "flysch", introduced into the literature by Studer (1827), is used to refer to marine geosynclinals sediments of considerable thickness (Kelling et al., 2007).

Hydrographically, the study area is unique due to its location in the European watershed, which ensures that the Bug and San basins belong to the Baltic Sea basin, while the Dniester basin belongs to the Black Sea. These river basins are represented in the study area with their upper parts (springs). In the Bug catchment there is a slight hypsometric differentiation in the area of 150–180 m above sea level; in the San and Dniester catchments the absolute heights range from 210 to 1200 m above sea level, due to the mountainous nature of the catchment. Due to the orographic factor, the Bug and its tributaries in the study area show minimal longitudinal slopes (0.01–0.5‰), which slows down the outflow of water and contributes to the formation of fluviogenic wetlands. The average annual river runoff in the study area in the Bug catchment is about 120 mm; the unit runoff varies from 3 to 4 l/s/km^2; and the share of groundwater in the river runoff is about 50% (Nazaruk, 2018). In the catchments of the San and Dniester, the main factor influencing the amount of runoff and the features of the river regime is atmospheric precipitation, which – combined with the low retention capacity of the Carpathian flysch and the dense erosion network – favour the occurrence of rapid surface runoff. The average annual river runoff in the San catchment in the foreland area is approx. 170–200 mm; this increases with the average height of the catchment, giving the upper part a runoff layer of 660–780 mm and a unit runoff of 23–27 l/s/km^2 (Michalczyk et al., 2002). The share of underground recharge of rivers in this area ranges from approx. 21% to 45%, and the lower values are characteristic of the mountainous part of the catchment area.

1.2 Geology and hydrogeological conditions

The shape of the land surface clearly refers to the geological structure. The area designated for modelling studies covers three main tectonic units. Looking from the south, these are: the Carpathian thrust, the Carpathian Foredeep and the Lublin basin.

The Carpathians are a young fold orogeny with a nappe structure. The model area covers a small fragment of the marginal zone of the Outer Carpathians, built of folded and flaked flysch rocks. In this area, the landscape is shaped by low mountain ranges running from NW to SE, mainly associated with outcrops of rocks resistant to weathering (mainly sandstones). The maximum elevations of the terrain only slightly exceed 550 m above sea level (Figure 3).

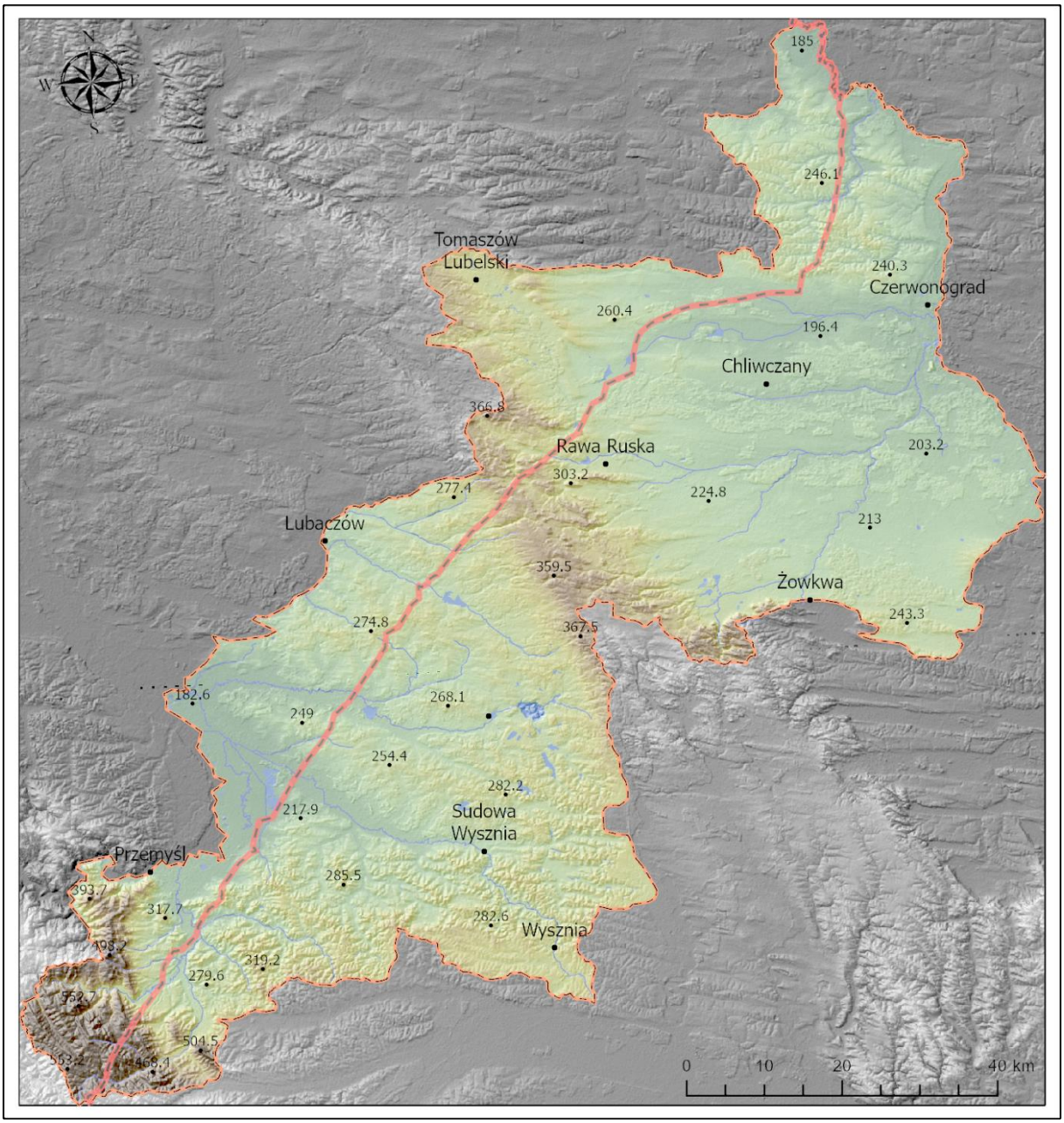

Figure 3. Terrain topography (based on SRTM-3 data)

In the foreland of the Carpathians, there is a clearly lowered and heavily denuded area of the Carpathian Foredeep. The Foredeep is a foreland rift filled with clastic Miocene deposits. The Miocene formations are tectonically weakly involved and occur under the cover of Quaternary sediments. The surface of the area is formed by old, heavily denuded post-glacial uplands cut by river valleys. At the eastern border of the area, loess covers formed at the end of the Pleistocene have been preserved. In this area, the relief is diversified by numerous ravines. To the north of the Carpathian Foredeep, the area of the Lublin Basin stretches. Both units are separated by a clear morphological edge of the Lublin-Lviv Upland, already included in the Lublin Basin. The upland is built of Upper Cretaceous and Palaeocene deposits developed mainly as carbonate facies. These formations are often exposed on the ground surface or occur under a thin cover of Quaternary sediments. Further to the north, the model covers the area of the Volyn-Podolia Upland. Elevations of the terrain clearly decrease here, which results from the tectonic lowering of the top of the Upper

Cretaceous formations. The cover of the Quaternary formations is thicker here, with loess covers dominating the uplands while the valleys of the Bug and its left tributaries are filled with sand and gravel alluvium. The surface geological structure of the research area is shown in Figure 4.

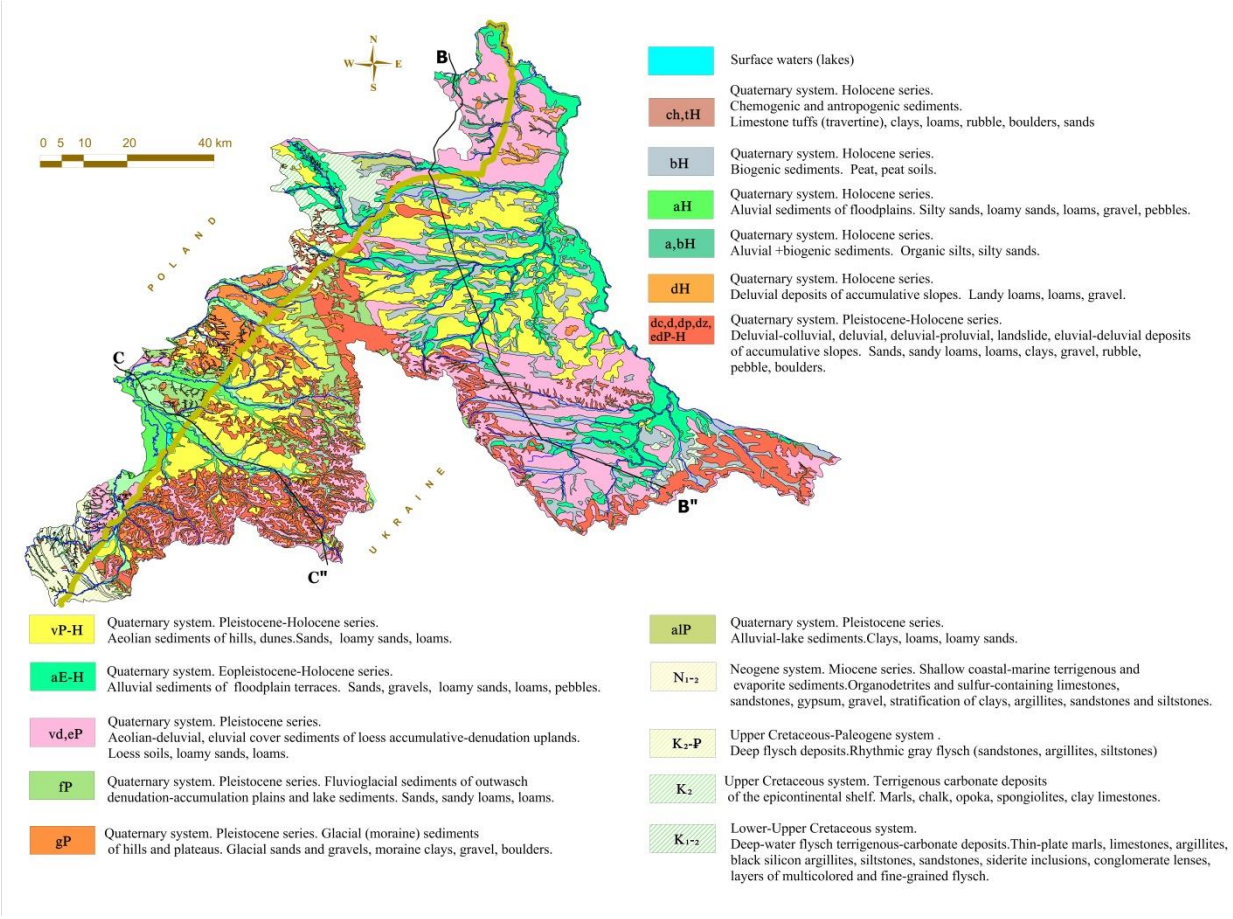

Figure 4. Geological map of the pilot area and lines of hydrogeological cross-section shown in Figure 5 (line BB") and Figure 6 (line CC")

The conditions of groundwater occurrence and circulation are different in individual tectonic units. In the area of the Carpathian overthrust, groundwater occurs in cracked flysch formations (mainly sandstones). The aquifer here has a fissure character, and its water permeability is determined by a network of block, dislocation cracks resulting from interbed surfaces separateness. The most favourable conditions for water circulation concern the near-surface zone, where a network of cracks is revealed as a result of rock mass stress-relief. Nevertheless, the water permeability of flysch sandstones is generally low. Filtration coefficients usually range from 10^{-5} to 10^{-6} m/s and decrease rapidly with depth. More favourable conditions are observed in river valleys, where groundwater occurs in sand and gravel alluvium.

In the valley zones, the filtration coefficient is usually 10^{-4} m/s.

In the area of the Carpathian Foredeep, ordinary groundwater is most often exploited from the Quaternary level. Affluent horizons occur here primarily in valley units filled with well-permeable sand and gravel alluvium. In the valleys of large rivers, the thickness of alluvial deposits locally exceeds 30 m, and the filtration coefficients are of the order of 10^{-4} m/s. In the area of the old post-glacial uplands, aquifers are mainly associated with sandy strata of

fluvioglacial origin, which are characterized by variable thickness and limited spread. The total thickness of the aquifers in the uplands usually does not exceed 25 m. The Miocene level in the area of the Carpathian Foredeep is usable only in its northern part and in Ukraine, where horizons of cracked limestones, sandstones, gypsum and gravels are exploited (the Baden (N1b1-N1b2). A typical structure of an aquifer in this area is shown in Figure 5. The Miocen aquifer is mainly confined (drilled at a depth of 11.0 - 46.0 m, the potentiometric surface was at a depth of 5.0-13.0 m below the surface). In Ukraine this aquifer is also associated with the presence of sulphate medicinal waters (Kamzist & Shevchenko, 2009).

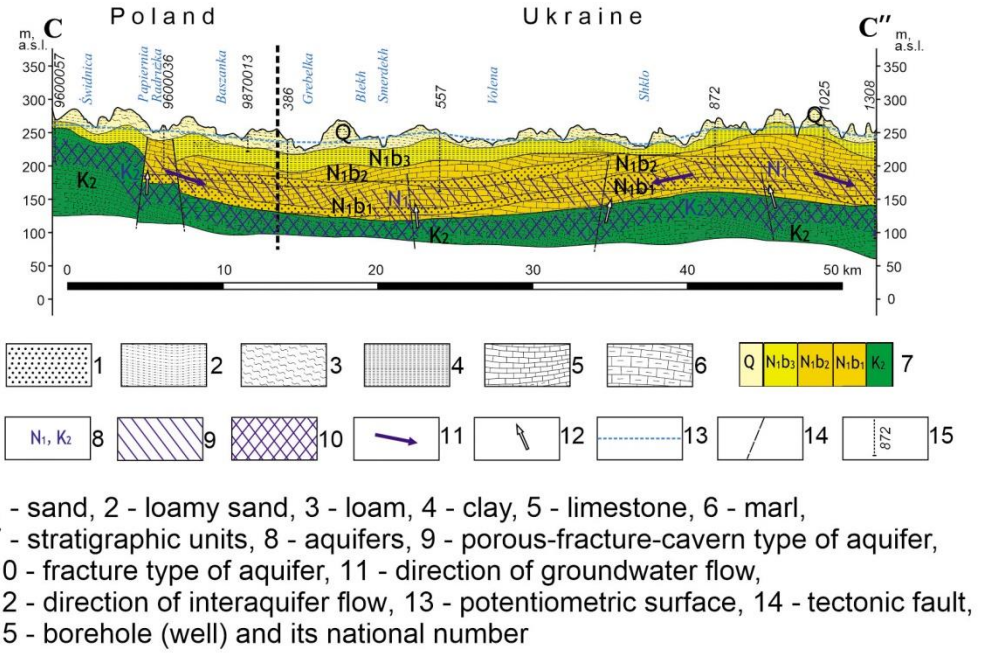

1 - sand, 2 - loamy sand, 3 - loam, 4 - clay, 5 - limestone, 6 - marl,
7 - stratigraphic units, 8 - aquifers, 9 - porous-fracture-cavern type of aquifer,
10 - fracture type of aquifer, 11 - direction of groundwater flow,
12 - direction of interaquifer flow, 13 - potentiometric surface, 14 - tectonic fault,
15 - borehole (well) and its national number

Figure 5. Hydrogeological cross-section characteristic for the cross-border part of the Carpathian Foredeep within the San sub-basin

In the area of the Lublin Basin, the main usable aquifer is mainly associated with the Upper Cretaceous formations (K_2). This aquifer is of key importance in shaping strategic drinking water resources, and is classified in Poland as the main groundwater reservoir with a regional range and large resources (Paczyński & Sadurski, 2007). The Upper Cretaceous rocks in the study area are formed in carbonate facies and are characterized by a varied content of silica and clay minerals. Among the lithological types of Upper Cretaceous rocks, writing chalk, marls, rocks and gauze predominate. These rocks form a fissured groundwater reservoir of a continuous character and variable water permeability. The water permeability of the massif depends on the lithological types of rocks and their tectonic involvement. Rocks occurring in the strongly fractured near-surface zone have the highest ability to conduct water. The filtration coefficients are in the order of 10^{-4} - 10^{-5} m/s, and the thickness of the permeable zone, depending on the lithological types of rocks, is estimated at 100 - 150 m. The Quaternary aquifer is of utility importance primarily in river valleys, where the thickness of alluvial deposits can reach up to 40 m, and the filtration coefficients are of the order of 10^{-4} m/s.

The hydrogeological conditions in this area are reflected in the hydrogeological profile of BB" (Figure 6). The first from the top, Quaternary (Q) aquifer occurs on a local scale and is hardly used. It is built of alluvial sandy sediments in the river valleys of the Bug and its tributaries –

the Rata, Solokiia, and others – are built from fluvioglacial sands in the watershed zone (Pankiv et al., 2013). The water table is unconfined and occurs at a depth of 0.4 m in river valleys and up to 12–15 m below ground level in the watershed zone. In the area of the greatest accumulation of alluvial sediments (the Bug River valley), its thickness is 15–20 m. The second aquifer, K_2, is the main usable aquifer; it has a sustained spread. Within Poland, the Upper Cretaceous aquifer is usually unconfined, while in Ukraine it is mainly confined. The depth of the intensive water exchange zone is 100-150 meters (Janiec, 1984). The water table is usually unconfined and its level depends on the topography. In river valleys the depth to the groundwater table is 0-10 m, at elevations 30-70 m.

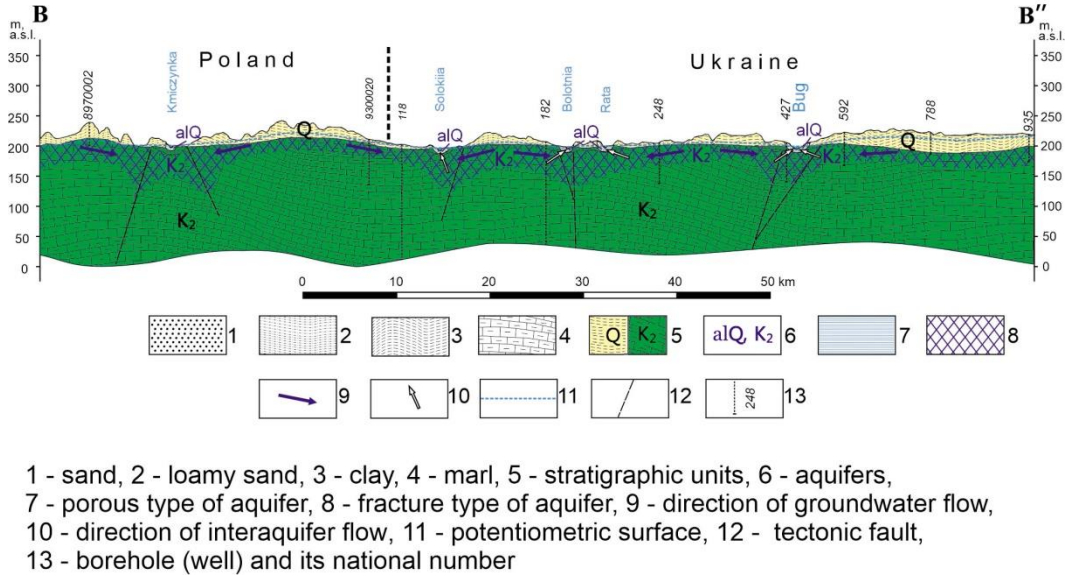

1 - sand, 2 - loamy sand, 3 - clay, 4 - marl, 5 - stratigraphic units, 6 - aquifers,
7 - porous type of aquifer, 8 - fracture type of aquifer, 9 - direction of groundwater flow,
10 - direction of interaquifer flow, 11 - potentiometric surface, 12 - tectonic fault,
13 - borehole (well) and its national number

Figure 6. Hydrogeological cross-section characteristic for the cross-border part of the Lublin Basin within the Bug sub-basin

1.3 Spatial development

Mapping of surface water bodies, wetlands and other types of areas based on Sentinel-2 space image processing data

The detection of water bodies, watercourses, wetlands and their changes over time are clearly recorded in the satellite images. At the current level of scientific and technical development, we are able to monitor, study and forecast changes in water reservoirs using remote sensing (RS) methods. This method is inexpensive, fast and effective for scientific research and eco-monitoring of the water surface.

Review of the methods of using remote sensing data to study and monitor water bodies

Most researchers successfully use the RS technologies to solve hydrogeological problems using optical and radar data from the Sentinel-2 and Sentinel-1 satellites, which are publicly available on the platform Copernicus Open Access Hub.

For mapping watercourses and their surroundings, scientists (Jiang et al, 2021, Kseňak 2022) use the RS data complex: SAR (Sentinel-1) technologies and Sentinel-2 spectral data - for the development of water indicators - NDWI (Normalized Difference Water Index), MNDWI (Modified Normalized Difference Water Index), AWEI (Automated Water Selection

Index). As a result, long-term observational data on changes in the behaviour of rivers and river systems can be obtained.

Using a complex of optical (Landsat-8) and radar (Sentinel-1A) data for detailed studies of Lake Poyang, the largest freshwater lake in China, scientists (Shen et al. 2022, Tian et al. 2017) obtained basic high-frequency data for environmental monitoring and wetland management.

Optical satellite data is also used for mineral mapping and lithology. For example, in the territory of north-eastern Morocco, using a combination of the ASTER and Sentinel-2A spectral bands in RGB composition, scientists (El Kati et al. 2018) identified lithological units and updated geological maps on a scale of 1: 50,000. Using data from Sentinel-2, scientists (Du et al., 2016) in their research used a technique based on the spectral index of water, MDNWI and NDWI. As a result, accurate monitoring was obtained according to the RS data, which has become an important element in mapping water bodies with a resolution of 10 m and 20 m.

Due to the use of SAR (Sentinel-1) radar data only, it is important to use various filters in the processing of space images (Kseňak et al. 2022, Kumar 2021) in order to reduce noise and improve the transparency of water bodies' boundaries. Use of various combinations of VV and VH polarities (Kseňak et al. 2022, Abdikan et al., 2016) with combinations of optical data (Yesou et al. 2016) allows to obtain optimal results for studying the dynamics of water surface and wetlands. Integrated RS data processing methods (De Luca et al., 2022) with the implementation of controlled classification, indexes, filters and programming elements (open source software and libraries (SNAP, Google Earth Engine, Scikit-Learn) in Python are gaining popularity.

Based on the experience of scientists and the technical capabilities of RS, at this stage of the research it was decided to use the data from optical multispectral images of the Sentinel-2 satellite to detect water surface areas, wetlands and other types of land.

The main task of the research was to designate areas with an open water surface (lakes, rivers, artificial reservoirs), wetlands, anthropogenically transformed areas (infrastructure, areas of human activity), forests and ecosystems (forests, trees, parks, reserves) and agricultural land (arable land and land permanently or periodically used and cultivated - gardens, fields, arable lands) in the basins of the Bug, San and Dniester river basins, using satellite data for 2018 and 2021. The selection of this type of land allowed to determine the proportion of the area and to determine the regularities found in the area of water reservoirs, wetlands, agricultural land, forests and urban areas in the above-mentioned river basins. A separate area (model area) was selected for the analytical description, covering the western part of Ukraine and eastern Poland, and part of the Bug and San basin (Figure 7).

Figure 7. Overview map of the locations of the river basins of the Bug, the San, the Dniester and the modelling area

Methodology

The task was performed using the method of data analysis from the multispectral Sentinel-2 satellite (Table 1) with specific RGB combination characteristics (band 11, 8, 2) suitable for the identification of water reservoirs and wetlands.

Table 1 Spectral characteristics of Sentinel-2 images

Band	Description	Resolution [m]	Central Wavelength [µm]
Band 1	Coastal Aerosol	60	0.443
Band 2	Blue	10	0.490
Band 3	Green	10	0.560
Band 4	Red	10	0.665
Band 5	Vegetation Red Edge	20	0.705
Band 6	Vegetation Red Edge	20	0.705
Band 7	Vegetation Red Edge	20	0.783
Band 8	NIR	10	0.842
Band 8-A	Narrow NIR	20	0.865
Band 9	Water Vapour	60	0.945
Band 10	SWIR-Cirrus	60	1.380
Band 11	SWIR	20	1.610
Band 12	SWIR	20	2.190

The methodology can be conditionally divided into the following steps:

1. Analysis of the research area and selection of remote sensing data to solve the task. At this stage, it was decided to use the product S2A_MSIL1C_20181014T093031 of the Sentinel-2 satellite available on the portal: Copernicus Open Access Hub. Space images with 0% cloudiness were selected for optimal results.

2. Next, the Sentinel-2 space images were downloaded from the portal and processed in GIS programs, and RGB combinations were determined for further classification in order to select the areas of interest (soil types). At this stage, the RGB combination was selected:

- Red: (Band 11) SWIR – short-wave infrared channel;
- Green: (Band 8) VNIR – near infrared channel;
- Blue: (Band 2) BLUE – blue channel.

The shortwave infrared channel SWIR penetrates almost 80% of the atmosphere. SWIR measurements can help estimate how much water is present in soil and plants because water reflects SWIR light and can absorb near infrared waves. Therefore, thanks to the use of NIR and SWIR channels in the calculations, we can distinguish the contours of water bodies and moist soils.

3. In the next stage, Supervised Image Classification was carried out using the Maximum Likelihood Classification method and the additional Iso Cluster Unsupervised Classification method, which supplemented the data in small areas. The classification was made in order to select the following types of plots:
    a) water bodies (lakes, rivers, artificial reservoirs);
    b) wetlands (wetlands);
    c) forests and semi natural areas - (forests, trees, parks, nature reserves;
    d) agricultural areas (arable land and land permanently or periodically used and cultivated - gardens, fields, arable land);
    e) artificial surfaces.
4. In the final stage, smoothing was performed after classification with generalization and the use of filters: combined (Region drop up), majority (Majority filter), clear borders (border clean) and removal of too small areas. Next, analyses were carried out to describe the obtained results.

Obtained results

Using the methodology described above, it was possible to distinguish areas of the classified types of plots of interest within the catchment areas of the Bug, San and Dniester rivers, calculate their area and ratio as a percentage of the total area of the river basin district, identify the location of the areas with the greatest number of water bodies and wetlands and identify patterns and differences between river basins.

Results in the Dniester basin

As a result of mapping, after developing the RGB composite (11,8,2 band) in the Dniester basin (Figure 8), in accordance with the described method, it was possible to prepare the map (Figure 9) with water bodies, wetlands, forest and semi natural areas, agricultural areas and artificial surfaces.

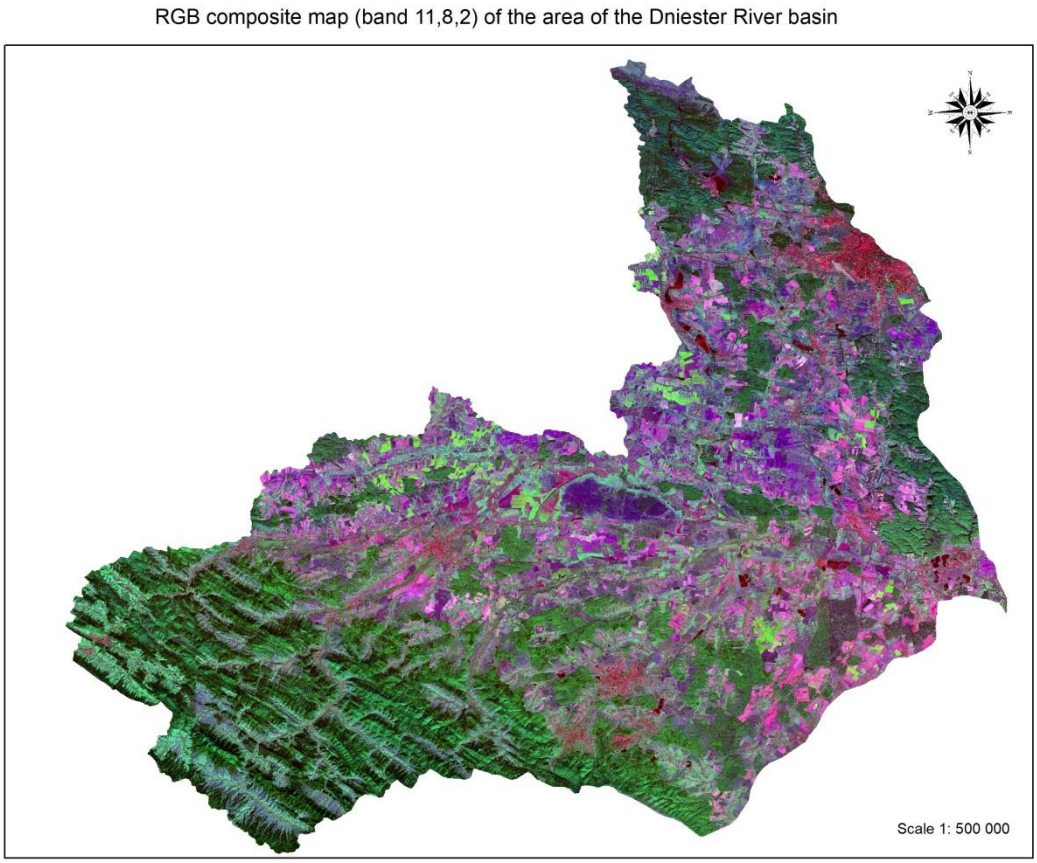

Figure 8. RGB composite (band 11,8,2) of the area of the Dniester River basin

The largest number of water bodies was found:

- near Ivano-Frankovo: Yanivskyi Stav with a number of smaller lakes and wetlands,
- near Horodek: Horodetsky lake and wetlands,
- near Otynevychi: Verenytsia River and Lake Otenevytskyi,
- Lake Karasivka, and
- lake near the town of Glynn.

The map clearly shows the mouth of the Dniester and Stryż and the run of Dniester in the south-eastern part of the basin. Wetlands are mainly found on the banks of rivers, lakes, depressions and ravines. In the south-western part of the catchment there is a minimal amount of water and wetlands, and the landscape is dominated by forests and semi natural areas (Figure 9).

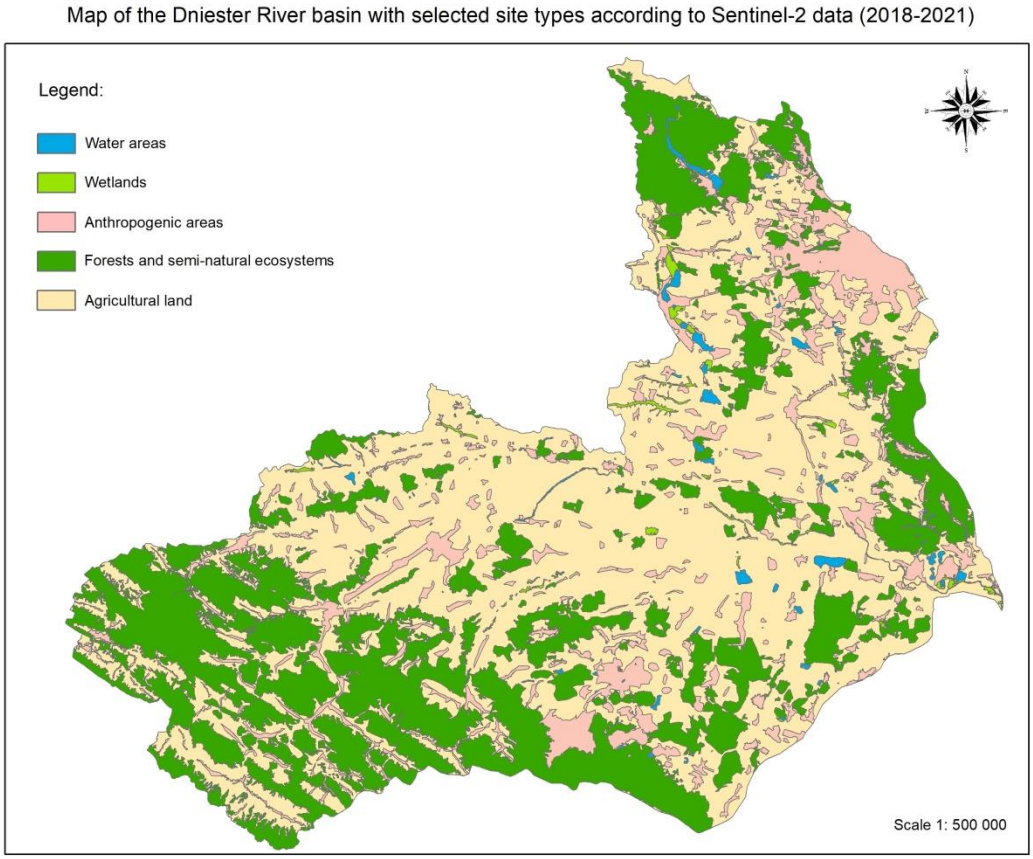

Figure 9. Map of the Dniester river basin with selected types of areas

The basin of the Dniester River occupies about 5919.55 km^2, the identified areas with water bodies occupy 54.23 km^2, and wetlands – 32.22 km^2, which is 0.92% and 0.54% of the entire area of the basin, respectively (Table 2).

Table 2 Ratio of classified site types to the total area for the Dniester river Basin

	Types of classified areas	km^2	(%)
1	Water bodies	54,23	0,92
2	Wetlands	32,22	0,54
3	Forests and semi natural areas	2002,44	33,83
4	Agricultural areas	3193,69	53,95
5	Artificial surfaces	636,97	10,76
Total area		5919,55	100

Description of results on the territory of the Bug river basin

The map of the Bug river basin with selected types of surface (areas) was created on the basis of the developed composite RGB map (band 11,8,2) (Figure 10) in the same area (Figure 11).

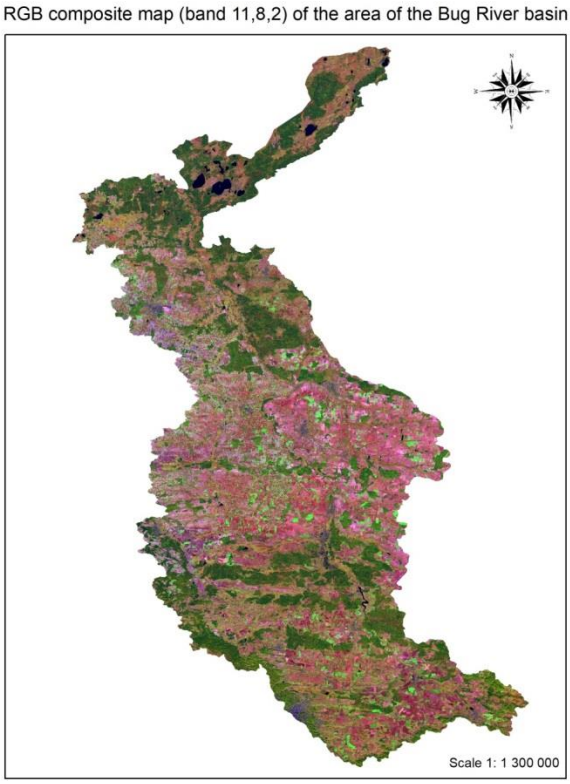

Figure 10. RGB composite (band 11,8,2) of the area of the Bug river basin

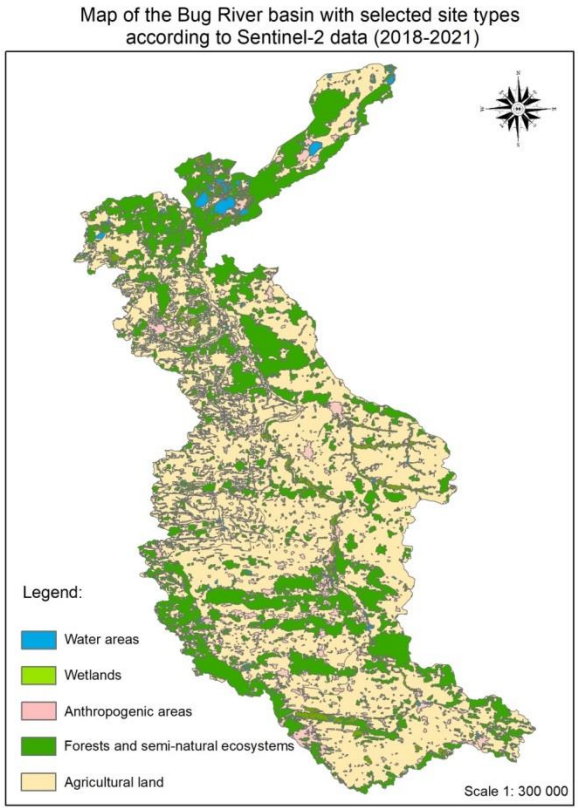

Figure 11. Map of the territory of the Bug river basin with selected types of areas

According to the obtained data, the Bug basin covers approximately 15,555.97 km^2, areas with water bodies cover ca. 157.95 km^2, and wetlands 435.77 km^2, which is approximately 1.02% and 2.8%, respectively (Table 3). Wetlands are mainly concentrated in river valleys and around lakes.

Table 3 The ratio of classified types of areas to the total area of the Bug River basin

Types of classified areas		km^2	%
1	Surface waters	157,95	1,02
2	Wetlands	435,77	2,8
3	Anthropogenically transformed areas	729,37	4,69
4	Forests and semi-natural ecosystems	4534,95	29,15
5	Arable (plowed) land	9697,93	62,34
Total area		15555,97	100

Almost 80% of the water bodies is located in the Shatsky National Nature Park of Ukraine in the northern part of the Bug basin. The Szackie Lakes are shown on the map (Figure 11): Svityaz Lake, Pulemetske Lake, Pisochne Lake, Chorne Velike Lake, Lyutsymer Lake, Ostrivyanske Lake, Prybich Lake, and Tur Lake.

Description of areas of the San River basin

As a result of mapping with the construction of RGB composite (band 11,8,2) and using the methodology for the territory of the San river basin (Figure 12), we received a map of the territory of the San river basin with selected types of areas (Figure 13).

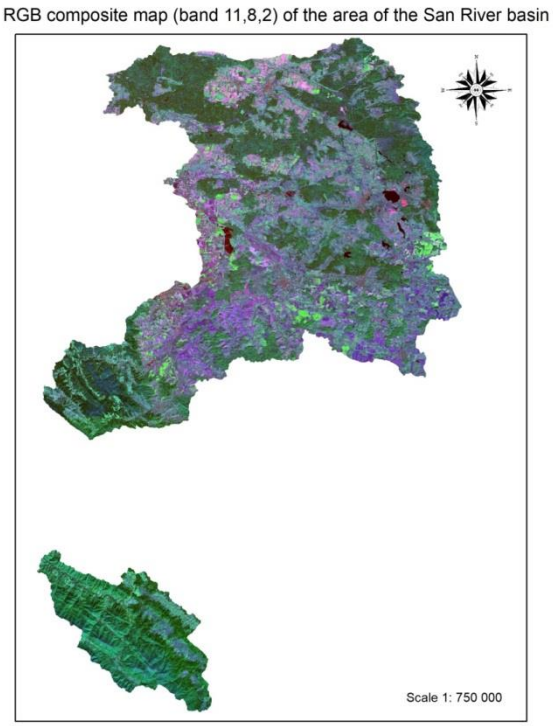

Figure 12. RGB composite (band 11,8,2) of the area of the San river basin

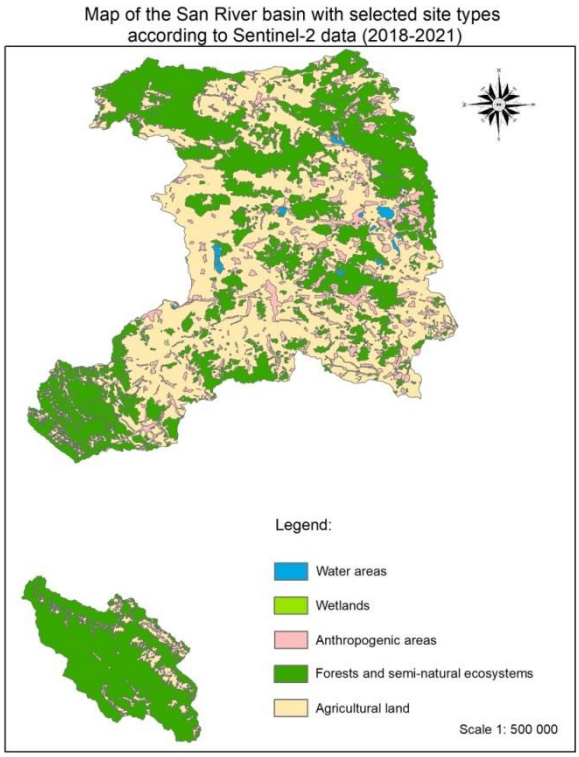

Figure 13. Map of the territory of the San river basin with selected types of sites

The predominant types of water bodies in the San river basin are lakes and reservoirs on both sides of the state border. On the Ukrainian side they are concentrated near the cities of Krakovets, Yavoriv and Hrushiv. On Polish side of the border lake Starzhava (Poland). Wetlands occupy only 0.66% and are concentrated mainly in ravines or river valleys.

The basin of the San river occupies ca. 4558.26 km^2, according to the obtained data, areas with an water bodies occupy 37.06 km^2, and wetlands – 30.03 km^2, which is about 0.81% and 0.66%, respectively (Table 4).

Table 4 The ratio of classified site types to the total area for the San river basin

Types of classified sites		square (km^2)	square (%)
1	Water bodies	37,06	0,81
2	Wetlands	30,03	0,66
3	Artificial surfaces	305,41	6,7
4	Forest and semi-natural areas	2085,21	45,75
5	Agricultural areas	2100,55	46,08
Total area		4558,26	100

Comparing the obtained statistics of the percentage ratio division of the basins of all three rivers, the following conclusions can be drawn (Table 5):

- The largest indicator of areas with water bodies was recorded within the Bug river basin, and it is 1.02% of the total area of the basin.
- The second place in terms of the area covered by water bodies is the Dniester river basin with an indicator of 0.92%.

- The lowest value of the indicator has been noted in the San basin and it equals to 0.81%.
- Wetlands are most abundant in the Bug river basin. They cover which is 2.8% of the area.
- The San river basin is in second place in terms of share of wetlands cover of the area with an index of 0.66%.
- The Dniester basin takes the third place in terms of share of wetlands cover of the area with an index of 0.54%.

There is a proportional regularity of the water surface in relation to agricultural areas, the greater the percentage of the water bodies, the greater the area of agricultural areas. The territory of the Bug river basin has the largest indicator of areas with a water bodies and wetlands.

Table 5 Comparison of areas of classified types of areas of the Bug, San and Dniester river basins

	Types of classified sites	Bug square (%)	Dniester square (%)	San square (%)
1	Water bodies	1,02	0,92	0,81
2	Wetlands	2,8	0,54	0,66
3	Artificial surfaces	4,69	10,76	6,7
4	Forest and semi-natural ecosystems	29,15	33,83	45,75
5	Agricultural areas	62,34	53,95	46,08

Description of the results for the modelling area

The analysed area is under the influence of the Bug and San rivers, the basins of which cover the areas of 3368.34 km^2 and 3526.31 km^2, which make up approximately 50% of the total area (7108.55 km^2) of the simulation (Figure 13). Within the modelling area, an RGB composite was constructed (Figure 14) and a map of the territory with classified types of areas was obtained (Figure 15).

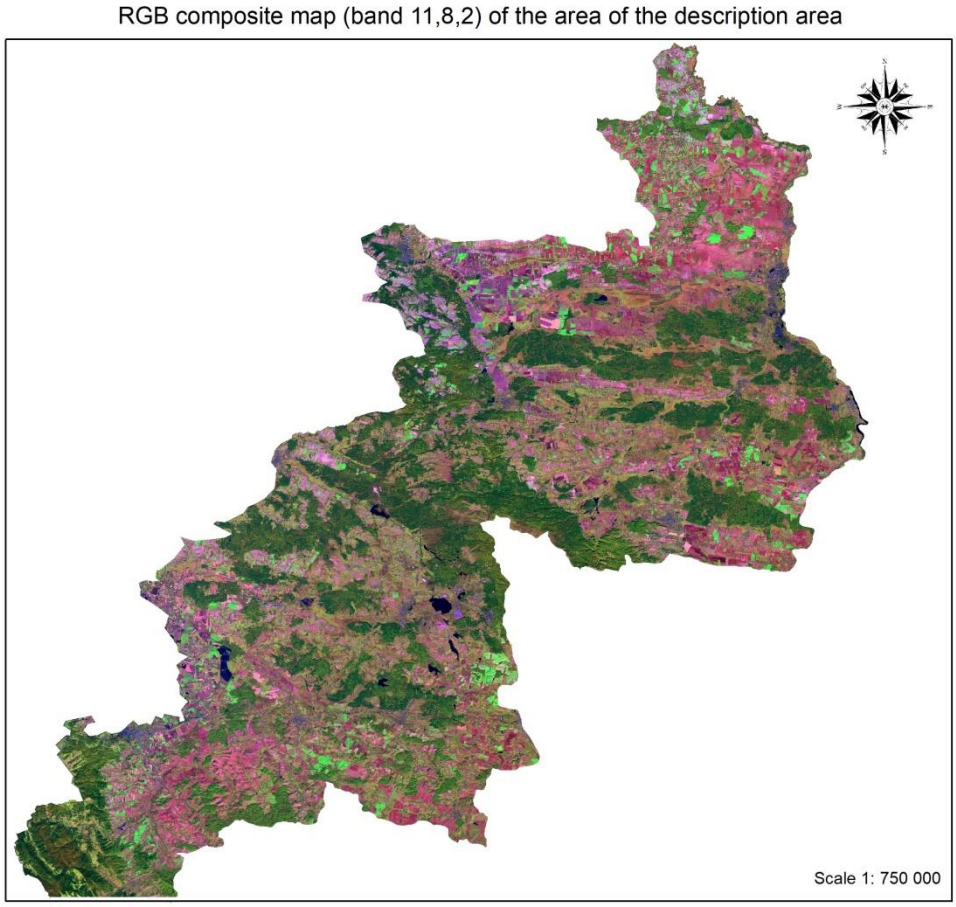

Figure 14. RGB composite (band 11,8,2) of the simulation area

The water bodies that are the most significant in the San basin are: Dobrotvyriv reservoir, Lake Yavorivske More, Lake Oselya, Hrushivskie reservoir a number of nameless lakes near Mageriv, Ugniv, Kornie.

Wetlands cover only 0.66% and are concentrated mainly in ravines or river valleys, near lakes. The largest number of the wetlands is concentrated in the valley of the Western Bug river near the city of Chervonograd and near the Nature Reserve Starzawa (Poland) and water reservoirs in Krakowiec and Hrushiv (Ukraine).

RGB composite map (band 11,8,2) of the area of the description area

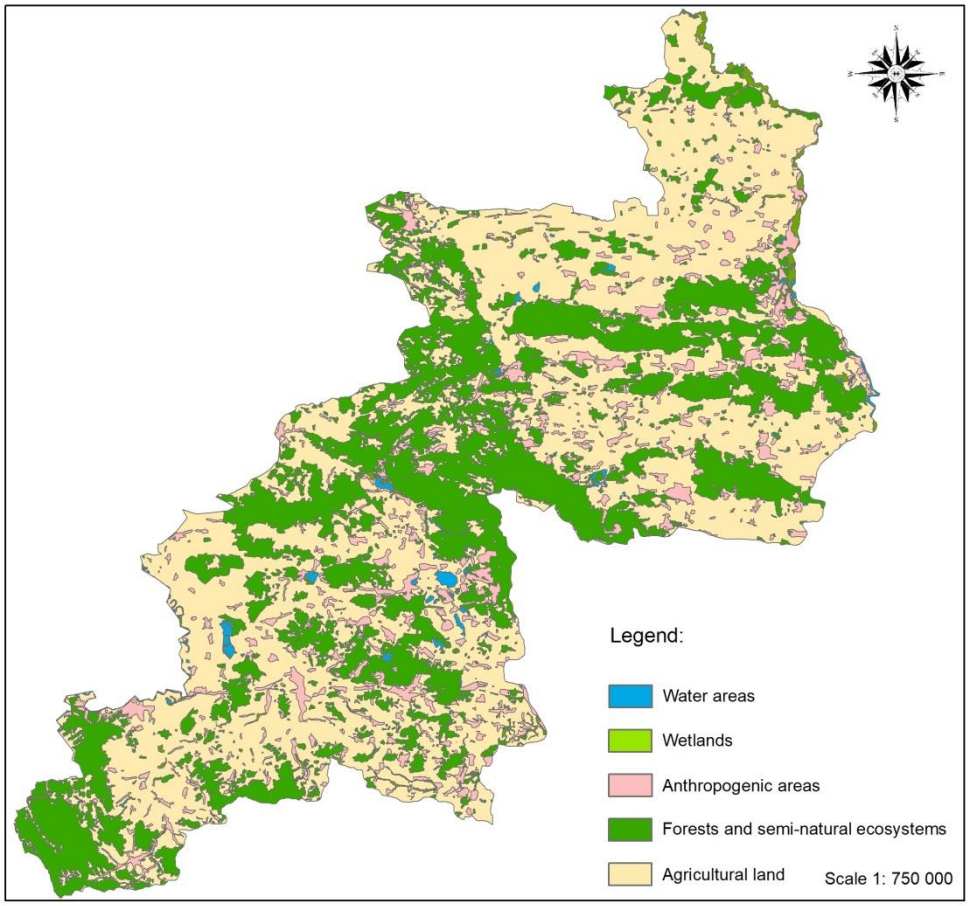

Figure 15. Map of the modelling area with selected site types

Areas of water bodies make up 0.78% while wetlands cover 1.11% of the area. More than half of the area (55.88%) is occupied by agricultural areas, more than a third of the area (34.51%) is occupied by forests and semi natural areas. Artificial surfaces make up almost 8% of the entire study area (Table 6).

Table 6 The ratio of classified types of plots to the total area of simulation

	Types of classified sites	square (km^2)	square (%)
1	Water bodies	55,07	0,78
2	Wetlands	78,7	1,11
3	Artificial surfaces	548,75	7,72
4	Forest and semi natural areas	2453,62	34, 51
5	Agricultural areas	3972,41	55,88
Total area		7108,55	100

The obtained data have a slight error. Small areas of arable land located in the middle of the settlement can be identified as areas of anthropogenic activity, but they have a small area and do not significantly affect the result. Waterlogged territories (swamp areas) do not always have clear boundaries and change depending on the season, in the summer during the drought there is a decrease in the area of swamps, and in spring and autumn, on the contrary, an increase (monitoring was carried out in the dry season – autumn). The boundaries of forests have the ability to change, it depends, in particular, on the felling and

development of the forest fund associated with the expansion of cities and the increase of urbanization in general. Therefore, to update data on changes in water bodies, it is necessary to carry out monitoring with a certain frequency (every year).

2. Transboundary groundwater flow model

2.1 Model structure

For the purposes of numerical calculations of the filtration field, a section of the hydrogeological space designated by the boundary surface described in Polish-Ukrainian pilot area characterization was separated / defined. This area was entered / placed / introduced into a rectangular frame of the model with sides parallel to the axis of the national geographical coordinate system PUWG 1992. Therefore, the location of the calculation area in geographical space can be uniquely described by the coordinates of the opposite corners of the frame expressed in this system ((x1: 754500 m; y1: 190000 m), (x2: 886500; y2: 330000)). The model frame represents a rectangular area of 132 x 140 km. The area was divided into computational blocks using a fixed step of discretization $\Delta x = \Delta y = 500$ m. Thanks to this procedure, a discretization grid consisting of 264 columns and 280 rows was created, which gave a total of 73,920 calculation blocks. Then, blocks located outside of the previously described boundary surface were excluded from the calculations, treated as inactive, and the calculation space was divided into two layers. After this procedure, each of the distinguished numerical layers consisted of 28,768 active blocks.

The next stage of work consisted of adapting the calculation area to the adopted model of the conceptual aquifer system. According to this model, in the area of the Carpathians, the upper layer of the model should represent a continuous aquifer within fractured flysch rocks occurring in the near-surface zone. The deeper parts of the system within the fold are represented by the second layer of the model. Since the water permeability of the medium within the flysch rocks decreases rapidly with depth, the blocks in the second layer of the model in the Carpathian area were excluded from the calculations.

In the Carpathian Foredeep, the upper layer of the model mainly represents the Quaternary aquifer. In river valleys, this layer imitates aquifers developed within well-permeable sand and gravel alluviums. In the uplands, the first layer of the model represents the aquifer created as a result of aggregation of inter-moraine levels of varying thickness and spread. At the bottom of the Quaternary layer / strata there are usually very poorly permeable Kraków clays, which is why the blocks in the second layer were excluded from the calculations here as well.

In the area of the Lublin Basin, the aquifer is associated mainly with the Upper Cretaceous carbonate rocks and is generally characterized by good water permeability throughout the active exchange zone. It is estimated that the thickness of this zone may reach 120 m and this value was used in the calculations. In the area of the Lublin Basin, the computational blocks in both layers were left active, which made it possible to take into account the spatial nature of the groundwater stream and the water permeability of the medium, which decreases with depth, in the calculations.

The practical implementation of the system schematization method described above required mapping the surface of the top and bottom of the individual numerical layers of the model.

The upper boundary surface of the model was related to the terrain surface and the SRTM-3 digital terrain model was used for this purpose (Figure 3).

In order to map the bottom surface of the lower layer, a spatial analysis was carried out, in which a raster information layer representing the spatial distribution of the piezometric level of groundwater table in the tested system was used. This layer was prepared by a team of employees of the PGI-NRI on the basis of data on the ordinate of the groundwater table obtained from 811 wells. Then, using algorithms in the field of map algebra, the course of the bottom surface was interpreted (**Błąd! Nie można odnaleźć źródła odwołania.**), which would meet the following boundary conditions:

- in the area of the Carpathian Fold, the surface is to represent the zone of occurrence of cracked flysch rocks, reaching a maximum of 30 m below the surface of the water table,
- in the area of the Carpathian Foredeep, the surface should represent the course of the bottom of the Quaternary aquifer, the thickness of which should not exceed 25 m in uplands and 35 m in river valleys,
- in the area of the Lublin Basin, the surface should correspond to the range of occurrence of the most fractured carbonate rocks, which was assumed *a priori* at a depth of 30 m.

The bottom surface of the lower layer of the model in the area of the Lublin Cretaceous Basin was established at a depth of 120 m below the surface of the groundwater table, which corresponds to the average depth range of the permeable zone within the Upper Cretaceous formations.

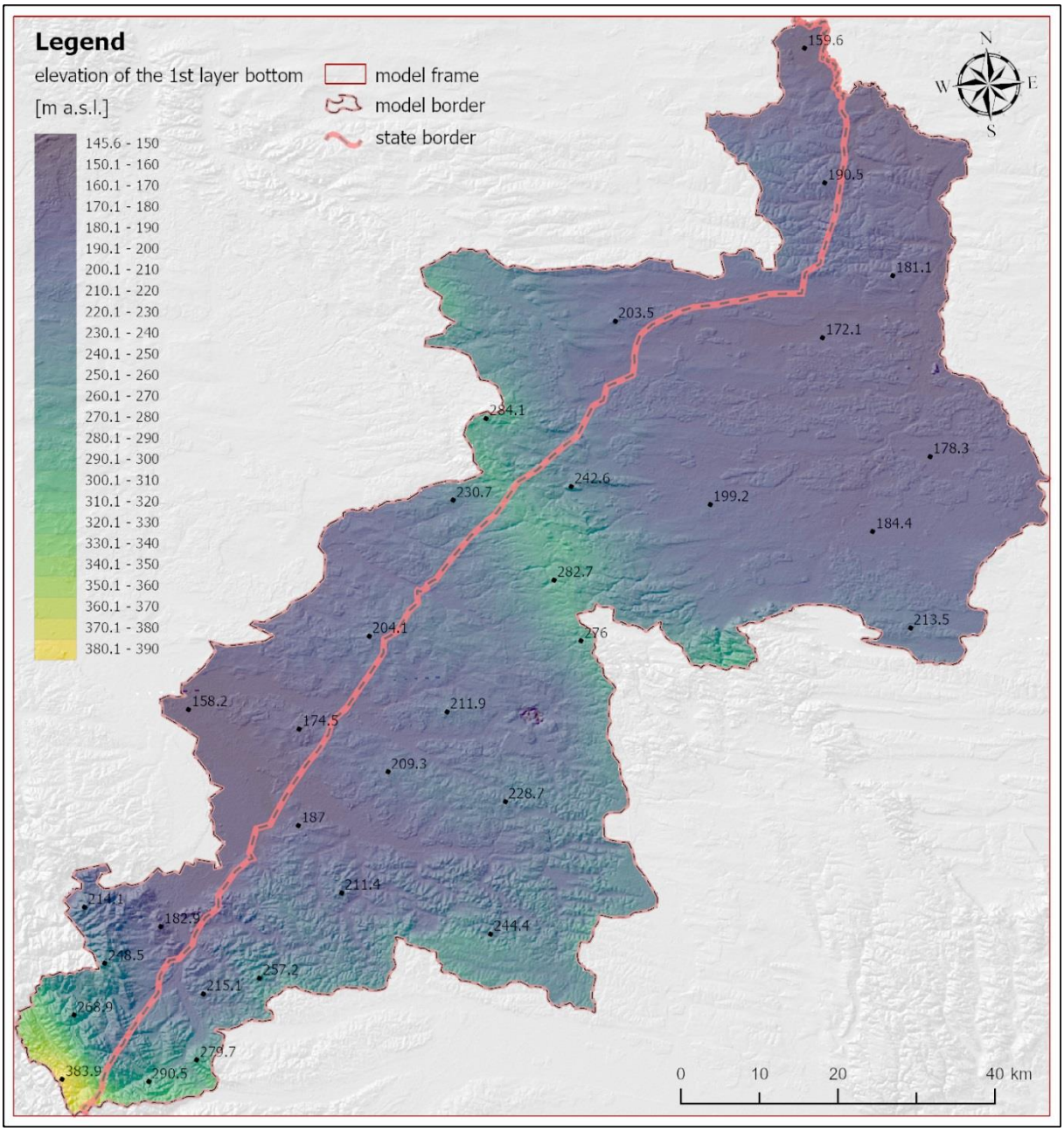

Figure 16. Distribution of the ordinate of the bottom of the first layer of the model against the morphology of the area

The variable water permeability of the medium was represented by a table of numbers representing the spatial distribution of the filtration coefficient values. Initially, the highest values of this parameter were assigned to points representing valley units filled with well-permeable alluvial deposits and upper parts of carbonate rocks of the Lublin Cretaceous Basin. Slightly lower parameter values were assumed for the Quaternary strata in areas occupied by post-glacial plateaus. An order of magnitude lower values of the filtration coefficient were assigned to the points representing the deposits developed within the Carpathian flysch and to the deeper parts of the system in the area of the Lublin Basin. The final distribution of the filtration coefficient values (Figure 17) was obtained at the model tarring stage.

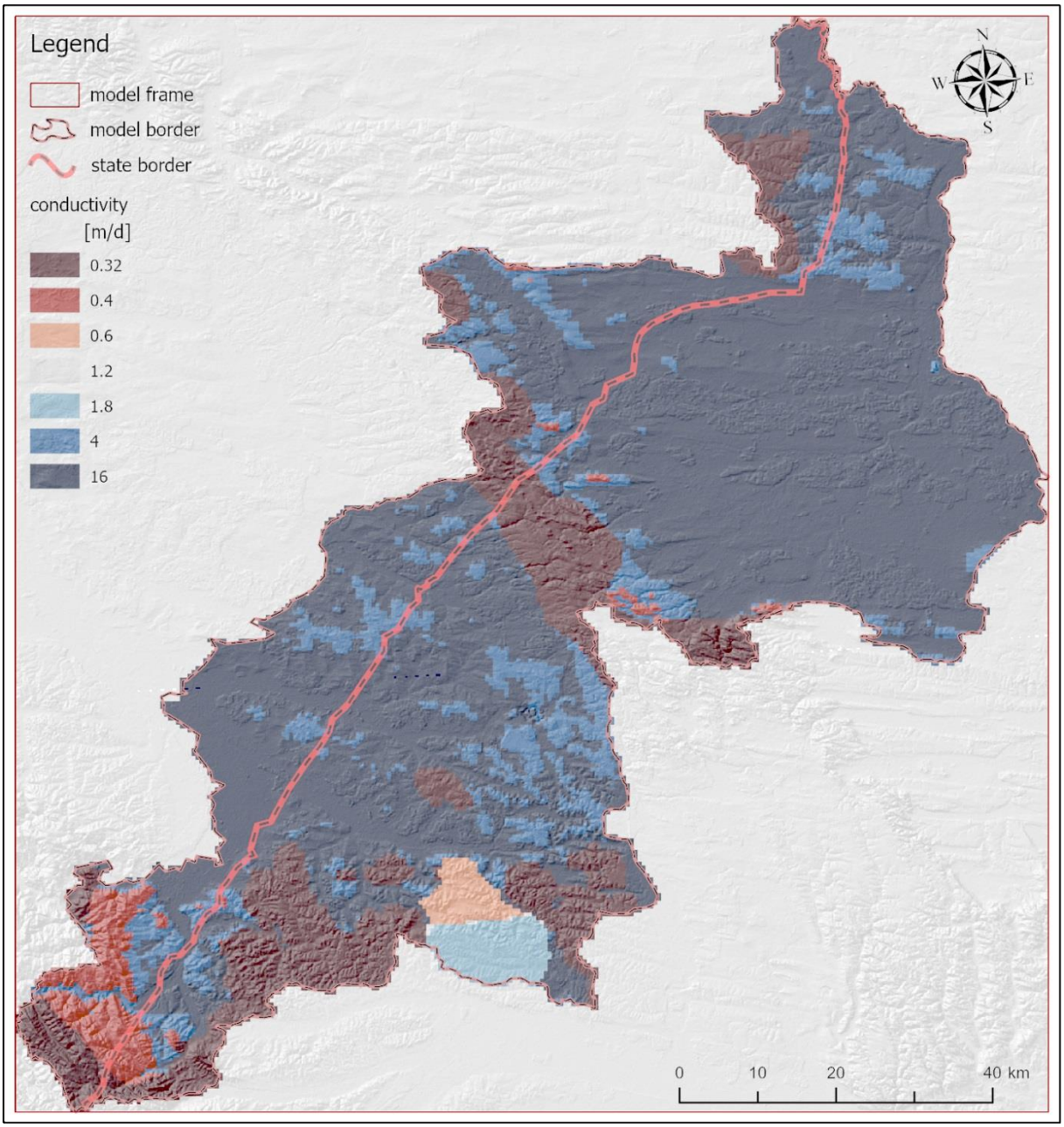

Figure 17. Distribution of the filtration coefficient in the first layer of the model

2.2 Boundary conditions

The boundaries of the model study area presented in Polish-Ukrainian pilot area characterization indicate the course of the outer boundary surface of the separated aquifer system. This surface separates the modelled system from the environment, and its character can only be locally and temporarily closed. This means that the system creates specific relations and couplings with the environment through the boundary surface. These relationships can be described by the water flow rate between the system and the environment. The amount of water exchange considered in the direction normal to the edge surface depends on the parameters and condition of the system in the vicinity of this surface. The internal state of the system in the vicinity of the boundary surface must be taken into account in a special way when assigning boundary conditions to the boundary surface. This

is due to the fact that a given type of boundary condition can describe the relationship of the system with the environment with a good approximation only under certain internal states of the system. This problem was particularly evident in the case of the considered aquifer system, the boundary surface of which was largely determined along morphological watersheds. This was intended to allow the application of the zero flow condition to this surface (a special case of the Neumann condition where the flow along the direction normal to the boundary is equal to zero). Such an approach would be justified only if the course of the underground watersheds fully corresponded to the course of the morphological watersheds, and the hydrodynamic state of the system in all variants of the calculations remained unchanged. In the case under consideration, none of the above conditions was met. In practice, this means that the application of the zero-flow condition in relation to the watershed zones did not allow for the inclusion of the lateral groundwater inflow in the water balance. Even worse, the zero-flow condition did not allow for the change of the nature of the boundary surface from closed to open during the simulation of intensive groundwater abstraction. In this situation, it was decided to assign the conditions of type III to the outer boundary surface of the system, with the General Head condition applied to the sections of the border related to the watershed zones, and the River condition applied to the sections along the riverbeds (Figure 18). This solution made it possible to take into account both, the state and parameters of the system in the vicinity of the boundary surface in the calculations. In addition, it was possible to take into account the variable nature of the surface during the groundwater abstraction simulation and to quantify the groundwater inflow through the boundary surface.

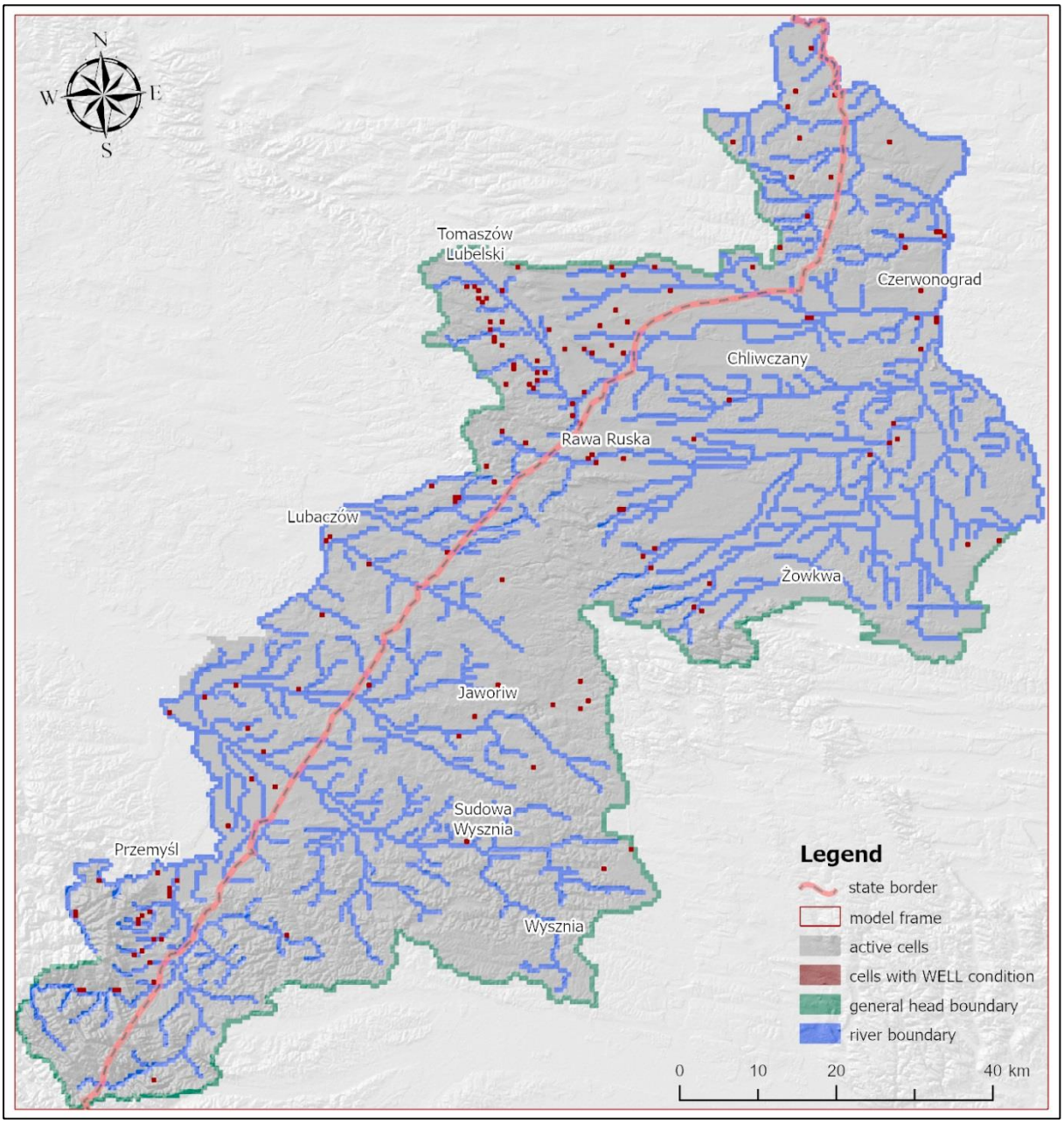

Figure 18. Types of boundary conditions used in the first layer of the model

General Head Condition

The *General Head* condition is one of the variants of the III type condition offered by the Modflow program. It is based on the equation describing the flow of water from the environment of the system (external source) to a point in space (block) belonging to the boundary surface:

$$Q_{bi,j,k} = C_{bi,j,k}\left(h_{bi,j,k} - h_{i,j,k}\right),$$

where $Q_{bi,j,k}$ means inflow to the block *i,j,k* from an external source, and $C_{bi,j,k}$ is the hydraulic conductivity between the block and the external source. In this equation, the inflow to block *i,j,k* from an external source is proportional to the difference of the hydraulic head assigned

to the boundary surface $h_{bi,j,k}$ and the hydraulic head in block $h_{i,j,k}$. The direction of water exchange depends on the difference in surface of the piezometric pressure of the groundwater table between the block and the external source.

The *General Head* condition was applied to sections of the outer boundary surface that corresponded to the course of surface watersheds. To formulate the condition, it was necessary to determine the state of the system surrounded by the boundary surface. For this purpose, a map of hydroisohips prepared by a team of employees of the PGI-NRI was used on the basis of archival information about the ordinate of the water table in the wells. This information was saved in the form of a vector linear layer, and then processed into a raster GIS information layer using the thin plate interpolation method. On this basis, it was possible to obtain information about the state of the system at a predetermined distance Δ*L* (1000 m) counting outwards from the boundary surface. The values of the groundwater table ordinate obtained in this way were then assigned to all points of the boundary surface representing the watershed zones (Figure 19).

The General Head condition required additional conductivity values to be assigned to the boundary surface using the $C_{bi,j,k}$ parameter. The following formula was used to determine the conductivity value:

$$C_{bi,j,k} = \frac{k_{sr} \cdot A}{\Delta L},$$

where k_{sr} is the average value of the filtration coefficient over an elongated section of the stream, *A* is the surface of the block perpendicular to the flow direction, and ΔL describes the distance by which the groundwater stream has been extended. The values of the filtration coefficient were obtained from the map of the spatial distribution of this parameter prepared for the purposes of calculations by a team of PGI-NRI employees. The ΔL value corresponded to the assumed value of elongation of the groundwater stream, and the surface area A resulted directly from the geometry of the calculation blocks in the space discretization scheme adopted for the calculations (see: Groundwater abstraction). The value of the parameter $C_{bi,j,k}$ calculated in this way was modified at the stage of taring the model.

In the area of the Carpathian Fold and the Carpathian Foredeep, the GHB condition was assigned only to the highest layer of the model. This was due to the fact that the blocks of the second layer in the area of these units represent a very poorly permeable medium and were excluded from the calculations. On the other hand, in the case of the Lublin Basin, the condition was set in both layers of the model, which guaranteed that the flow through the boundary surface was taken into account in the calculations of both the shallow and deep parts of the system.

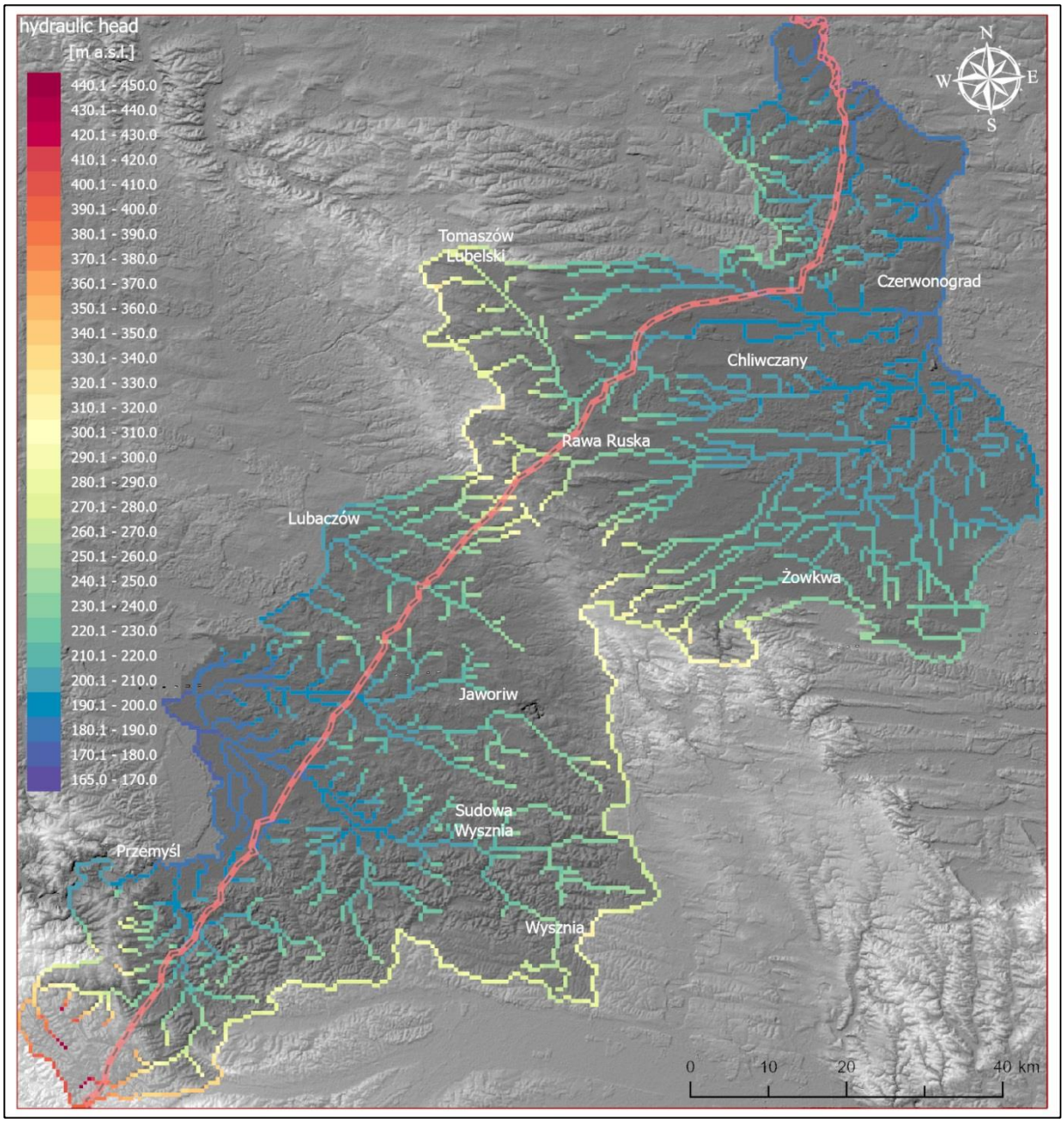

Figure 19. The values of the groundwater table elevation assigned to the blocks with the III type condition

River condition

The River condition is mathematically similar to the General Head one. The difference is in the introduction of additional restrictions and a different methodology for estimating the conductivity parameter $C_{bi,j,k}$, which is intended to correctly describe the relationship between the aquifer system and surface watercourses. Condition of the third type was applied both to surface watercourses on the outer boundary surface and to watercourses inside the modelled area (Figure 18). By using the River condition, it was possible to include the filtration resistance of the river bed in the calculations. This resistance results from the colmatation of the near-channel zone and the incompleteness of the channel and can be expressed by the value of the conductivity parameter $C_{bi,j,k}$. This value can be estimated on the basis of the thickness M and water permeability K of the bottom sediment layer:

$$C_{bi,j,k} = \frac{KLW}{M},$$

where L is the length of the river section in the block, and W is the average channel width in the block. In practice, both the water permeability of bottom sediments and their thickness are usually unknown, and the value of the $C_{bi,j,k}$ parameter is selected by trial and error at the model calibration stage. This methodology was also adopted in the described model studies.

The River type condition allows one to simulate a situation in which the groundwater table has been lowered below the bottom of the river bed (the so-called "detachment" of the water table from the river bed). In practice, this means that this condition requires the determination of two variables relating to the state function: the ordinate of the water table in the river $H_{Ri,j,k}$ and the ordinate of the bottom of the river bed R_{dna}. The $H_{Ri,j,k}$ variable was interpreted on the basis of the ordinates obtained from the SRTM-3 model. For this purpose, procedures in the field of spatial statistics implemented in the GIS environment were used. The first stage of the applied procedure consisted of identifying all computational blocks through which surface water flows. This task was accomplished by a simple intersection of vector layers representing the computational blocks and the river network of the area. This procedure returned a set of blocks in which the condition of the III type should be set. Then, within each of these blocks, a subset of the SRTM-3 layer raster containing therein could be determined. Finally, from the subset of raster in each block, the one with the lowest value of the terrain elevation was selected, and this value was assigned to the HRi,j,k variable (Figure 19).

In turn, the R_{dna} value was calculated on the basis of $H_{Ri,j,k}$ and the assumed (constant for a given watercourse) depth value. Water exchange between the aquifer system and the environment via the River condition was calculated as:

$$Q_{bi,j,k} = C_{bi,j,k}(H_{Ri,j,k} - h_{i,j,k}), \qquad \text{when } h_{i,j,k} > R_{dna},$$

$$Q_{bi,j,k} = C_{bi,j,k}(H_{Ri,j,k} - R_{dna}), \qquad \text{when } h_{i,j,k} \leq R_{dna}.$$

The River type condition was set only in the first layer of the model. It was used to map the impact of all the main watercourses forming the hydrographic network of the area on groundwater.

To describe the relationship of the separated aquifer with the environment, in addition to the conditions of the III type, the conditions of the II type were also used. This condition was used to map the groundwater intake, infiltration recharge of the system and the relationship with the environment on selected sections of the outer border surface. Various variants of the Type II condition offered by the Modflow software were used for this purpose, and these were the Well condition, the Recharge condition and the zero flow condition, respectively.

Well condition

The Well condition makes it possible to take into account water intake and injection through wells in the calculations. It consists of assigning the value of the outflow expressed in a unit of volume per unit of time to a point or points of discrete space contained in the well filter interval. Assigning a positive extraction value is synonymous with injection (absorbing well),

and a negative value with groundwater extraction. The condition also allows to simulate the operation of a well intaking more than one aquifer / water bearing horizon. However, this requires that each of the recognized levels is represented in the model by a separate layer. In such a situation (after indicating which levels are included), the total discharge of such a well is divided into individual layers in proportion to their water conductivity.

In case of the described model, the Well condition was first used to map the registered groundwater intake. For this purpose, the available information on the volume of extraction on both sides of the state border was used. The data concerned both intakes securing water to the municipal supply system and industrial installations. During data collection, a clear disproportion of information available in the Polish and Ukrainian parts of the area was found. While in Poland it was possible to obtain data also for small intakes (with a capacity of less than 100 m^3/d), in Ukraine the available data concerned primarily the largest intakes (with a capacity of over 1000 m^3/d).

As a result, the spatial distribution of extraction mapped on the model is clearly uneven (Figure 20). However, this does not result from the density of the settlement network and the demand for water, but from the different legal conditions in both countries determining the management of information on the volume of abstraction. Based solely on official data on abstraction, the model included the 112 intakes, the total capacity of which was 46,024.5 m^3/d, of which 25,670 m^3/d was assigned to layer I of the model, and 20,354.5 m^3/d to layer II.

The issue of unregistered extraction required a separate approach. This problem, although with different intensity, occurs on both sides of the border and should be taken into account in the calculations so that the result can be considered reliable. This issue is discussed in more detail in Groundwater abstraction.

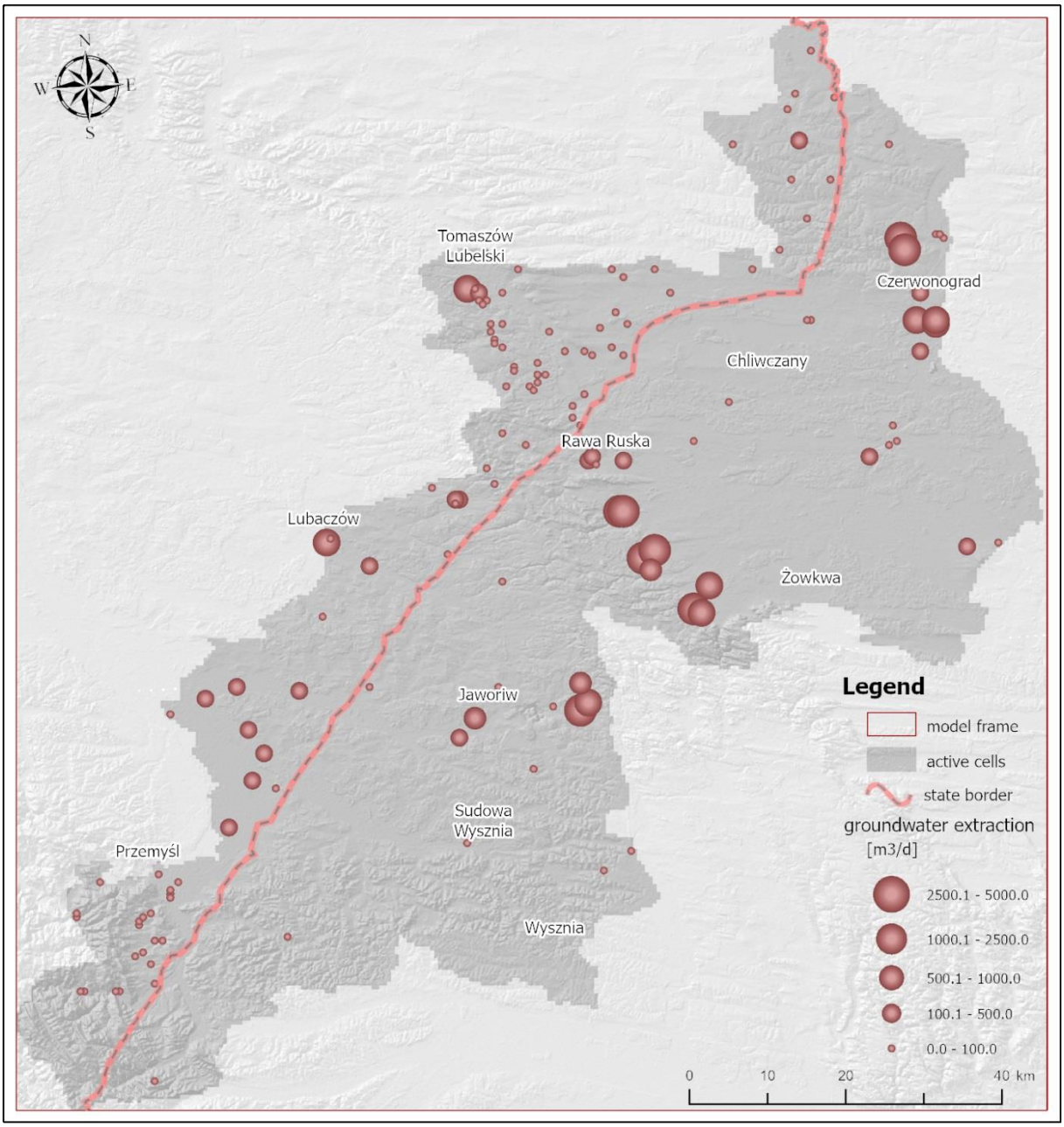

Figure 20. Spatial distribution of registered groundwater abstraction mapped in the model using the Well condition.

Recharge condition

The Recharge condition was developed to simulate the spatial distribution of the recharge of an aquifer system. The infiltration rate $Q_{Ri,j}$ is calculated as the product of the effective infiltration rate $I_{Ei,j}$ and the area of the calculation block:

$$Q_{Ri,j} = I_{Ei,j} \cdot \Delta X \Delta Y$$

where Δx and Δy stand for the size of the space discretization step taken along the X and Y axes, respectively. The application of the Recharge condition required the preparation of a data table representing the spatial distribution of effective infiltration intensity. This table was developed by a team of PGI-NRI employees participating in the project. The main criterion

differentiating the spatial distribution of the recharge was the lithological formation and the related water permeability of the formations of the near-surface zone. The total amount of the system's renewable resources was assessed on the basis of the analysis of flow hydrographs in selected sections of water gauges. Then, this quantity was distributed in space using the constant-volume transformation and the GIS information layer representing the water permeability of formations in the near-surface zone.

Zero flow condition

This condition was applied in the lower layer of the model in the section of the boundary surface corresponding to the course of the Bug river bed. This measure was used to imitate the character of the river, which is the main drainage base for the regional groundwater circulation system. In this context, the application of the zero flow condition must be considered together with the River type condition, which was set in the upper layer of the model on the analogous section of the boundary. By this solution, it was possible to imitate the hydrodynamic situation in the model in which the Bug is draining and fully penetrating in relation to the considered system. This made it possible to take into account the spatial nature of the groundwater stream in the vicinity of the riverbed in the calculations, i.e. it allowed to map the vertical component of the movement under the riverbed. At the same time, leaving the boundary closed in the second layer is consistent with the hypothesis of hindered transfer of hydrodynamic impacts under the bottom of a large river under conditions of its good hydraulic connection with the aquifer.

2.3 Calibration of the model

After determining the internal structure of the system and setting the boundary conditions, it was possible to formulate a system of linear equations, which was solved using an iterative procedure. The initial result of the calculations was the spatial distribution of the hydraulic head, which could be compared with the set of empirical data describing the position of the groundwater table. For this purpose, archival measurements of the groundwater table ordinate in 811 wells were used, of which 376 were representative of the first layer and 435 of the second layer. The spatial distribution of these points is shown in Figure 21. At each point, it was possible to calculate the error value as the difference between the calculated and measured state. The distribution of the model's error values and its numerical parameters were the measures of adjustment to the modelled reality and could be controlled at every stage of work related to taring the model. The model tarring procedure consisted of selecting a set of system parameters that would minimize the difference between the calculated and measured state. For this purpose, the method of successive approximations was used, where the control parameters were primarily the filtration coefficient assigned to the numerical layers of the model and the conductivity parameter assigned to the calculation blocks with the condition of the third type.

The tarring procedure was stopped after achieving a match expressed by the value of the mean error and the mean absolute error at the level of -3.17 m and 4.96 m, respectively. It was considered that the achieved fit is sufficient in view of the regional nature of the calculations, their resolution (500x500 m blocks) and the scale of the applied simplifications. The distribution of modelling residuals obtained at this level of fit is close to the normal distribution with the parameters μ=-3.17 m and σ=6.15 m (Figure 22). In the obtained

empirical distribution, the residuals are grouped mainly in the range -4.16 – 4.76 m (519 out of 811 points, which is 64% of the population of results). In the fit plot of the calculated values to the measured values (Figure 23), the points are grouped around a straight line with a slope equal to 1, and the value of the coefficient of determination R2 is 0.96. The obtained error values indicate that the developed model of the filtration field, despite the adopted simplifications, is a good approximation of the considered aquifer system, and after verification can be the basis for the calculation of the groundwater flow balance. The result of the calculations provides the basis not only for the description of the current hydrodynamic state, but it can also be used to simulate the behaviour of the system with the intensification of groundwater abstraction.

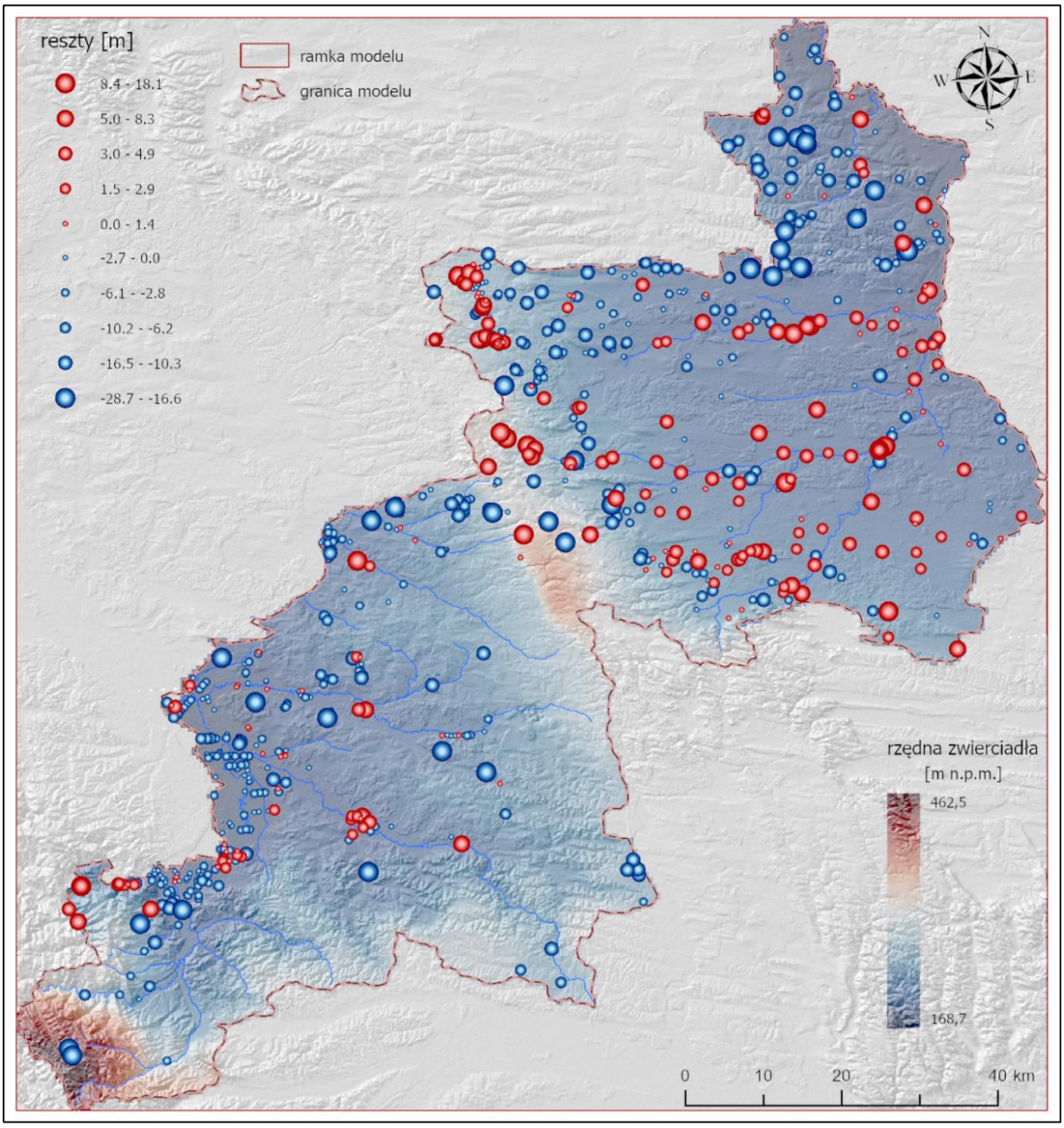

Figure 21. Spatial distribution of the model error against the background of the calculated state of the system

The calculation result obtained for the current hydrodynamic state is consistent with the adopted model of the water circulation in the tested system. The highest calculated ordinates

of the groundwater table exceed 450 m above sea level and concentrate on the morphologically elevated area of the Carpathian overthrust (Figure 24). In the San and Bug valleys, which are the main axes of groundwater drainage in the studied system, the ordinates of the water table go below the value of 180 m above sea level. In the area of the Lublin - Lviv Plain, a clear watershed zone is formed between the underground catchment of the Bug and the catchment of the San, and the elevation of the groundwater table locally exceeds 340 m above sea level. The beds of smaller rivers form local drainage zones, and in upland areas, lower-order watershed zones are clearly marked.

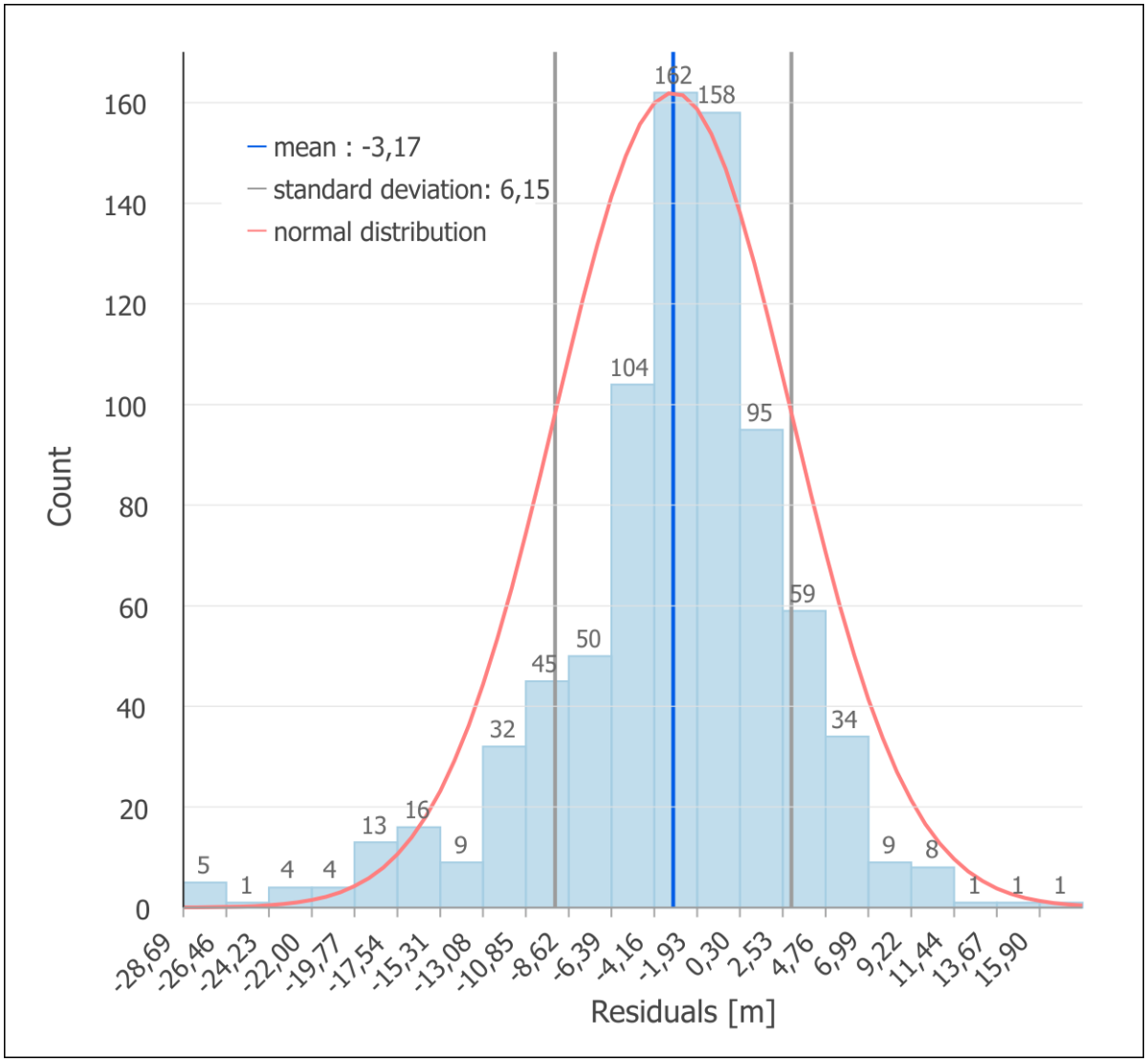

Figure 22. Distribution of residuals against a normal distribution

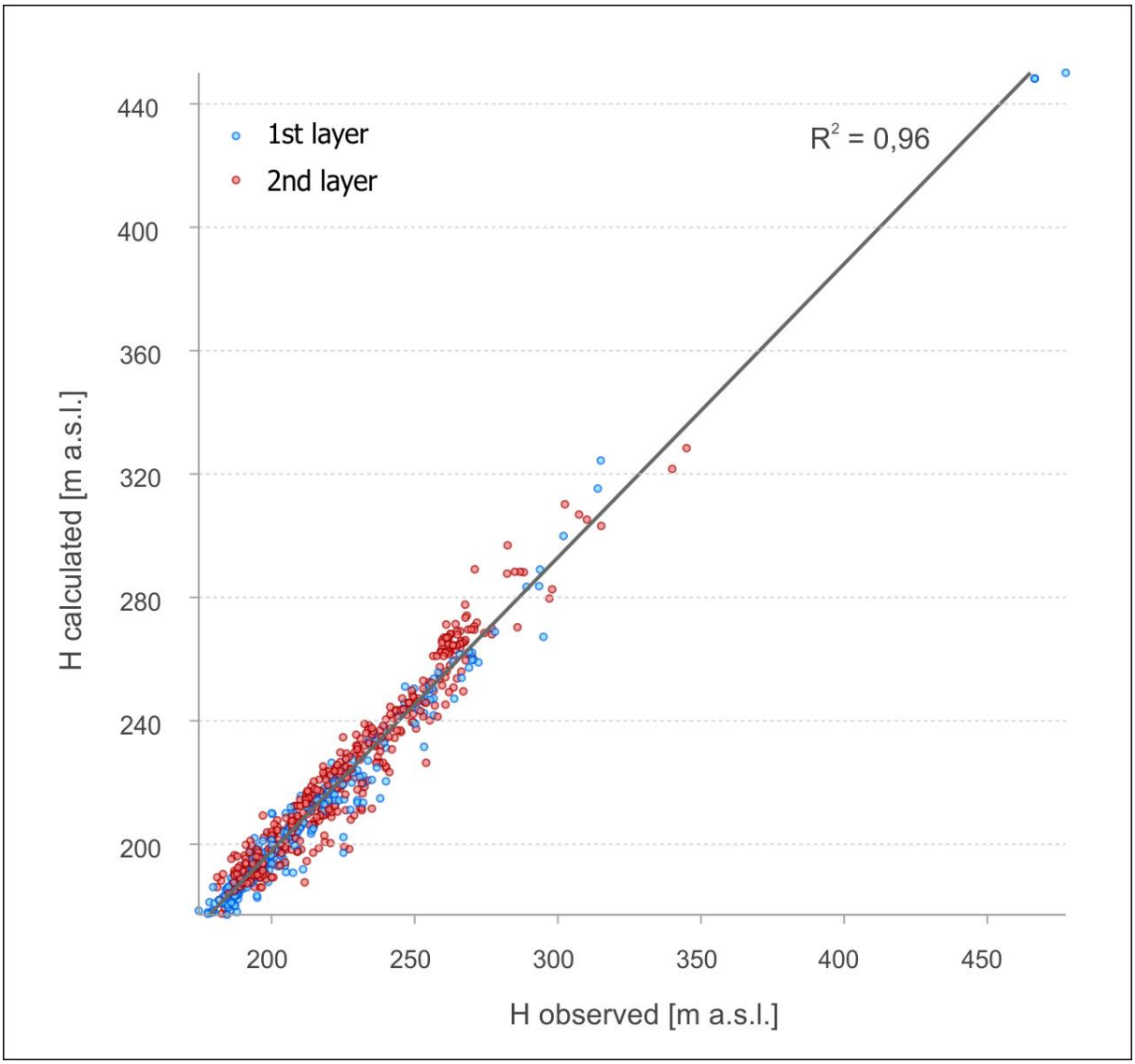

Figure 23. Fitting curve between measured and calculated values

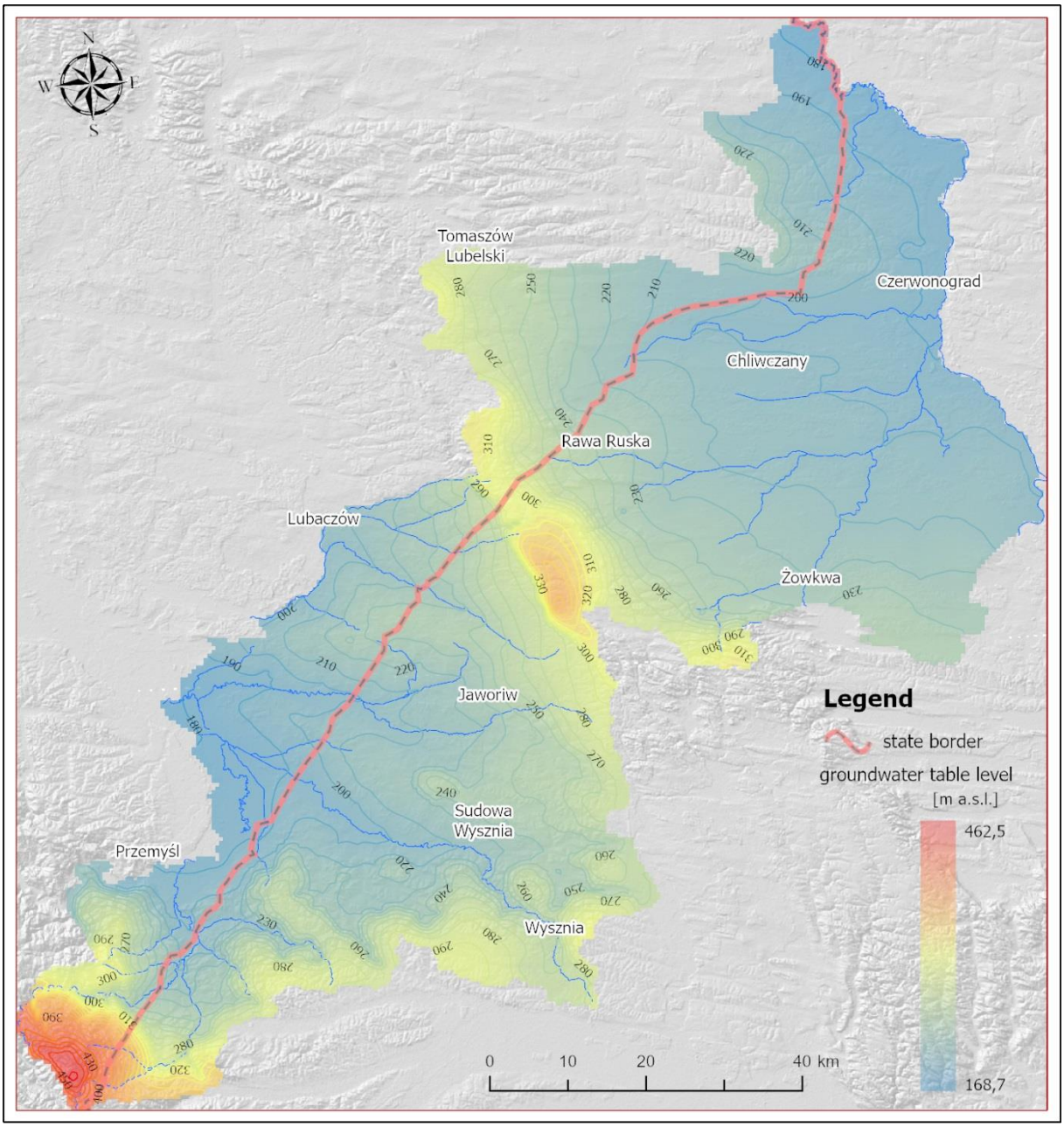

Figure 24. Calculated system state (first layer of the model)

3. Groundwater abstraction

3.1 Characteristics of registered groundwater abstraction

The exploitation of groundwater in the research area in the currently functioning intakes (1128 intakes) concerns mainly K2 aquifer or combined Q_{al}-K_2 (70% intakes), the other aquifers are Q_{al}, N_1, Q_{al}-N_1. The average daily intensity of groundwater exploitation in 2018-2020 is at the level of 53,984 m^3/d, of which 80% is in Ukraine. Spatial diversification of the volume of exploitation at the average level from the last 3 years is shown in Figure 25.

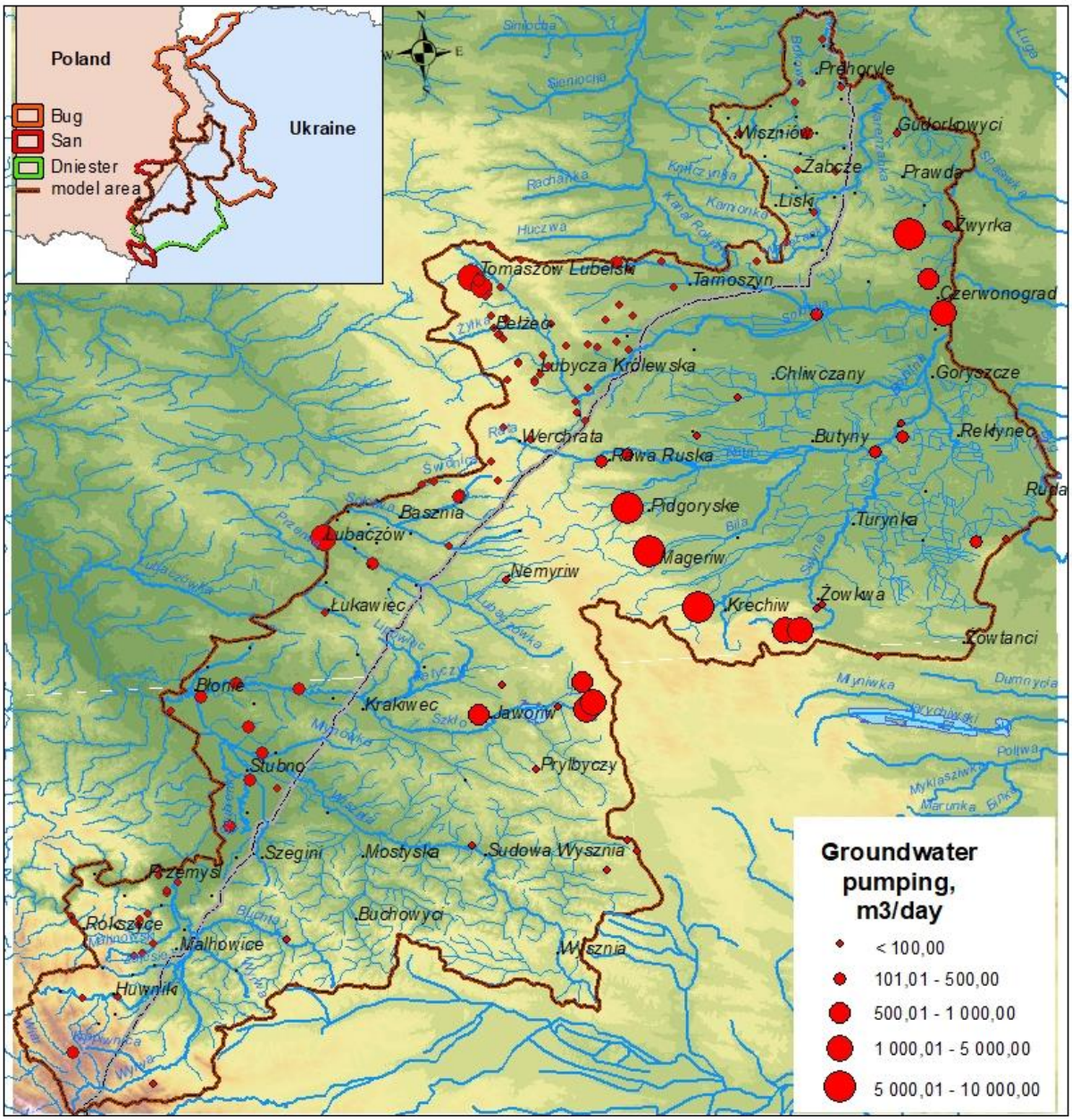

Figure 25. Average daily groundwater pumping in the operating intakes, 2018–2020

A characteristic feature of the Polish part of the study area is the dispersion of the groundwater intake at unit volumes generally below 100 m^3/d. The largest amount of water is extracted from the intakes in Pasieki, approx. 3,300 m^3/d, that belong to the municipal water supply system of the city of Tomaszów Lubelski. The average daily total water extraction from all 87 intakes in 2018-2020 was approx. 11,000 m^3/d. The largest 17 intakes (with an average daily extraction above 100 m^3/d) account for 88% of the total extraction from all 87 intakes in the Polish part of the study area. The main intakes are, for the most part, multi-borehole ones. Table 7 presents the amounts of groundwater abstraction in 2018-2020, from 17 intakes, where the average daily abstraction was greater than 100 m^3/day.

Table 7 Groundwater abstraction from the largest intakes located in the Polish part of the study area, 2018–2020

No.	National number of intake	Role of the intake	Location of intake (city/town/village)	County	Intaken aquifer	Mean daily abstraction (m^3/d)
1	9280025	Communal (collective supply)	Pasieki	tomaszowski	Cr3	3274.5
2	9860018	Communal (collective supply)	Lubaczow	lubaczowski	Q	1962.4
3	9280015	No data	Tomaszow Lubelski	tomaszowski	Cr3	958.5
4	10080024	Communal (collective supply)	Chotyniec	jarosławski	Q	471.9
5	10080049	Communal (collective supply)	Torki	przemyski	Q	400.1
6	10090008	Communal (collective supply)	Kobylnica Ruska	lubaczowski	Q	335.8
7	9600018	No data	Horyniec-Zdroj	lubaczowski	Pg+Ng	332.6
8	10080041	Communal (collective supply)	Stubno	przemyski	Q	291.7
9	9860044	Communal (collective supply)	Wolka Krowicka	lubaczowski	Q	246.4
10	8980008	Communal (collective supply)	Dolhobyczow	hrubieszowski	Cr3	243.9
11	9850024	No data	Charytany	jarosławski	Q	225.1
12	9600027	Communal (collective supply)	Horyniec-Zdroj	lubaczowski	Cr3	207.2
13	10430005	Communal (collective supply)	Braniow	bieszczadzki	Cr3	166.9
14	9290058	Communal (collective supply)	Lubcze	tomaszowski	Cr3	156.3
15	10080083	Communal (collective supply)	Lazy	jarosławski	Q	109.4
16	10080081	Communal (collective supply)	Kalnikow	przemyski	Q	108.3
17	9280022	No data	Tomaszow Lubelski	tomaszowski	Cr3	102.6

In the Ukrainian part, the exploitation of groundwater is concentrated in municipal intakes with an average unit volume of abstraction at the level of 1,100 m^3/d. The largest amount of water is extracted from the intakes in Stare Selo, approx. 10,000 m^3/d. The average daily total water extraction from all intakes in 2018-2020 was approx. 43,030 m^3/d. The largest 18 intakes (with an average daily extraction above 100 m^3/d) account for 98% of the total extraction from all 39 intakes in the Ukrainian part of the study area.

Table 8 presents the volumes of groundwater abstraction in 2018-2020, from 18 intakes, where the average daily abstraction was greater than 100 m^3/day.

Table 8 Groundwater abstraction from the largest intakes located in the Ukrainian part of the study area, 2018–2020

	National number of intake	Role of the intake	Location of intake (city/town/village)	County	County	Mean daily abstraction (m^3/d)
1	463001400	Communal (collective supply)	Stare Selo	Lvivski	Cr3	9981
2	463001300	Communal (collective supply)	Maheriv	Lvivski	Cr3	6844.7
3	463001500	Communal (collective supply)	Kunyn	Yavorivski	Cr3	5965.7
4	463003800	Communal (collective supply)	Zhvyrka	Chervonohradski	Cr3	5359
5	463000800	Communal (collective supply)	Novoiavorivsk	Yavorivski	M	2986.3
6	463001100	Communal (collective supply)	Mokrotyn	Lvivski	Cr3	2491.7
7	463004000	Communal (collective supply)	Chervonohrad	Chervonohradski	Cr3	2343
8	463001000	Communal (collective supply)	Shklo	Yavorivski	Q-M	2070.3
9	463005501	Communal (collective supply)	Mokrotyn	Lvivski	Cr3	1221
10	460066101	Individual	Starychi	Yavorivski	M	849
11	463004300	Communal (collective supply)	Ostriv	Chervonohradski	Cr3	625.7
12	460056600	Communal (collective supply)	Yavoriv	Lvivski	Q-M	533
13	460055200	Communal (collective supply)	Rava-Ruska	Lvivski	Cr3	320.7
14	460062200	Industrial	Volytsia	Chervonohradski	Cr3	210
15	460008801	Industrial	Batiatychi	Lvivski	Cr3	208.7
16	460026400	Communal (collective supply)	Velyki Mosty	Chervonohradski	Cr3	130.7
17	460025600	Communal (collective supply)	Belz	Chervonohradski	Cr3	120.3
18	460012100	Industrial	Rava-Ruska	Lvivski	Cr3	109.7

3.2 Assessment of unregistered abstraction of groundwater

The actual volume of groundwater abstraction is difficult to determine and can only be estimated with some approximation. This is due to the fact that a significant part of the consumption eludes official statistical summaries, that contain data only on intakes supplying water to the municipal networks and industrial installations. However, there is the remaining problem of individual intakes, which are usually not monitored and their operation is not reported in any way. This is especially true in rural areas, where intakes of this type are commonly used for economic purposes and irrigation of crops. Although individual intakes usually work with low efficiency, together they constitute an important component of the water balance, which cannot be neglected in model studies. This necessitated the development of a methodology that would allow estimating the volume of unregistered abstraction and its spatial distribution within the study area. This required, in the first place, recognition of the structure of the water supply system for the population. Data for Poland were obtained from the Central Statistical Office. In a similar way, information was obtained

for border administrative units on the territory of Ukraine. The information obtained concerned the condition of the water supply network and the volume of consumption in 2021 and was compiled in relation to administrative units (municipalities on the Polish side and regions on the Ukrainian side).

Both on the Polish and Ukrainian side of the border, groundwater is mainly used for supplying the water to the municipal network (Figure 26). Surface waters are taken in communes located in the southern part of the area, where at the junction of the Carpathian overthrust and the Carpathian Foredeep, aquifers have poor parameters and limited resources. The total water abstraction in the communes located in the vicinity of the model study area is 48,814,334.2 m^3/year, of which 41,237,471.2 m^3/year is from groundwater and 7,576,863 m^3/year from surface waters. On the Polish side, surface waters account for as much as 39% of the total volume of water supplying the municipal network, while on the Ukrainian side it is less than 9%. This disproportion is partly due to the fact that on the Polish side, the water supply network serving the commune with the highest population density (the Przemyśl commune) is supplied from surface waters.

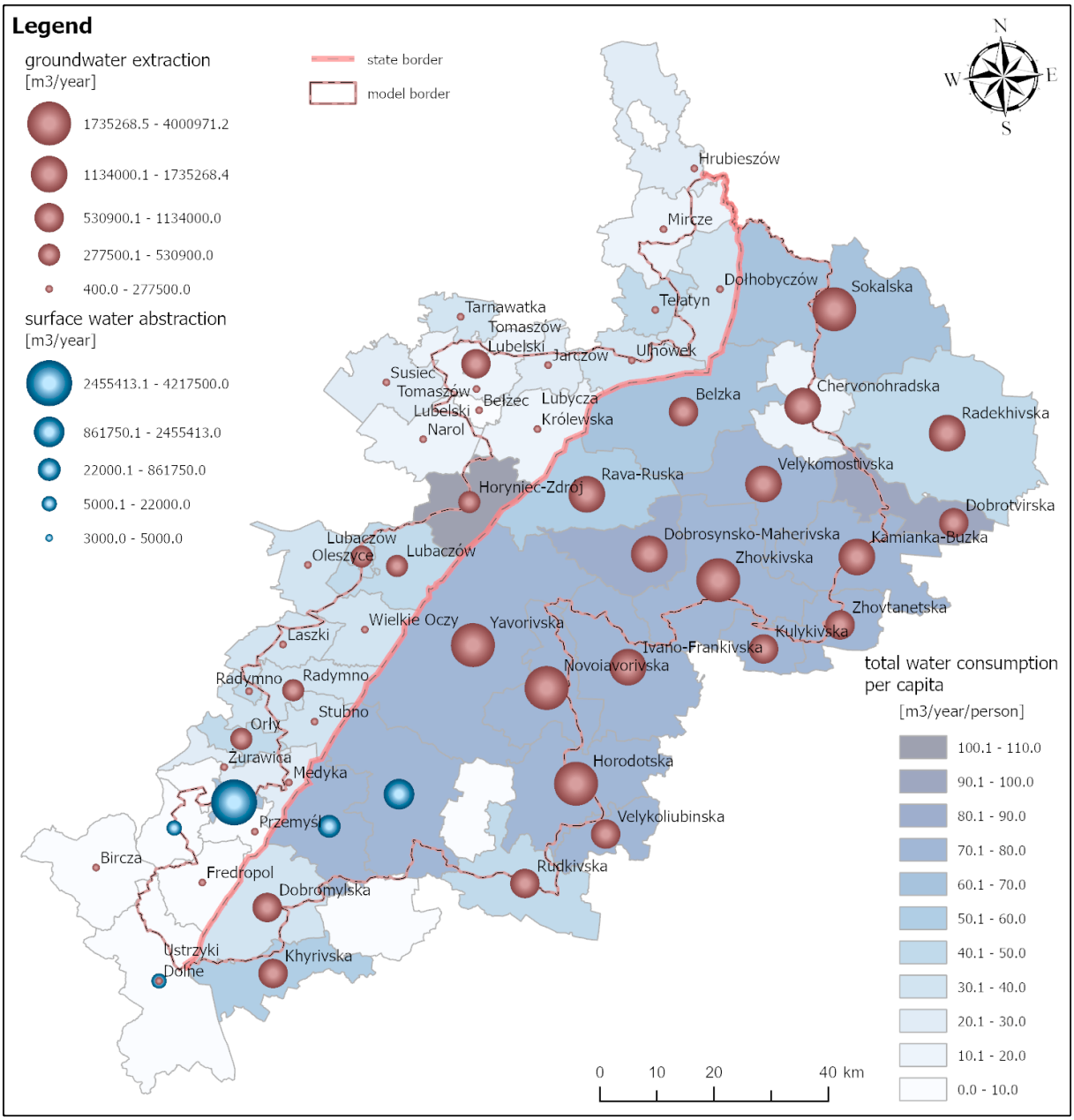

Figure 26. The structure of water supply in communes located in the vicinity of the study area

The analysis of data on water supply to the population showed significant differences in the development of the water supply network on both sides of the border (Figure 27). On the Polish side, in nearly half of the communes (14 out of 31), the percentage of the population using the group water supply system exceeds 90%, and only in two communes this percentage is lower than 10%. On average, in communes on the Polish side, the water supply network is used by 75.3% of the total population, and the median is 87.4%. On the Ukrainian side, the development of the water supply network is definitely poorer. In the majority of communes (13 out of 24), the percentage of the population connected to the water supply system does not exceed 10%, and only in one commune does it exceed 75%. On average, in communes on the Ukrainian side, only 16.3% of the population uses group water supply (median 5.5%). Against this background, the data on the average water consumption from the network supply system per capita looks interesting. Data obtained for communes on the Polish side of the border indicate that this value is usually in the range of

0.04 - 0.17 m^3/d/person (Figure 28), and the average demand value is 0.11 m^3/d/person. Meanwhile, on the Ukrainian side, the average value of demand for water is almost twice as high and amounts to 0.18 m^3/d/person, while in most communes it is a value from a narrow range of 0.2 - 0.23 m^3/d/person (Figure 29).

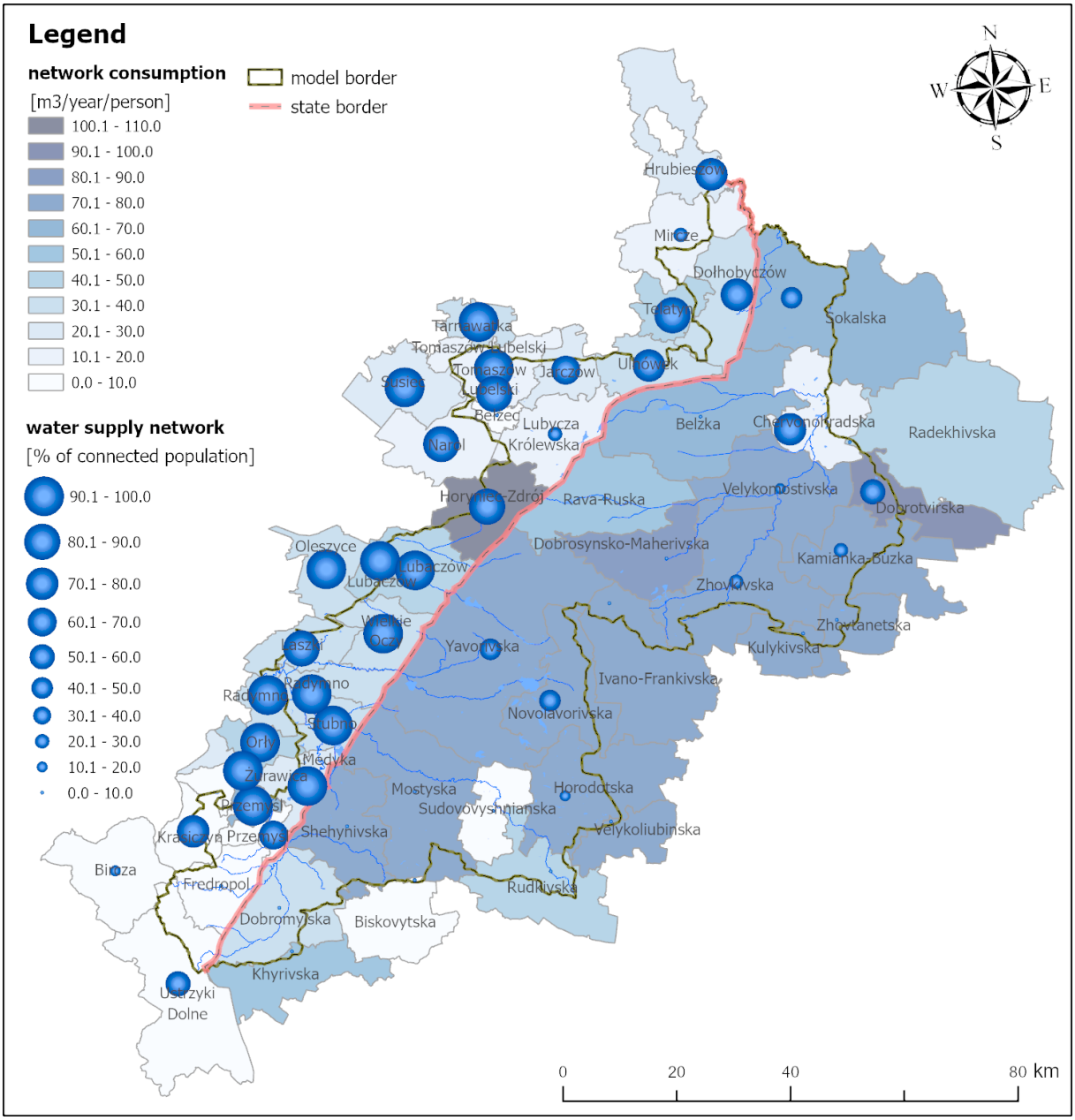

Figure 27. Percentage of population connected to the water supply network and average water consumption in 2021 per commune inhabitant (based on statistical data)

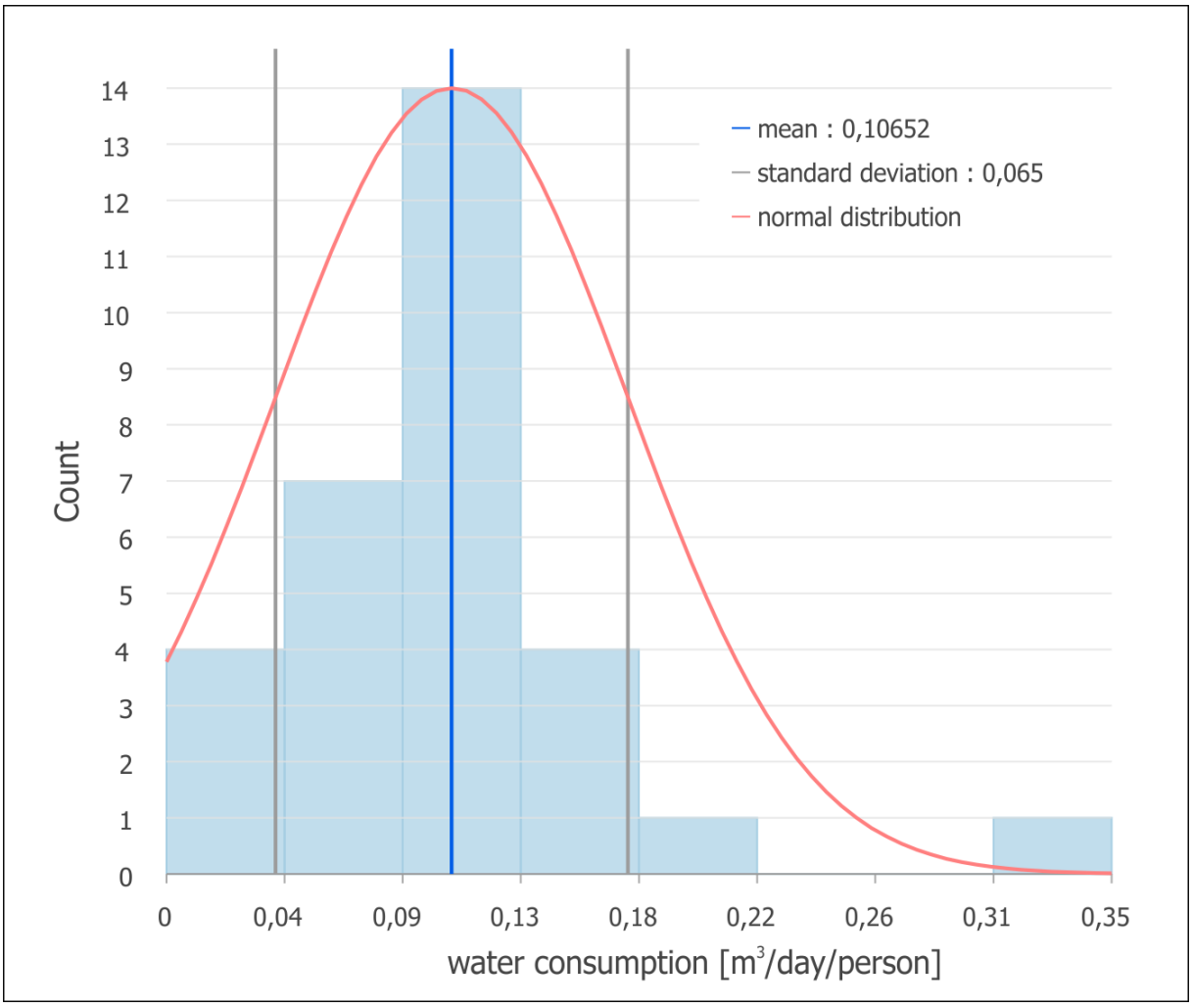

Figure 28. Distribution of the average demand for water in communes on the Polish side of the border (based on GUS data for 2021)

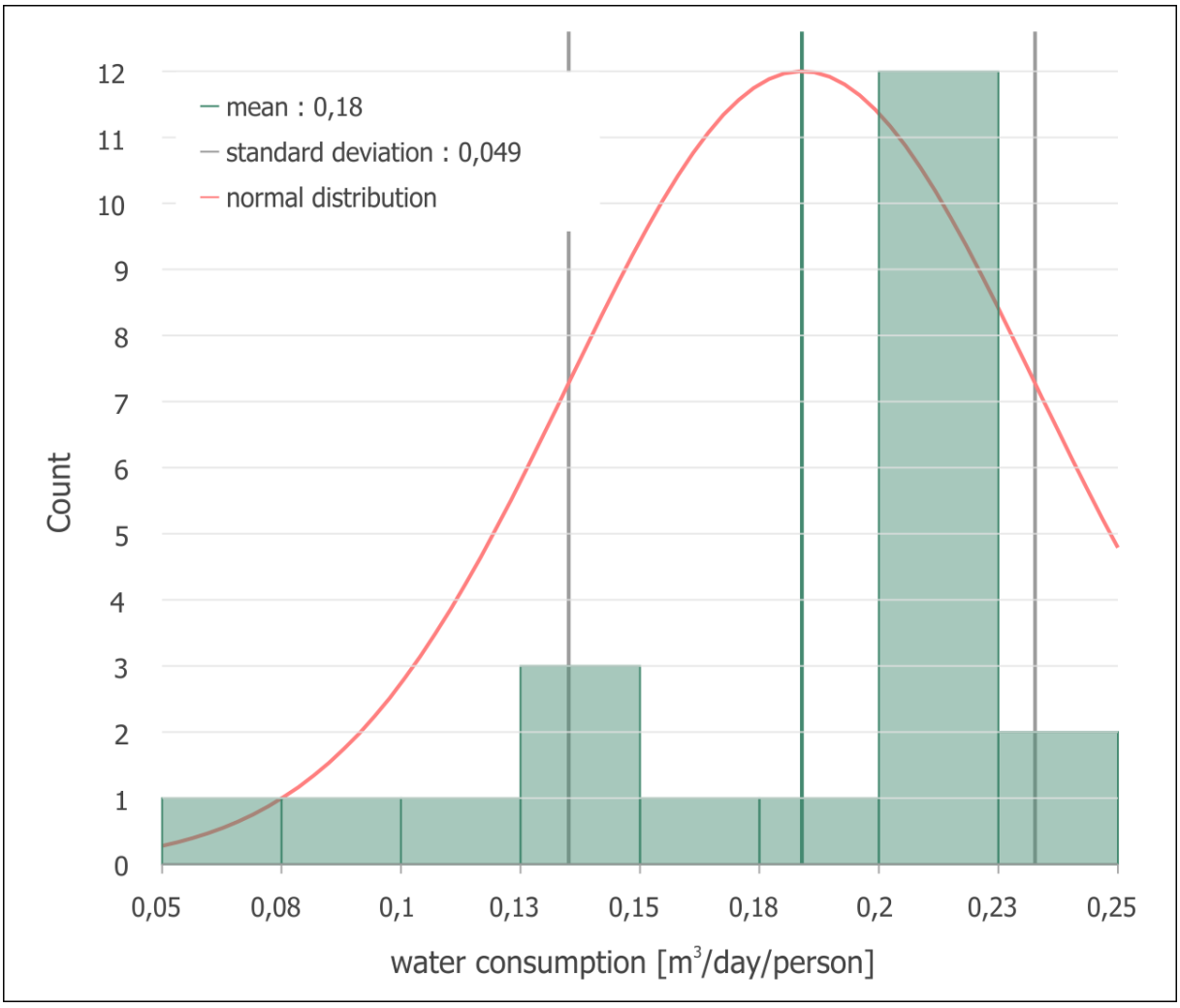

Figure 29. Distribution of the average demand for water in communes on the Ukrainian side of the border (based on statistical data for 2021)

It should be noted that the above-mentioned differences in water consumption do not result from the diversified demand for water per capita, but only testify to a different scale of the problem of hidden consumption, for which individual intakes are responsible. This phenomenon can be traced in a particularly vivid way in the communes on the Polish side of the border. If we look at urban communes (Przemyśl, Tomaszów Lubelski), it turns out that the volume of water consumption is close to the value of 0.2 m^3/d/person. Therefore, these values are similar to those prevailing in municipalities in Ukraine. Meanwhile, in rural communes, consumption values do not exceed 0.13 m^3/d/person (excluding the commune of Horyniec Zdrój, where medicinal waters are additionally included, which means that the average water consumption reaches the value of 0.38 m^3/d/person). These data may seem surprising, because higher water consumption should be expected in rural areas, where water is used not only to meet living needs, but also for economic purposes and for irrigation of crops. This indicates that in rural areas, the population uses water from the network to meet only part of the actual demand, and the remaining part is covered from numerous individual intakes that escape official statistical summaries. On the other hand, in urban areas the problem of unregistered consumption is much less important.

The above analysis shows that the actual demand for water per capita remains unknown and must be assumed a priori in order to include unregistered consumption in the calculations. In case of the described model studies, the demand at the level of 0.4

m^3/d/person was considered a safe value, i.e. a value approximately twice as high as the maximum registered consumption in both the Polish and Ukrainian part of the area (excluding Horyniec Zdrój). It was also assumed that the problem of unregistered groundwater abstraction will concern primarily rural communes. The assumed value of the demand made it possible to estimate the total demand for water according to the formula:

$$C = ZW \times POP,$$

where:
C – estimated demand for water within the administrative unit,
ZW – water demand per capita,
POP – the number of residents.

Knowing the total demand for water within each administrative unit, it was possible to estimate the total amount of unregistered consumption. A simple balance equation was used for this purpose:

$$ND = C - (P_{pow} + P_{pod})$$

where:
ND – estimated value of unregistered consumption,
P_{pow} – supply of the water supply network from surface waters,
P_{pod} – supply of the water supply network from groundwater.

Unfortunately, the amount of unregistered consumption obtained according to the above methodology could not be used directly in the filtration field model. This was due to the fact that in case of some administrative units, the model covered only a fragment of their area, and the consumption data concerned the entire unit. Therefore, it was necessary to estimate what part of the consumption falls on the fragment of the unit within the limits of the model. For this purpose, it was assumed that unregistered consumption is evenly distributed over the entire area of the administrative unit, so its value within the model can be estimated as:

$$NDM = PJAM / PJA \times ND$$

where:
NDM – unregistered consumption in a part of the administrative unit within the model limits,
PJAM – area of the administrative unit within the model limits,
PJA – total area of the administrative unit.

The obtained abstraction volume had to be then decomposed into individual abstraction point / intake, which could be represented in the model using the Well condition. It was assumed that the abstraction would be concentrated primarily in the vicinity of the towns forming the settlement network of the area. Then, spatial data on land cover from the Corine Land Cover database were used (in the Ukrainian part of the study, these were data prepared by members of the project team based on the analysis of satellite images). From this database, a polygon layer representing built-up areas was selected, and then each polygon was assigned a point located in its geometric centre. This way, a set of points was obtained that could be counted within each administrative unit within the limits of the model. By this solution, it was possible to determine the volume of abstraction at each abstraction point / intake within the commune:

$$QPP = NDM / LPP$$

where:

QPP – recharge of a single abstraction point / intake,
PJAM – number of abstraction points / intakes within the administrative unit.

As a result, a point information layer representing the spatial distribution of unregistered consumption in the area of model research was created (Figure 30). Thanks to the applied methodology, the obtained distribution takes into account the population density and the structure of the settlement network. The highest values of unregistered consumption were obtained in communes where only a small percentage of the population is supplied with water via the water supply system (areas with a large deficit in groundwater abstraction). The abstraction values for individual points vary and range from 79.9 to 1346.8 m^3/d. It should be noted that these amounts depend not only on the estimated volume of unregistered abstraction in a given administrative unit, but also on the number of settlement points within the boundaries of this unit. These values can be interpreted as the total abstraction of all individual intakes in the vicinity of a given settlement.

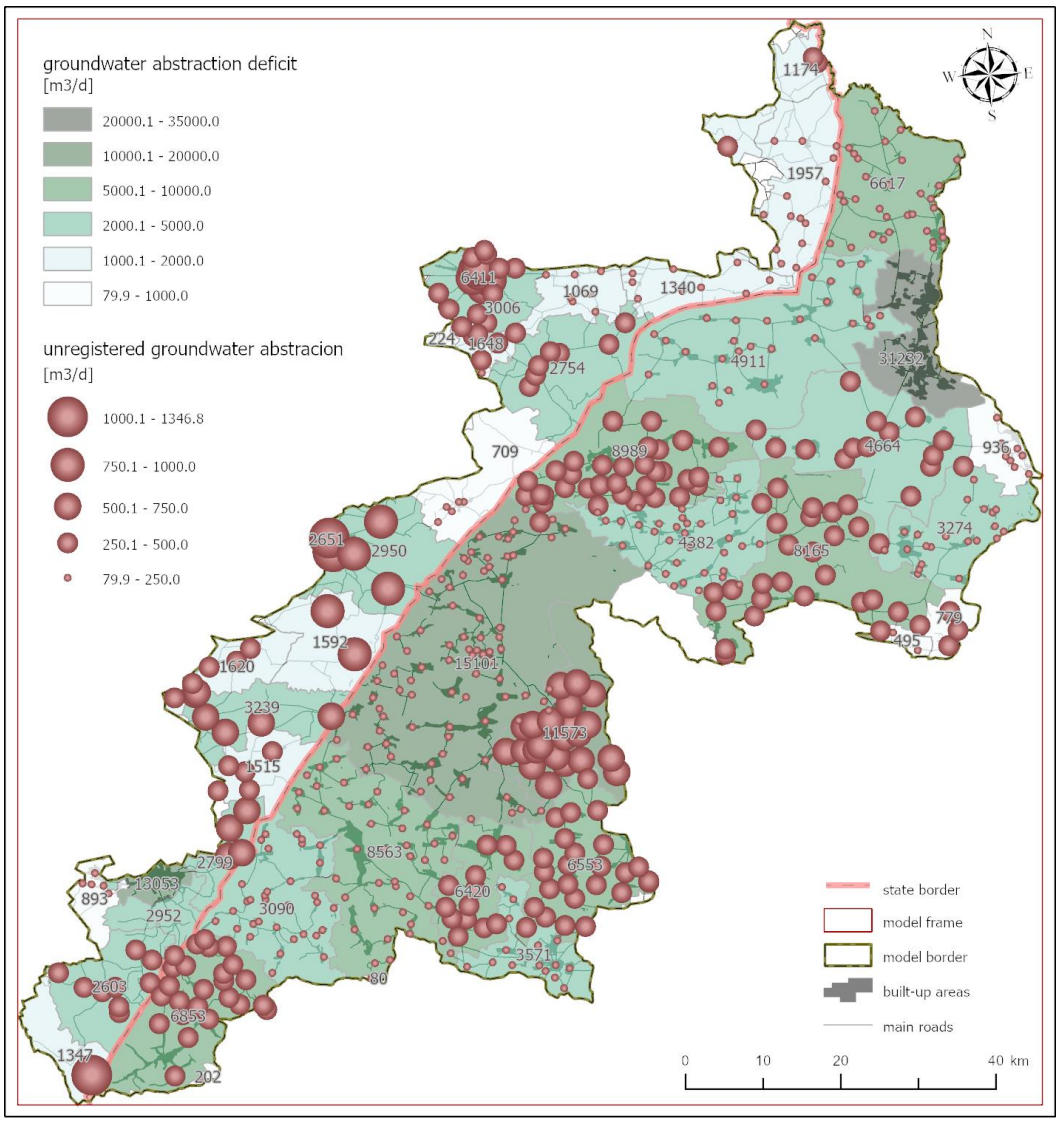

Figure 30. Distribution of unregistered abstraction within the area of model research

4. Impact assessment of groundwater abstraction on the dynamics of transboundary flows

4.1 Natural state simulation

A calibrated steady-state model was used to simulate natural conditions without groundwater exploitation. The calculation result obtained for the natural hydrodynamic state of the TBAs system is consistent with the gravitational principle of the circulatory system in an open groundwater system with an unconfined groundwater table recharged by rainwater infiltration. The simulated groundwater table elevation follows the surface water circulation system and imitates the isolines of the terrain. In the Bug sub-basin groundwater level descends from NW to SE from ~ 360 m a.s.l. in the watershed zone between the underground catchment of the Bug and the San (in Roztocze), going below 180 m a.s.l. in the Bug valley, which is the main axis of groundwater drainage in the Bug sub-basin (Figure 31).

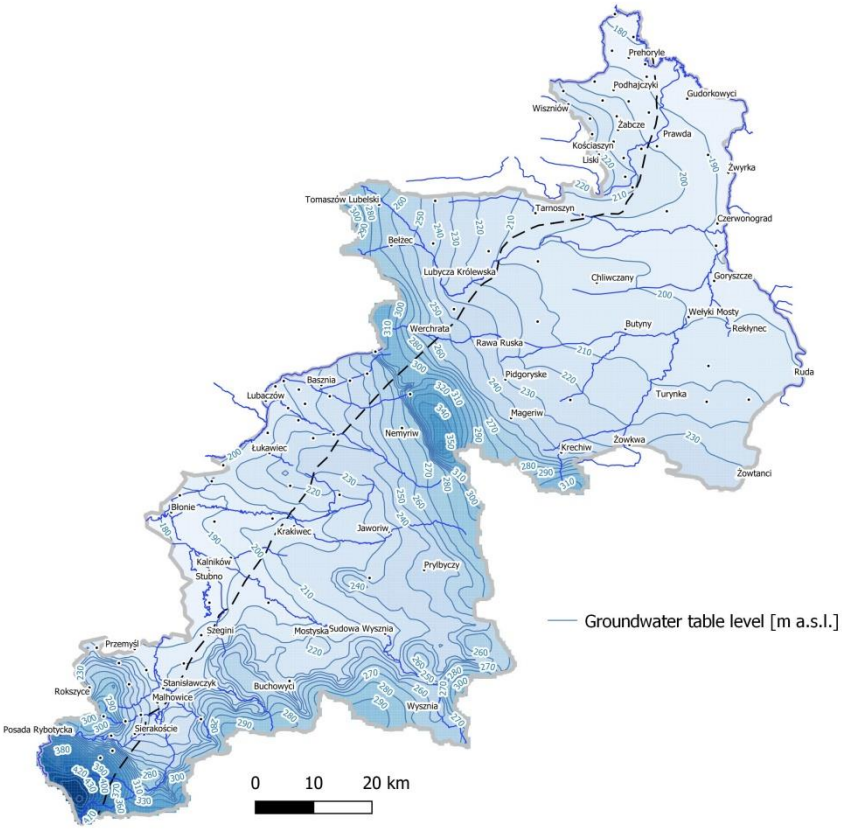

Figure 31. Calculated natural state of the Bug-San TBAs system without groundwater exploitation

In the San sub-basin, the highest calculated ordinates of the groundwater table are concentrated, exceeding 450 m a.s.l. and are located in the area of the Carpathian overthrust. Within the San sub-basin, due to the surrounding mountains, the hydraulic gradient is the highest, almost three times higher than the analogous one in the Bug alluvial plains. In the Carpathian part of the San sub-basin the elevation of groundwater table decreases from S to N due to the inflow of the Wiar River to the San River from 450 to 180 m a.s.l. In the northern, plain part of the San sub-basin groundwater level descends from E to W under the influence of the tributaries of the Szklo and Wisznia rivers to the San from 300

to 180 m a.s.l. and in the direction from NE to SW under the influence of the tributary of the Lubaczówka river to the San from 360 to 200 m a.s.l.

In balance terms, in a state close to natural conditions, the groundwater resources of Bug-San TBAs are as follows (Table 9):

- rainwater infiltration (72,3% - Poland; 81,3% - Ukraine),
- surface water infiltration (15,8% - Poland; 11,4% - Ukraine),
- groundwater inflow from outside the model area (3,7% - Poland; 1,1% - Ukraine).
- transboundary groundwater inflow (8,2% - Poland; 6,2% - Ukraine)

The outflow from Bug-San TBAs results mainly from (Table 9):

- drainage through river (85,8% - Poland; 93,5% - Ukraine),
- evapotranspirationi (0,2% - Poland; 0,8% - Ukraine),
- groundwater outflow outside the model area (3,2% - Poland; 1,0% - Ukraine),
- transboundary outflow of groundwater (10,8% - Poland; 4,7% - Ukraine)

Table 9 Water budget of the Bug-San TBAs for a natural state

m^3/d	Poland	Ukraine
Surface water infiltration (Inflow)	101406,4	130086,2
Drainage through river (Outflow)	551803,9	1063499,0
Groundwater intake (Outflow)	0,0	0,0
Rainwater infiltration (Inflow)	465186,2	925250,2
Evapotranspiration (Outflow)	1190,5	9777,8
Groundwater inflow from outside the model area (Inflow)	23568,1	12378,9
Groundwater outflow outside the model area (Outflow)	20474,3	11145,9
Transboundary flow	- 69683,5	+ 69683,5
Transboundary flow	+ 52989,4	- 52989,4
Total Inflow	643150,2	1137398,8
Total Outflow	643152,2	1137412,1
Error, %	-0,0003	-0,0012

Particular commentary is required on the participation in the balance of the component of transboundary groundwater exchange. Calculations show that for Ukraine the cross-border exchange of groundwater in natural conditions is positive (the inflow of water at 16694.1 m^3/d exceeds the outflow), in contrast to Poland.

4.2 Impact assessment of registered groundwater abstraction on the hydrodynamic status of TBAs

The groundwater abstraction simulation was performed for different variants of the pressure of the tested aquifer system. The simulations used were a tool for assessing the impact of groundwater abstraction on the hydrodynamic condition of the system. The first scenario assumed the lowest level of pressure on the TBAs system and took into account only the registered groundwater abstraction, which is reported in official statistical summaries and

applies only to intakes supplying water supply networks and industrial installations (see: Characteristics of registered groundwater abstraction). This abstraction is far from reflecting the actual amount of groundwater exploitation as significant part of it eludes official statistical summaries.

In the analyzed scenario, taking into account the abstraction of groundwater from over 1,100 intaxes at the average level from the last 3 years, the simulation shows that drawdown cones on a scale noticeable in the regional model arise in the area of the largest intakes (Figure 32). In Poland, only a group of intakes in the area of Tomaszów Lubelski with a total abstraction of groundwater from K_2 aquifer in the size of about 4,000 m^3/d produces drawdown cones with a maximum lowering of the groundwater table to 3 m. Meanwhile, on the Ukrainian side, the maximum value of lowering the water table is about 31 m and occurs in the area of the intakes in Stare Seło, supplying water to the Lviv agglomeration with the exploitation of groundwater at the level of 10,000 m^3 /d. In addition, several other areas of lowering the groundwater table, caused by the abstraction of groundwater in excess of 3,000 m^3/d, should be mentioned. These include intakes in the towns of Mageriv, Kunyn, Chervonograd and Novoyavorivsk, which cause the maximum value of lowering the groundwater table level from 4 to 20 m.

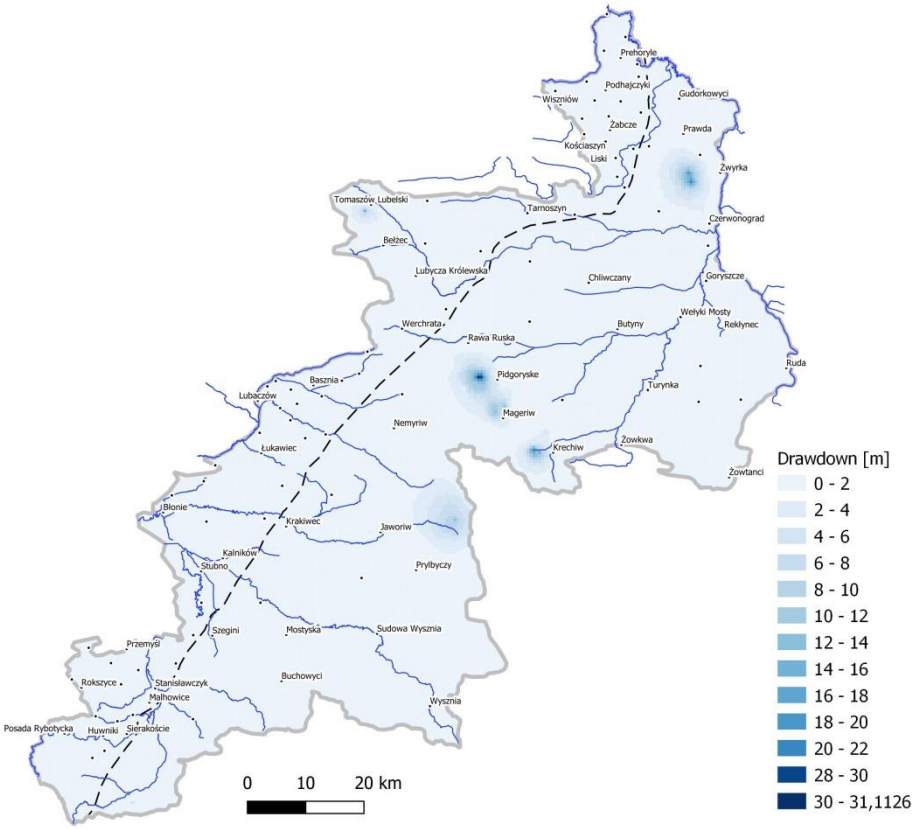

Figure 32. Simulated groundwater drawdown with exploitation at the level from 2018-2021 (taking into account only registered abstraction)

In balance terms, changes in the TBAs system under the influence of groundwater exploitation for the analyzed variant have been presented in Table 10.

Table 10 Water budget of the Bug-San TBAs in the current exploitation model (taking into account only the registered abstraction)

m^3/d	Poland, m^3/d	Poland*, %	Ukraine	Ukraine*, %
Surface water infiltration (Inflow)	103050,0	↑1,6	155908,7	↑19,8
Drainage through river (Outflow)	543549,7	↓1,5	1015984,2	↓4,5
Groundwater intake (Outflow)	10792,3	-	74537,2	-
Rainwater infiltration (Inflow)	465186,2	0	925250,2	0
Evapotranspiration (Outflow)	1190,5	0	9777,8	0
Groundwater inflow from outside the model area (Inflow)	23957,6	↑1,6	12657,0	↑2,2
Groundwater outflow outside the model area (Outflow)	19818,0	↓3,2	10375,0	↓6,9
Transboundary flow	- 69749,5	↑0,1	+ 69749,4	↑0,1
Transboundary flow	+ 52904,3	↓0,2	- 52904,3	↓0,2
Total Inflow	645098,1	↑0,3	1163565,3	↑2,3
Total Outflow	645100,0	↑0,3	1163578,5	↑2,3
Error, %	-0,0003	-	-0,0011	-

* - changes compared to the natural state

The average daily intensity of groundwater exploitation is at the level of 85,329.5 m^3/d and accounts for 6.1% of the recharge of the Bug-San TBAs, which can be considered a negligible impact. By country, abstraction accounts for 2.3% of groundwater supply by atmospheric precipitation in Poland, and approximately 8.1% in Ukraine. Groundwater abstraction is mainly compensated by an increase in surface water infiltration into the aquifer system (1.6% - in Poland and 19.8% - in Ukraine) and a slightly intensified inflow of groundwater from outside the model area (1.6% - in Poland and 2.2% - in Ukraine). In addition, the outflow of groundwater to rivers is slightly decreasing (to 1.5% - in Poland and 4.5% - in Ukraine) compared to the natural state. Other components of the budget do not change significantly during abstraction in the analysed case.

4.3 Impact assessment of registered and estimated unregistered groundwater abstraction on the hydrodynamic status of TBAs

The next two simulations, to a certain extent, reflect the impact of the actual pressure of the tested aquifer system as, apart from the registered abstraction, they also take into account the abstraction from individual intakes, which are usually not measured and their work is not reported in any way. Although individual intakes usually work with low efficiency, together they constitute an important component of the water balance, which cannot be neglected in assessing the impact of groundwater abstraction on the hydrodynamic condition of the system. The methodology of assessment of unregistered abstraction has been described in Assessment of unregistered abstraction of groundwater.

In the first simulation, abstraction is the sum of registered (analyzed in chapter Impact assessment of registered groundwater abstraction on the hydrodynamic status of TBAs) and unregistered abstraction at the level of 0.2 m^3/d/person - the average value of water demand in most municipalities on the Ukrainian side. In the analyzed scenario (Figure 33), the previously identified drawdown cones are joined by others located in the San sub-basin, in the region of the communes with the highest population density - the Przemyśl agglomeration (Poland) and the communes of Sudovovyshnianska and Dobromylska (Ukraine). The indicated communes on the Ukrainian side are not among the most populous,

but in combination with the low resources of the aquifer system in this area, they are at risk of lowering the groundwater table below 2 m, with maximum values reaching even 16 m - in the villages of Makunin, Dmytrowyczy, Dydiatyci.

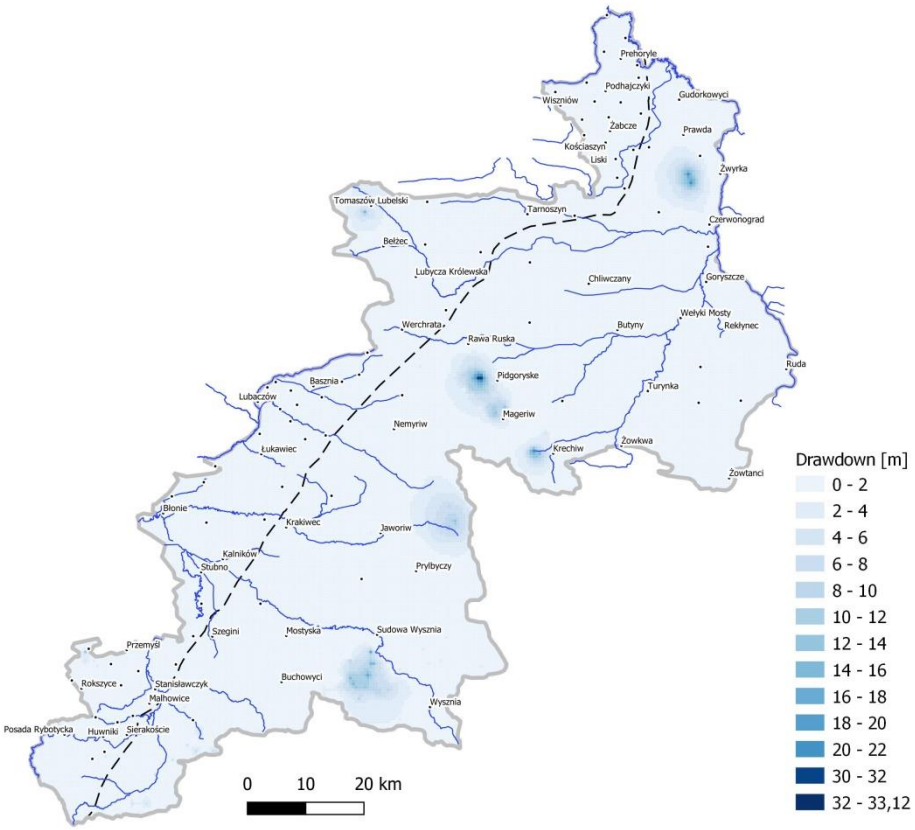

Figure 33. Simulated groundwater drawdown with exploitation at the level from 2018-2021

In balance terms, changes in the TBAs system under the influence of groundwater exploitation for the analyzed variant have been presented in Table 11.

Table 11 Water budget of the Bug-San TBAs in the current exploitation model (taking into account registered consumption and estimated unregistered consumption at the level of 0.25 m^3/d/person)

m^3/d	Poland, m^3/d	Poland*, %	Ukraine	Ukraine*, %
Surface water infiltration (Inflow)	105444,2	↑4,0	158582,5	↑21,9
Drainage through river (Outflow)	531498,5	↓3,7	998342,2	↓6,1
Groundwater intake (Outflow)	26801,3	-	95756,2	-
Rainwater infiltration (Inflow)	465186,2	0	925250,2	0
Evapotranspiration (Outflow)	1190,5	0	9777,8	0
Groundwater inflow from outside the model area (Inflow)	24580,9	↑4,3	13067,1	↑5,6
Groundwater outflow outside the model area (Outflow)	19041,2	↓7,0	9730,1	↓12,7
Transboundary flow	- 69358,6	↓0,5	+ 69358,6	↓0,5
Transboundary flow	+ 52676,8	↓0,6	- 52676,8	↓0,6
Total Inflow	647888,1	↑0,7	1166258,4	↑2,5

Total Outflow	647890,1	↑0,7	1166283,1	↑2,5
Error, %	-0,0003	-	-0,0021	-

* - changes compared to the natural state

The abstraction of groundwater is 122,557.5 m^3/d and is 1.4 times higher than the registered one (previous variant of the simulation - Impact assessment of registered groundwater abstraction on the hydrodynamic status of TBAs). In Poland, abstraction accounts for 5.8% of groundwater recharge by atmospheric precipitation, in Ukraine – approx. 10.3%. As in the previous variant, the changes caused concern the increased (several times greater) infiltration of surface waters into the aquifer system (at 4.0% - in Poland and 21.9% - in Ukraine) and the deepening reduction of surface water recharge (at 3.7% - in Poland and 6.1% - in Ukraine). There are no significant changes in the transboundary exchange of groundwater compared to the natural state, the values are insignificant and remain at the level of 0.5-0.6%.

The next simulation takes into account a greater pressure on the tested aquifer and is the sum of registered (analyzed in chapter Impact assessment of registered groundwater abstraction on the hydrodynamic status of TBAs) and unregistered abstraction at the level of 0.4 m^3/d/person (a value approximately twice as high as the previous option). In the analyzed scenario (Figure 34), the previously identified drawdown cones are joined by new ones. They only form in the San sub-basin. On the other hand, in the Bug sub-basin, the changes manifest themselves in the extension of the range and size of depressions of the already existing drawdown cones in the area of large municipal intakes. In the San sub-basin, new drawdown cones are formed mainly in the Ukrainian part in the area at the watershed, which is related to the low rsourcefulness of the system. The group of communes (Novoiavorivska, Sudovovyshnianska and Dobromylska) at risk of lowering the groundwater table is joined by the communes of Shehynivska, Mostyska and Horodotska. The indicated communes are at risk of lowering the groundwater table below 2 m, with maximum values reaching even 20 m - in Makunin, Dmytrowyczy, Dydiatyci, Novoiavorivsk. It should be noted that even if the abstraction of groundwater is more than doubled, no cross-border drawdown cones are formed.

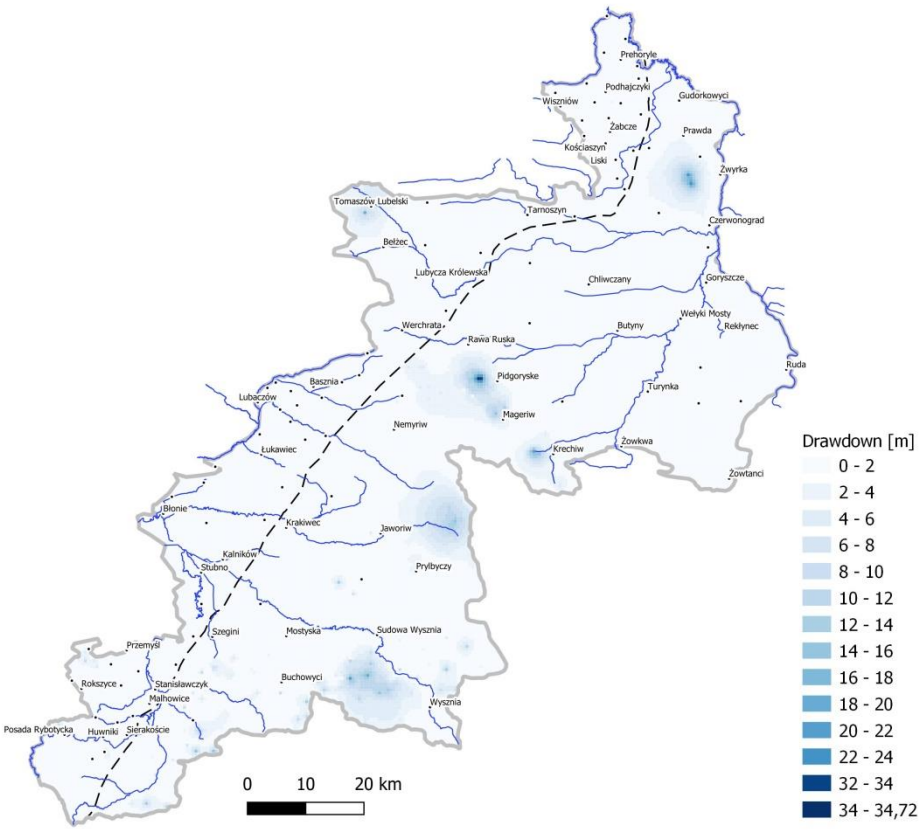

Figure 34. Simulated groundwater drawdown with exploitation at the level from 2018-2021 (taking into account registered abstraction and estimated unregistered abstraction at the level of 0.4 m^3/d/person)

In balance terms, changes in the TBAs system under the influence of groundwater exploitation for the analyzed variant are presented in Table 12.

Table 12 Water budget of the Bug-San TBAs in the current exploitation model (taking into account registered consumption and estimated unregistered consumption at the level of 0.4 m^3/d/person)

m^3/d	Poland, m^3/d	Poland*, %	Ukraine	Ukraine*, %
Surface water infiltration (Inflow)	108424,8	↑6,9	164999,0	↑26,8
Drainage through river (Outflow)	520210,9	↓5,7	961118,6	↓9,6
Groundwater intake (Outflow)	41946,3	-	141839,2	-
Rainwater infiltration (Inflow)	465186,2	0	925250,2	0
Evapotranspiration (Outflow)	1190,5	0	9777,8	0
Dopływ wód podziemnych z poza obszaru modelu (Inflow)	25207,9	↑6,9	14302,9	↑15,5
Odpływ wód podziemnych poza obszar modelu (Outflow)	18290,5	↓10,7	9000,8	↓19,2
Transboundary flow	- 69194,7	↓0,7	+ 69194,7	↓0,7
Transboundary flow	+ 52012,0	↓1,8	- 52012,0	↓1,8
Total Inflow	650830,9	↑1,2	1173746,8	↑1,2
Total Outflow	650832,9	↑1,2	1173748,4	↑1,2
Error, %	-0,0003	-	-0,0001	-

* - changes from the natural state

The groundwater abstraction is 183,785.5 m^3/d and it is 2.2 times higher than the registered one (Impact assessment of registered groundwater abstraction on the hydrodynamic status of TBAs). In Poland, the abstraction amounts to 9.0% of groundwater recharge by atmospheric precipitation, in Ukraine – approx. 15.3%. As in the previous variant, the changes caused concern the increased (several times greater) infiltration of surface waters into the aquifer system (at 6.9% - in Poland and 26.8% - in Ukraine) and the deepening reduction of surface water recharge (at 5.7% - in Poland and 9.6% - in Ukraine). In the analyzed scenario, there is a tendency to reduce the amount of transboundary groundwater exchange. Compared to the natural state, the decrease values are at the level of 0.7% for the transboundary groundwater flow from Poland to Ukraine and 1.8% - in the opposite direction. As a result, it can be concluded that more than doubling the abstraction of groundwater slightly reduces the transboundary groundwater flow in both directions, but the San sub-basin is affected to a greater extent.

4.4 Impact assessment of groundwater abstraction on the level of useful resources available for use

The EU Water Framework Directive (EU, 2000), the main purpose of which is to maintain good water status in the GWB, includes the term "groundwater resources available for management". According to the definition given in the WFD, the resources available for development are understood as the difference between the renewable resources of the groundwater system and the size of the river base flow. In practice, this expression means the volume of water available for management, which is the amount of groundwater that can be taken from the hydrogeological system constituting the balance area - without worsening their chemical status and maintaining the desired condition of groundwater-dependent ecosystems (Sadurski, 2016). The balancing hydrogeological system is the underground drainage basin of the river with the areas of groundwater flow to intakes located within the drainage basin (Szczepański, 2008). The possibility of assessing the resources available for management, including the hydrogeological and environmental effects of their abstraction, is only possible with the use of methods of mathematical modeling of the groundwater filtration process.

In the numerical model of groundwater flow developed in the EU-Waterres project, in which the distribution of recharge equal to the underground outflow to rivers was estimated, criteria for assessing resources available for management and weight factors controlling their distribution are defined. The spatial distribution of these resources is calculated using the constant-volume transformation algorithm (Śmietański, 2012). The method of this transformation directly links the resources available for management with the underground runoff to rivers in the computational process.

The main assumptions of the conducted simulation of groundwater abstraction at the level of resources available to management include:

1. The reference point was the piezometric surface obtained in the simulation, taking into account the registered and unregistered consumption in the amount of 0.25 m^3/d/person (Impact assessment of registered and estimated unregistered groundwater abstraction on the hydrodynamic status of TBAs);
2. The following areas were excluded from the abstraction simulation (the aquifer system was not under pressure).:

- Surroundings (1 km buffer) of model blocks with condition II - Well condition by means of which the registered groundwater abstraction was mapped;
- Surroundings (0.5 km buffer) of centroids with virtual intakes with unregistered abstraction;
- National Parks;
- Reserves;
- Groundwater dependent ecosystems;
- Natura 2000 areas.

3. In blocks located outside the excluded areas, the maximum possible abstraction was simulated so that the groundwater table depression calculated from the piezometric surface in the baseline simulation described above (current registered + unregistered abstraction at the level of 0.25 m^3/d/person) did not exceed the regional value of 2, 0 m, and locally, in the vicinity of large intakes - a maximum of 4 m.

The results of calculations of the additional maximum possible abstraction value shown in Figure 35 illustrate the so-called reserves of groundwater resources. Their value is usually in the range of 6-24 m^3/d. In the uplands, the lowest value is observed - below 12 m^3/d due to the low resources of the aquifer system, especially in the San basin - below 6 m^3/d. In the San River valley, the additional abstraction reaches maximum values - 42-48 m^3/d, while in the valleys of the main tributaries of the Bug - 30-42 m^3/d.

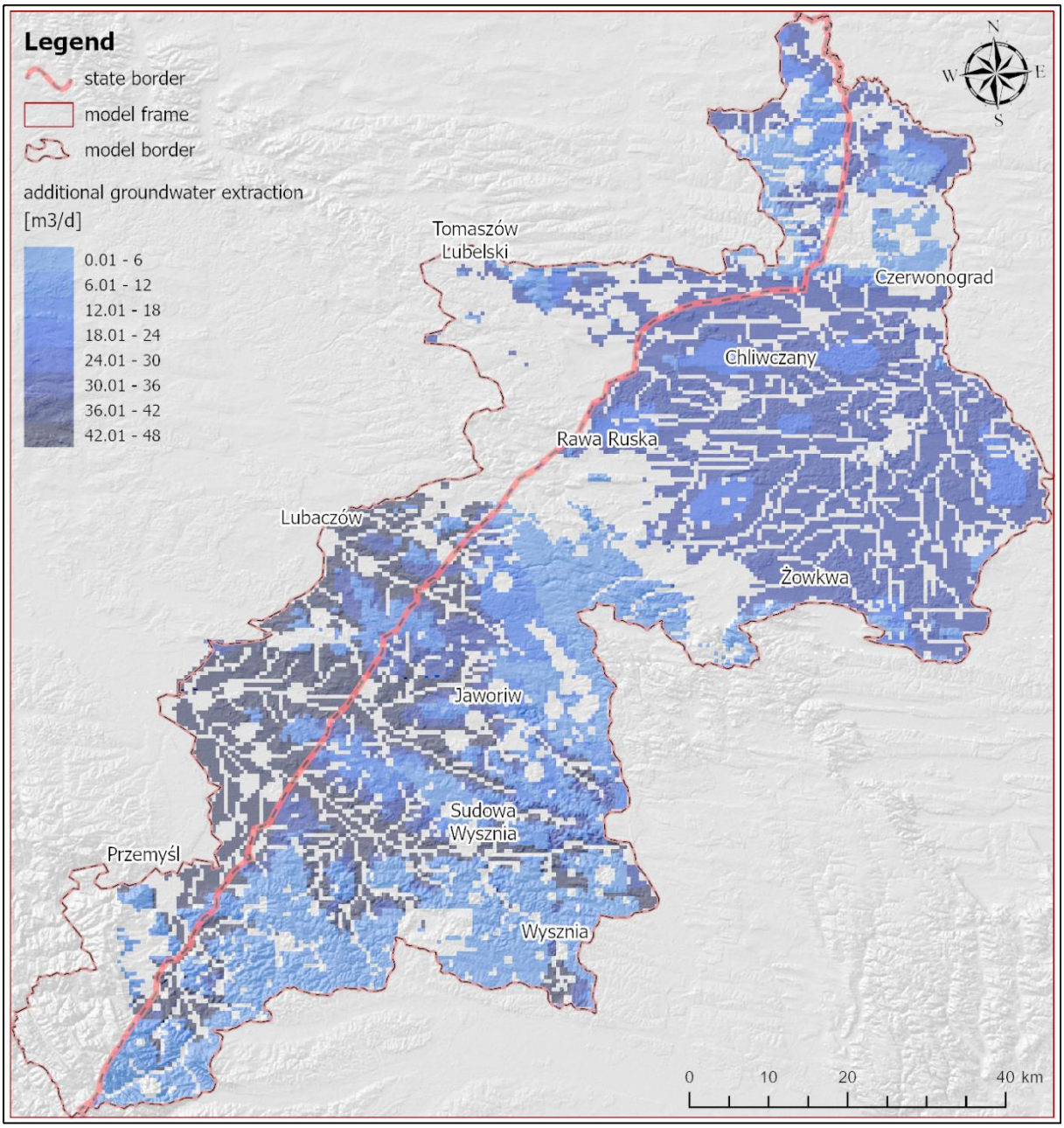

Figure 35. Additional maximum abstraction available for management - reserves of groundwater resources

The obtained additional, maximum abstraction available for management was then divided into groundwater abstraction points, which were mapped in the model using the Well condition. The results of the simulation of groundwater abstraction at the level of resources available for management are shown in Figure 36.

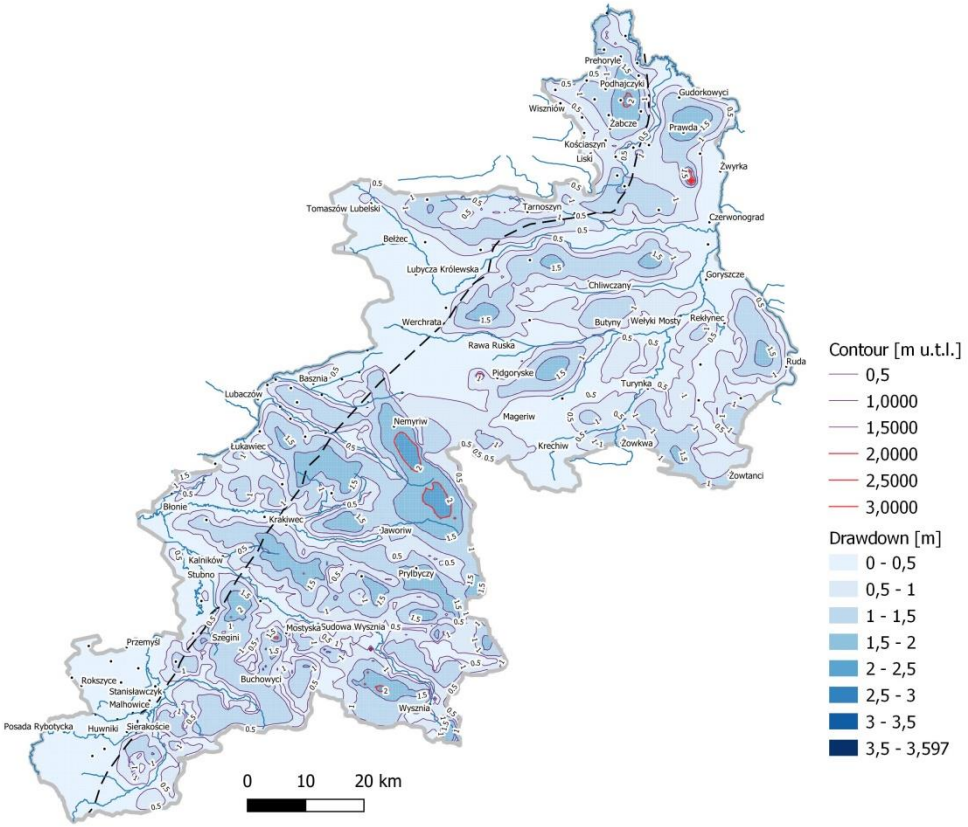

Figure 36. Simulated groundwater drawdown at the level of resources available for management

This scenario shows possible regional, not local as it was analyzed in the previous variants, lowering of the groundwater table with the maximum permissible pressure of the aquifer system with water abstraction. The obtained result of the calculations is consistent with the accepted regularity - the areas with low natural resourcefulness of the aquifer system in combination with significant groundwater abstraction are characterized by the highest sensitivity to the lowering of the groundwater table. The following regularities can be traced in the obtained spatial distribution:

- in general, the San sub-basin, compared to the Bug sub-basin, is characterized by greater sensitivity to the lowering of the groundwater table, mainly due to the low natural resourcefulness of the aquifer system;
- areas with a regional lowering of the groundwater table exceeding 1.0 m are located in non-valley zones of rivers, constituting groundwater drainage axes in the studied system. The exception is Roztocze - the watershed zone between the underground catchment of the Bug and the catchment of the San and the area of the Carpathian mountain overthrust, which were not included in the simulation of abstraction due to their location within the protected areas;
- the areas with the greatest lowering of the groundwater table, exceeding 2.0 m, are located in areas where two unfavorable factors coexist - low natural resourcefulness of the aquifer system and concentration of groundwater intakes.

In terms of administrative units, the areas with the greatest lowering of the groundwater table exceeding 2.0 m are located in the following towns:

- Poland: Dołhobyczów;

- Ukraine: Mostyska (OTG Mostyska), Melnyky (OTG Yavorivska), Shysherowychy, Dydiatychy, Dmytrovychy, Makuniv (OTG Sudovovyshnianska), Starychi (OTG Novoiavorivska), Zamok (OTG Dobrosynsko-Maherivska), Savchym (OTG Sokalska).

For these localities, optimization measures should be introduced first, because the current abstraction already exceeds the groundwater resources available for management. Particular attention should also be paid to localities located in the areas of lowering the groundwater table within 1.5-2 m. These areas can be considered deficient in terms of groundwater resources. Therefore, it is important to promote preventive measures here. The list of these localities includes:

- Poland: Krowica Lasowa, Malków Kolonia,
- Ukraine: Grabivnycia (OTG Dobromylska), Shehyni (OTG Shehynivska), Zaverhy, Hatky, Chyshky (OTG Mostyska), Malkivska Vola, Buniv, Glynycia, Drogomysl, Lypyna, Lypovec, Rogizna, Nemyriv (OTG Yavorivska), Orchovyci (OTG Rudkivska), Kulmatyci (OTG Sudovovyshnianska), Vola Starycka, Shklo, Prylbyci, Muzylovyci (OTG Novoiavorivska), Tuchapy, Lisnovyci (OTG Horodotska), Richky, Kryvokamjanka, Nowa Kamjanka (OTG Rava-Ruska), Horodok, Cherlany (OTG Horodotska), Buchmy, Kulynyci, Byshkiv, Bobroidy (OTG Dobrosynsko-Maherivska), Domashiv (OTG Belzka), Pravda, Volynskie (OTG Sokalska).

5. Recommendations for sustainable exploitation of transboundary aquifers

5.1 Recommendations for transboundary groundwater management

Many approaches to transboundary groundwater management refer to sustainable water abstraction that do not disturb the long-term dynamic balance between recharge and discharge intensity (Doherty & Simmons, 2013; Højberg et al., 2007). In the researched cross-border area this is extremely important due to the presence of the Lublin-Lviv groundwater reservoir with strategic drinking water resources. The results of the simulation show that the regional quantitative status of Bug-San TBAs does not significantly deteriorate at the current level of exploitation, but in the light of the current geopolitical crisis and intensified migration of people in connection with the war in Ukraine and in the absence of joint management of groundwater resources, this problem will become an issue in the near future. It is recommended that the critical values of the regional drop in the groundwater level in TBAs should be introduced into the management practice and that groundwater resources available for management should be determined on their basis. This practice is already implemented in the Upper Pannonian transboundary area between Austria, Hungary, Slovakia, Slovenia and Croatia (Nádor et al., 2012; Tóth et al., 2016).
In this study, the critical value of the regional groundwater level drop at the level of 2 m was tested. The choice of this value was justified by the analysis of natural fluctuations of the groundwater table based on the results of monitoring from 23 observation points in a given region. In these calculations (for the period 2000-2021), a value of 1.8 m was obtained, which was considered typical for the seasonal amplitude of groundwater table fluctuations. Therefore, the assessment of groundwater resources available for management was based on the critical value of the regional groundwater level drop at the level of 2 m. The

methodology for assessing groundwater resources available for management is described in Impact assessment of groundwater abstraction on the level of useful resources available for use. The results of the assessment of groundwater resources available for management were analysed in terms of the size corresponding to administrative units (Figure 37), the resource module per 1 km2 (Figure 38) and 1 person (Figure 39).

The assessment of groundwater resources available for management for the balance unit (model area) performed in this study, selected according to the criterion of possible transboundary groundwater exchange within the meaning of international law, which applies to transboundary groundwater resources (Eckstein and Eckstein, 2003), is tantamount to an assessment of transboundary groundwater resources. The volume of transboundary groundwater resources available for management between Poland and Ukraine is shown in Figure 37 and Table 13.

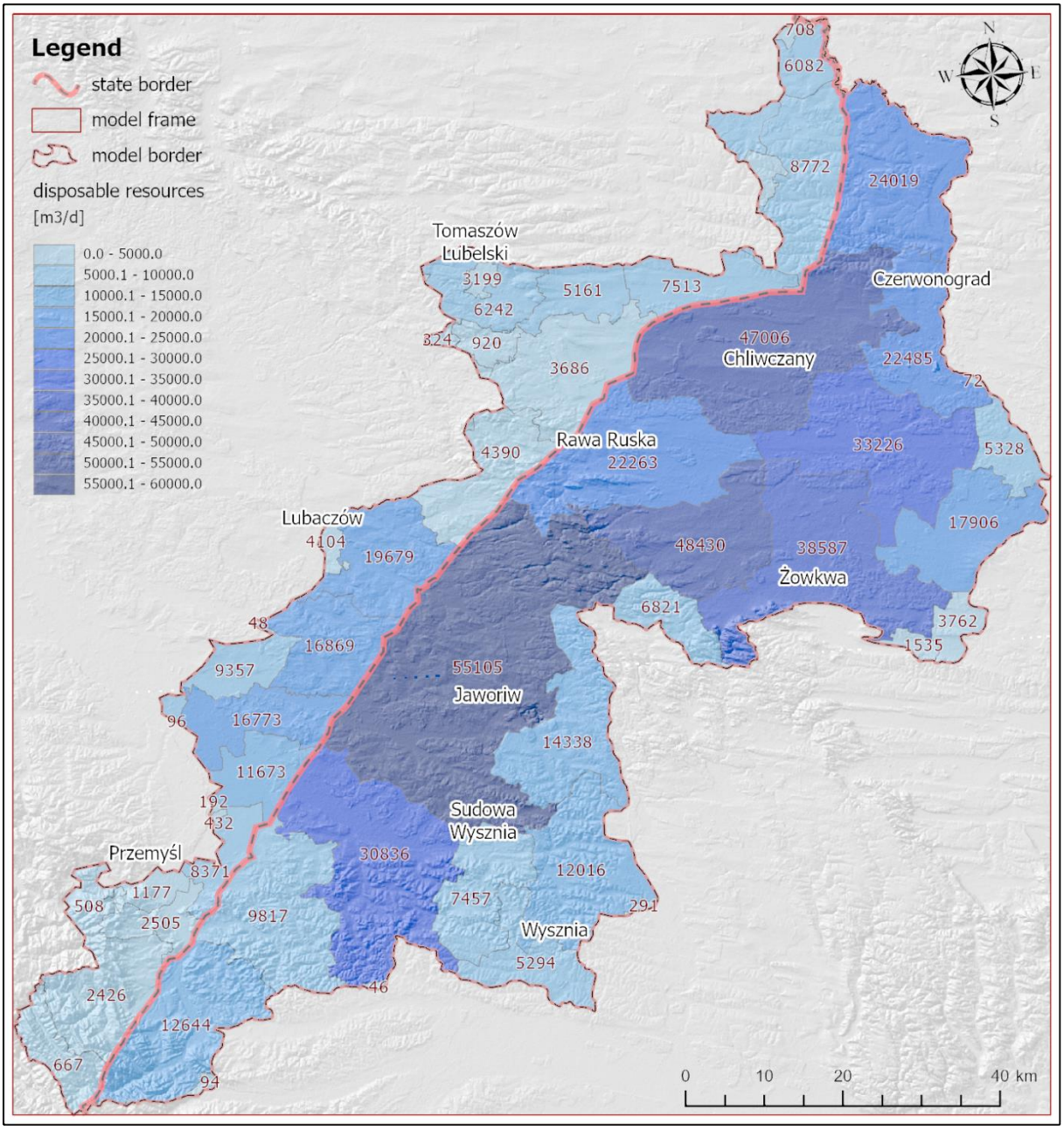

Figure 37. Cross-border groundwater resources available for management (available) within the boundaries of administrative units

Table 13 The volume of transboundary groundwater resources available for management between Poland and Ukraine

Poland		Ukraine	
Municipality	**Resources, m^3/d**	**Territorial communities**	**Resources, m^3/d**
Lubaczów *	19679	Yavorivska *	55105
Wielkie Oczy	16869	Dobrosynsko-Maherivska	48430
Radymno *	16773	Belzka	47006
Stubno	11673	Zhovkivska *	38587
Laszki *	9357	Velykomostivska	33226
Dołhobyczów *	8772	Mostyska *	30836
Medyka	8371	Sokalska *	24019
Ulhówek *	7513	Chervonohradska *	22485
Tomaszów Lubelski *	6242	Rava-Ruska	22263
Mircze *	6082	Kamianka-Buzka *	17906
Jarczów *	5161	Novoiavorivska *	14338
Horyniec-Zdrój *	4390	Dobromylska *	12644
Lubaczów (gm. miejska) *	4104	Horodotska *	12017
Lubycza Królewska *	3686	Shehynivska *	9817
Tomaszów Lubelski	3199	Sudovovyshnianska	7457
Przemyśl	2505	Ivano-Frankova *	6821
Fredropol *	2426	Dobrotvirska *	5328
M. Przemyśl *	1177	Rudkivska *	5294
Bełżec	920	Zhovtanetska *	3762
Hrubieszów *	708	Kulykivska *	1535
Ustrzyki Dolne - obszar wiejski *	667	Velykoliubinska *	291
Krasiczyn *	508	Khyrivska *	94
Żurawica *	432	Radekhivska *	72
Narol- obszar wiejski *	324	Biskovytska *	46
Orły *	192		
Radymno *	96		
Oleszyce *	48		

* - administrative units, occurring fragmentarily (within less than the entire area) within the study area

These results indicate that the value of transboundary groundwater resources, broken down by administrative units, ranges from 46 to 55,105 m3/d. It should be noted that the spatial distribution and size of transboundary groundwater resources shown in Figure 37 and Table 13 may introduce inaccuracies in interpretation, because relatively larger resources on the Ukrainian side are the result of a larger area of administrative units in this area, and not the actual abundance of the aquifer system. Therefore, converting these resources into a module gives an objective picture of the situation (Figure 38).

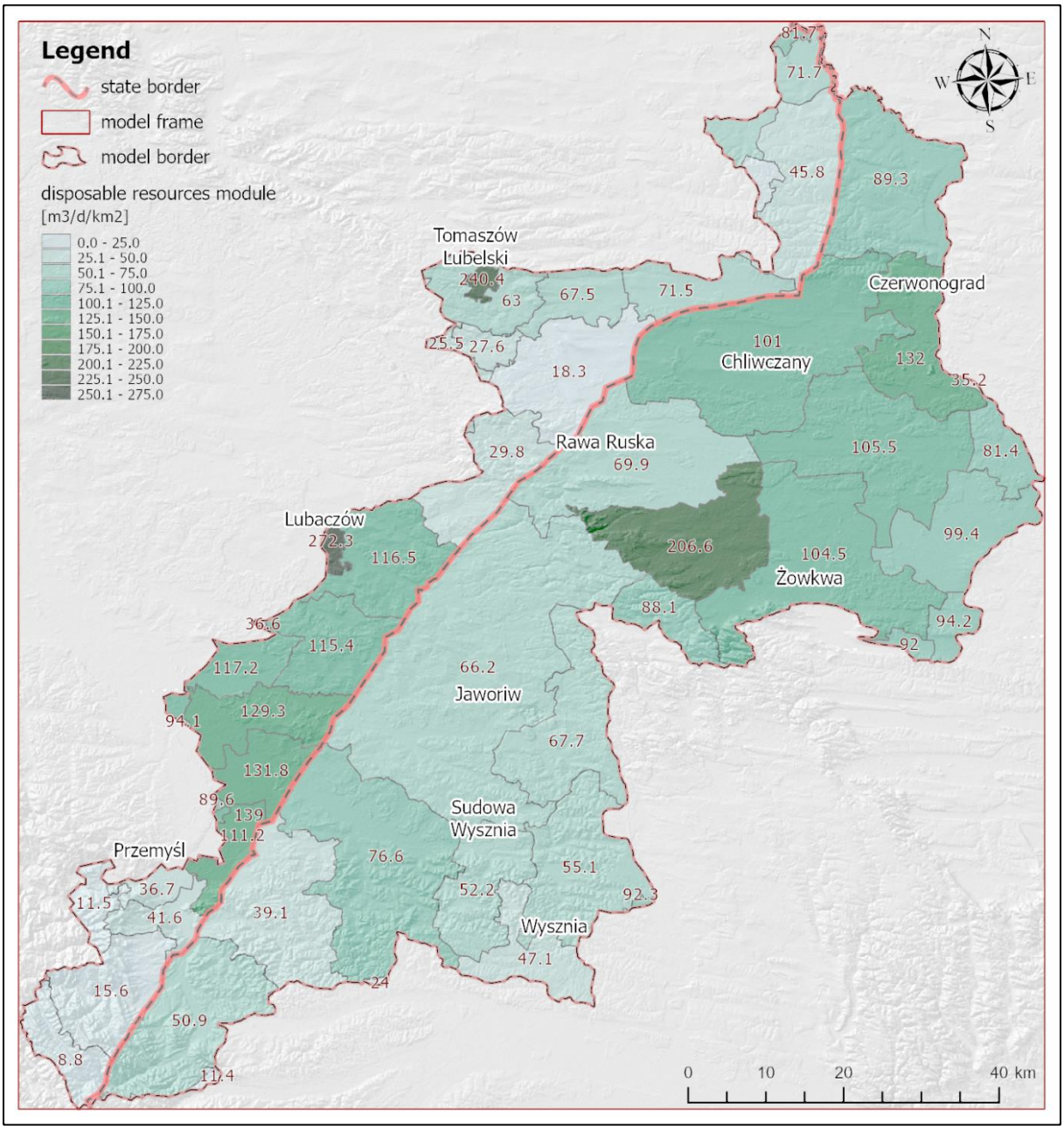

Figure 38. Cross-border groundwater resources available for management (disposable) within the boundaries of administrative units, converted into a module - $m^3/d/km^2$

If we look at Figure 38, we can see a larger modulus of transboundary groundwater resources in the Bug catchment in Ukraine, and in the San catchment in Poland. This is explained by the general rule - the gravitational groundwater circulation system is characterized by greater abundance in river valleys, which are the axes of groundwater drainage in the studied system. Therefore, in the study area, the drainage base in the Bug catchment is located in Ukraine, and the San River in Poland. This naturally determined regularity is somewhat disturbed by the current abstraction of groundwater. Therefore, in administrative units with drainage of mining areas (Ukraine - OTG Sokalska and Chervonohradska) and a high concentration of municipal intakes (Ukraine - OTG Rava-Ruska, Yavorivska, Shehynivska), the modulus of transboundary groundwater resources is lower than naturally determined.

The ranking of administrative units according to the size of transboundary groundwater resources available for management between Poland and Ukraine is presented in Tab. 14. In Poland, the modulus of transboundary groundwater resources available for management ranges from 9 to 272 $m^3/d/km^2$, on average 71 $m^3/d/ km^2$. The largest resources (over 100 $m^3/d/km^2$) are found in 9 communes: Lubaczów, Tomaszów Lubelski, Medyka, Stubno, Radymno, Laszki, Lubaczów, Wielkie Oczy and Żurawica. All these communes, apart from Tomaszów Lubelski, are located within the non-mountainous part of the San river basin. In Ukraine, the modulus of transboundary groundwater resources available for management ranges from 11 to 207 $m^3/d/km^2$, on average 79 $m^3/d/km^2$. The largest resources (above 100 $m^3/d/km^2$) occur in the OTG: Dobrosynsko-Maherivska, Chervonohradska, Velykomostivska, Zhovkivska and Belzka. All these territorial communities occur within the catchment area of the Bug River.

Table 14 Ranking of administrative units according to the size of transboundary groundwater resources between Poland and Ukraine available for management

Poland		Ukraine	
Municipality	**Resources, $m^3/d/km^2$**	**Territorial communities**	**Resources, $m^3/d/km^2$**
Lubaczów (gm. miejska) *	272	Dobrosynsko-Maherivska	207
Tomaszów Lubelski	240	Chervonohradska *	132
Medyka	139	Velykomostivska	106
Stubno	132	Zhovkivska *	104
Radymno *	129	Belzka	101
Laszki *	117	Kamianka-Buzka *	99
Lubaczów *	116	Zhovtanetska *	94
Wielkie Oczy	115	Velykoliubinska *	92
Żurawica *	111	Kulykivska *	92
Radymno *	94	Sokalska *	89
Orły *	90	Ivano-Frankova *	88
Hrubieszów *	82	Dobrotvirska *	81
Mircze *	72	Mostyska *	77
Ulhówek *	71	Rava-Ruska	70
Jarczów *	68	Novoiavorivska *	68
Tomaszów Lubelski *	63	Yavorivska *	66
Dołhobyczów *	46	Horodotska *	55
Przemyśl	42	Sudovovyshnianska	52
M. Przemyśl *	37	Dobromylska *	51
Oleszyce *	37	Rudkivska *	47
Horyniec-Zdrój *	30	Shehynivska *	39
Bełżec	28	Radekhivska *	35
Narol- obszar wiejski *	25	Biskovytska *	24
Lubycza Królewska *	18	Khyrivska *	11
Fredropol *	16		
Krasiczyn *	11		

Ustrzyki Dolne - obszar wiejski *	9

* - administrative units, occurring fragmentarily (within less than the entire area) within the study area

The key indicator in planning the management of groundwater resources is the number of people whose water needs can be satisfied from available resources. For this purpose, specific transboundary groundwater resources available for management (disposable) were recalculated in relation to the population size, assuming an average water consumption of 0.25 m3/d/person (Figure 39).

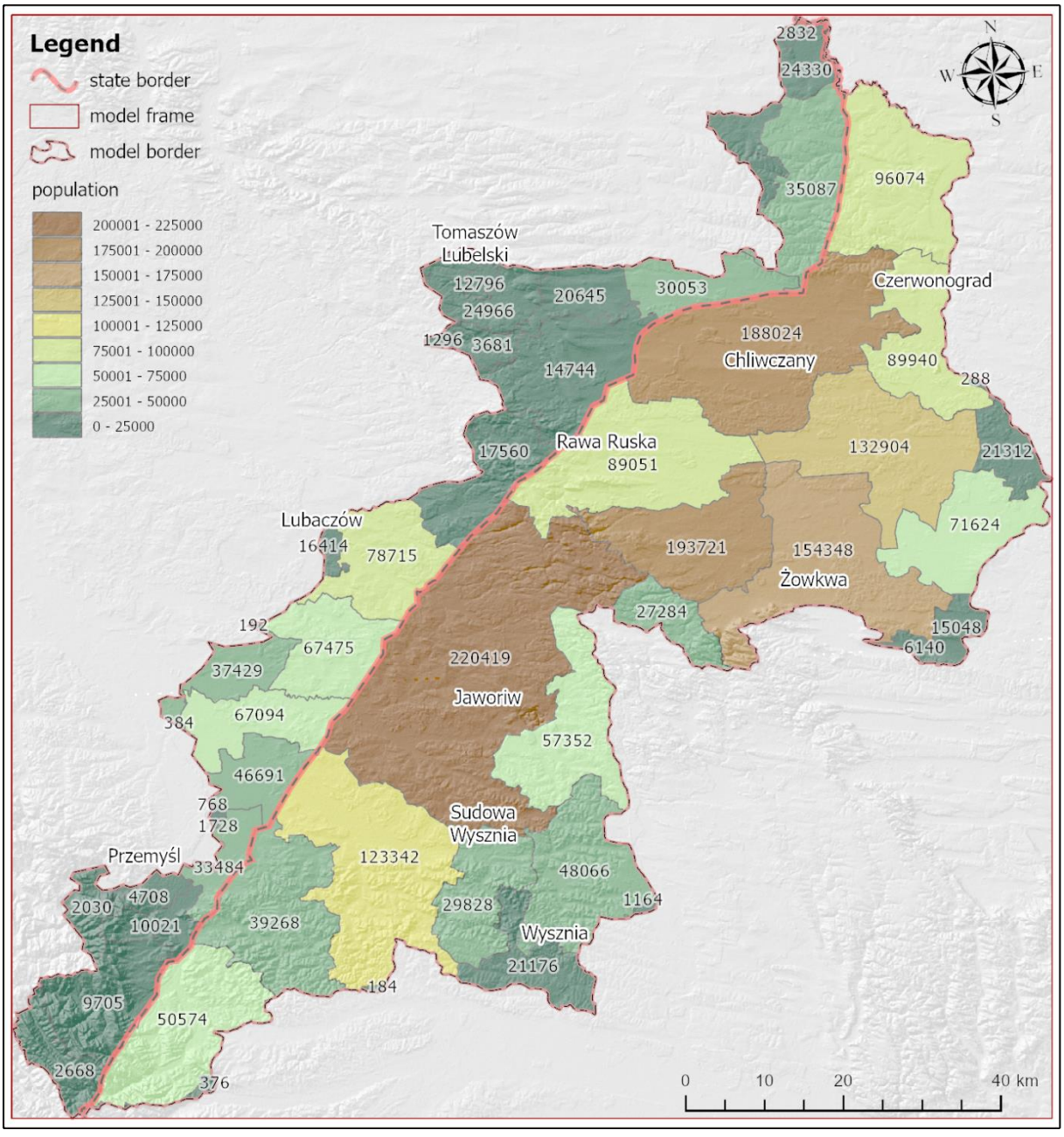

Figure 39. Population within administrative units whose water needs can be met from transboundary disposable groundwater resources (assuming average water consumption of 0.25 m^3/day/person)

The data in Figure 39 indicate the maximum possible number of consumers of transboundary available groundwater resources within the boundaries of administrative units or their parts. On their basis, it is possible to calculate the reserve number of consumers after subtracting

the current number, which is of particular importance in the light of the migration crisis caused by the war in Ukraine (Table 15).

Table 15 Ranking of administrative units according to the number of people whose water needs can be met from transboundary disposable groundwater resources

Poland		Ukraine		
Municipality	**Max no of consumers**	**Territorial communities**	**Max no of consumers**	**Reserve number of consumers**
Lubaczów *	78 715	Yavorivska *	220 419	168 372
Wielkie Oczy	67 475	Dobrosynsko-Maherivska	193 721	177 483
Radymno *	67 094	Belzka	188 024	173 197
Stubno	46 691	Zhovkivska *	154 348	121 246
Laszki *	37 429	Velykomostivska	132 904	116 820
Dołhobyczów *	35 087	Mostyska *	123 342	93 828
Medyka	33 484	Sokalska *	96 074	75 348
Ulhówek *	30 053	Chervonohradska *	89 940	20 385
Tomaszów Lubelski *	24 966	Rava-Ruska	89 051	63 357
Mircze *	24 330	Kamianka-Buzka *	71 624	60 398
Jarczów *	20 645	Novoiavorivska *	57 352	17 461
Horyniec-Zdrój *	17 560	Dobromylska *	50 574	33 653
Lubaczów (gm. miejska) *	16 414	Horodotska *	48 066	24 967
Lubycza Królewska *	14 744	Shehynivska *	39 268	28 617
Tomaszów Lubelski	12 796	Sudovovyshnianska	29 828	16 987
Przemyśl	10 021	Ivano-Frankova *	27 284	23 628
Fredropol *	9 705	Dobrotvirska *	21 312	16 703
M. Przemyśl *	4 708	Rudkivska *	21 176	11 778
Bełżec	3 681	Zhovtanetska *	15 048	12 363
Hrubieszów *	2 832	Kulykivska *	6 140	1 639
Ustrzyki Dolne - obszar wiejski *	2 668	Velykoliubinska *	1 164	939
Krasiczyn *	2 030	Khyrivska *	376	-200
Żurawica *	1 728	Radekhivska *	288	115
Narol- obszar wiejski *	1 296	Biskovytska *	184	24
Orły *	768			
Radymno *	384			
Oleszyce *	192			

* - administrative units, occurring fragmentarily (within less than the entire area) within the study area

The data **in** Figure 39 **indicate the maximum possible number of consumers of transboundary available groundwater resources within the boundaries of administrative units or their parts. On their basis, it is possible to calculate the reserve number of consumers after subtracting the current number, which is of particular importance in the light of the migration crisis caused by the war in Ukraine (**Table 15**).**

Table 15 shows that in the Polish part of the study area, the possibilities of meeting water needs from transboundary disposable groundwater resources (assuming average water consumption at the level of 0.25 m^3/d/person) are more than twice lower, but this is only due to significantly smaller share of its area within the area of occurrence of TBAs. For the Ukrainian part, a reserve number of consumers of transboundary available groundwater resources was additionally calculated, comparing the maximum possible number with the current state for 2020. These results indicate that the largest reserves (more than 10 times) taking into account the current number of consumers are characteristic for OTG - Dobrosynsko-Maherivska and Belzka. Also high reserves (more than 5 times) typical for OTG - Velykomostivska, Kamianka-Buzka and Ivano-Frankova. The following OTGs have the lowest reserve (below 100%):

- Radekhivska – the potential to increase consumers reaches 66% compared to the current number;
- Novoiavorivska – 44%;
- Kulykivska – 36%;
- Chervonohradska – 29%;
- Biskovytska – 15%.

It is worth mentioning the Khyrivska OTG, where there is no reserve for increasing consumers, and the current level of use of groundwater resources already exceeds (by 35%) the value of available resources that can be used taking into account the needs of the environment.

This study, the first such assessment of the state of transboundary aquifers, provides important scientific support for the establishment of a joint management system for transboundary groundwater resources between Poland and Ukraine. Very important elements of this study are:

- a uniform and coherent database on the state of TABs;
- specified size of transboundary disposable groundwater resources;
- analysis of the effects of various pressure scenarios of the TBAs system.

On the other hand, the interpretation of the data obtained in the context of the management of transboundary groundwater resources is difficult because the status of international law applicable to transboundary groundwater resources has not yet been specified. The rules governing the use, allocation, protection and management of this resource across borders are still unclear. UNECE Water Convention – a key issue in international law in the field of transboundary waters, leaves many unanswered questions.

Another issue is the lack of a management plan for transboundary groundwater resources between Poland and Ukraine, which would establish mutually acceptable rules for sharing common resources. There is no trade water rights in Poland and Ukraine. The only legal document where the groundwater extraction limit is registered is the water permit. The user may not transfer or sell the excess allocated water resources to other users, although he has paid for the reservation of water in accordance with the limit. This issue is neglected because there is no shortage of groundwater resources in the Polish-Ukrainian border area and there is no incentive to use the trade water rights to solve cross-border water conflicts. Our simulations show the likelihood of conflicts when all users start using the allowed limits. It is recommended to create a joint Polish-Ukrainian platform for the coordination of water permits, as the conducted research confirmed the impact of groundwater exploitation on the neighbouring country's water resources. Considering the fact that Ukraine is in a disadvantageous situation in the Bug sub-basin, because it is located in the lower reaches of

the river, and in the San sub-basin the situation is the opposite, both countries are motivated to implement the water rights system. The concept of interstate trade in water rights would include compensation for the downstream state for excess water used in the upstream state.

6. Conclusions

The assessment of the impact of groundwater exploitation on the condition of TBAs was carried out using an improved numerical model originally created for the implementation of tasks in WP3. The development of the existing dynamic model involved transforming it into a form enabling the simulation of filtration field constraints in the vicinity of the boundary surface. A new conceptual model of the TBAs aquifer system was developed, which guaranteed the continuity of the filtration field in the model area, and at the same time allowed the calculations to take into account the complex structure of the regional system, including three large tectonic units with different geological characteristics. The structure of the numerical flow model was designed, which took into account the complex conditions of groundwater occurrence and circulation in the studied system. Tables of input data were prepared in the format of GIS information layers, which, after being imported into the filter field model, allowed to take into account the complex geometry of the system and the spatial variability of parameters. A method of implementing the boundary problem in the vicinity of sections of the boundary surface representing morphological watersheds was developed. For this purpose, the condition of the III type in the General Head variant was used, which allowed the mapping of the variable nature of the boundary surface and guaranteed the correct description of the system's relationship with the environment during the simulation of groundwater abstraction.

The Bug-San TBAs model is characterized by high numerical stability, and thanks to the continuity of the filtration field, it is a unique tool used to simulate various variants of groundwater abstraction and quantitative assessment of cross-border flows between Poland and Ukraine. Four TBAs (porous alluvial, fractured Upper Cretaceous, fractured-cavernous Lower Neogene and porous Quaternary fluvioglacial) were jointly simulated to properly account for the main water exchange processes that are caused by two separate regional flow systems controlled by the Bug and San rivers. For the first time, an area with significant transboundary flows was identified, which covers only 28% of the border area defined along the boundaries of the transboundary river sub-basins. The balance of interstate groundwater exchange turned out to be positive for Ukraine and negative for Poland. The volume of flow from Poland to Ukraine is more than 1.5 times higher than from the opposite direction. The largest cross-border flows occur within the Bug sub-basin, in the fractured Upper Cretaceous aquifer.

The exploitation of groundwater at the current level does not cause inter-state interception of resources and the formation of transboundary dropdown cones, but there are noticeable effects of impacts on river water resources and transboundary groundwater flow. It was estimated that groundwater outflow to rivers decreased by 6.9% and 26.8% respectively for Poland and Ukraine, and infiltration losses of water through the riverbed increased (to 5.7% - in Poland and 9.6% - in Ukraine). In the analysed scenario, there is a tendency to reduce the amount of transboundary groundwater exchange. Compared to the natural state, the decrease values are at the level of 0.7% for the transboundary groundwater flow from Poland to Ukraine and 1.8% - in the opposite direction. As a result, it can be concluded that more

than doubling the abstraction of groundwater slightly reduces the transboundary groundwater flow in both directions, but the San sub-basin is affected to a greater extent.

The last element of the work was the assessment of transboundary groundwater resources available for management. Larger resources of transboundary groundwater occur in the catchment area of the Bug River than in the catchment area of the San River. The largest resources (over 100 $m^3/d/km^2$) are found in 9 Polish communes (Lubaczów, Tomaszów Lubelski, Medyka, Stubno, Radymno, Laszki, Lubaczów, Wielkie Oczy and Żurawica) and 5 in Ukraine (Dobrosynsko-Maherivska, Chervonohradska, Velykomostivska , Zhovkivska and Belzka).

This study, the first of its kind to assess the status and resources of TBAs, provides important scientific support for the establishment of a joint management system for transboundary groundwater resources between Poland and Ukraine. Currently, a broader legal consensus, improvement of institutional relations, integration of monitoring and assessment systems of water status are needed to implement the suggested transboundary management in practice. Particular attention should be paid to GDEs as their sustainability depends on appropriate environmental policies and groundwater management practices. GDEs are often not sufficiently taken into account in the management of groundwater resources. With the help of the created model of TBAs, a better understanding of the functioning of the GDE can be achieved.

7. References

Abdikan, S., Sanli, F.B., Ustuner, M., Calò, F., 2016. Land cover mapping using Sentinel-1 SAR data. The international archives of the photogrammetry, remote sensing and spatial information sciences XLI-B7, 757–761.

De Luca, G., João, M., Silva, N., Fazio, S.D., Modica, G., 2022. Integrated use of Sentinel-1 and Sentinel-2 data and open-source machine learning algorithms for land cover mapping in a Mediterranean region. European Journal of Remote Sensing 55(1), 52–70.

Doherty, J., Simmons, C.T., 2013. Groundwater modelling in decision support: reflections on a unified conceptual framework. Hydrogeol. J., 21, 1531-1537. https://doi.org/10.1007/s10040-013-1027-7

Du, Y., Zhang, Y., Ling, F., Wang, Q., Li, W., Li, X., 2016. Water bodies' mapping from Sentinel-2 imagery with Modified Normalized Difference Water Index at 10-m spatial resolution produced by sharpening the SWIR Band. Remote Sens. 8, 354–372.

Eckstein, G., Eckstein, Y., 2003. A Hydrogeological Approach to Transboundary Ground Water Resources and International Law. American University International Law Review 19, no. 2: 201-258.

El Kati I., Nakhcha Ch., El Bakhchouch O., Tabyaoui H., 2018. Application of Aster and Sentinel-2A images for geological mapping in arid regions: the safsafate area in the neogen Guercif basin, Northern Morocco. International Journal of Advanced Remote Sensing and GIS 2018, Volume 7, Issue 1, pp. 2782-2792 https://doi.org/10.23953/cloud.ijarsg.374

EU, 2000. Directive 2000/60/EC of the European Parliament and of the Council of 23 October 2000 establishing a framework for Community action in the field of water policy. https://eur-lex.europa.eu/eli/dir/2000/60

Højberg, A.L., Refsgaard, J.C., Geer, F., Jørgensen, L.F., Zsuffa I., 2007. Use of models to support the monitoring requirements in the water framework directive. Water Resour Manag, 21, 1649-1672. https://doi.org/10.1007/s11269-006-9119-y

Janiec, B., 1984. Wody podziemne w strefie południowo-zachodniej krawędzi Wyżyny Lubelskiej. Wyd. Geol., Warszawa.

Jiang, H., Wang, M., Hu, H., Xu, J., 2021. Evaluating the performance of Sentinel-1A and Sentinel-2 in small waterbody mapping over urban and mountainous regions. Water 13, 945–960.
Kamzist, Zh. S., Shevchenko, O.L., 2009. Hidroheolohiia Ukrainy. Navchalnyi posibnyk, Inkos. [in ukrainian].
Kati, I.E., Nakhcha, C., Bakhchouch, O.E., Tabyaoui, H., 2018. Application of Aster and Sentinel-2A images for geological mapping in Arid Regions: the Safsafate area in the Neogen Guercif basin, Northern Morocco. International Journal of Advanced Remote Sensing and GIS 7 (1), 2782–2792.
Kelling, G., Walton, E.K., Simpson, F., 2007. The contribution of Stanisław Dżułyński to flysch sedimentology: A 'Western' perspective. Annales Societatis Geologorum Poloniae. 77, 93–103.
Ksenak, L., Pukanská, K., Bartoš, K., Blišťan, P., 2022. Assessment of the usability of SAR and optical satellite data for monitoring spatio-temporal changes in surface water: bodrog river case study. Water 14, 299–321.
Kumar, D., 2021. Urban objects detection from C-band synthetic aperture radar (SAR) satellite images through simulating filter properties. Scientific Reports, 1-24.
Lorenc, H., 2005. Atlas klimatu Polski, IMGW. [in polish].
Michalczyk, Z., Bartoszewski, S., Turczyński, M., 2002. The water conditions of the Polesie Region. Acta Agroph., 66, 49-76.
Nádor, A., Lapanje, A., Tóth, G., Rman, N., Szőcs, T., Prestor, J., Uhrin, A., Rajver, D., Fodor, F., Muráti, J., Székely E., 2012. Transboundary geothermal resources of the Mura-Zala basin: joint thermal aquifer management of Slovenia and Hungary. Geologija, 55, 209-224. https://doi.org/10.5474/geologija.2012.013
Nazaruk, M., 2018. Pryrodni umovy ta pryrodni resursy Lvivshchyny, LNU. [in ukrainian].
Paczyński, B., Sadurski, A., 2007. Hydrogeologia regionalna Polski, t. I. Państwowy Instytut Geologiczny. [in polish].
Pankiv, R., Kost, M., Sakhnyuk, I., Harasymchuk, V., Maykut, O., Mandzya, O., Kozak, R., Palchykova, O., 2013. Ekolohichna otsinka yakosti vod verkhnoyi chastyny baseynu Zakhidnoho Buhu. Heolohiya i heokhimiya horyuchykh kopalyn, № 1–2, 62-74. [in ukrainian].
Sadurski A., 2016. Disposable groundwater resources of river basins in Poland in the light of sustainable management. Biuletyn Państwowego Instytutu geologicznego nr 466, pp. 261-270 [in Polish]
Solon, J., Borzyszkowski, J., Bidłasik, M., Richling, A., Badora, K., Balon, J., Brzezińska-Wójcik, T., Chabudziński, Ł., Dobrowolski, R., Grzegorczyk, I., Jodłowski, M., Kistowski, M., Kot, R., Krąż, P., Lechnio, J., Macias, A., Majchrowska, A., Malinowska, E., Migoń, P., Myga-Piątek, U., Nita, J., Papińska, E., Rodzik, J., Strzyż, M., Terpiłowski, S., Ziaja, W., 2018. Physico-geographical mesoregions of Poland: verification and adjustment of boundaries on the basis of contemporary spatial data. Geographia Polonica. 91, Issue 2, 143-170. doi:10.7163/GPol.0115.
Shen, G., Fu, W., Guo, H., Liao, J., 2022. Water body mapping using long time series Sentinel-1 SAR data in Poyang Lake. Water 14, 1902–1927.
Studer B., 1872. Index der Petrographie und Stratigraphie der Schweiz, Bern.
Szczepański A., 2008. Metodyka modelowego bilansowania zasobów wód podziemnych w ich zlewniowym zagospodarowaniu. Biuletyn Państwowego Instytutu Geologicznego no 431, pp. 201 – 208 [in Polish]
Śmietański L., 2012. Zastosowanie przekształcenia stałoobjętościowego do oceny odnawialności zasobów wód podziemnych wschodniej części pojezierza pomorskiego. Biuletyn Państwowego Instytutu Geologicznego no 451, pp. 227 – 234 [in Polish]
Tian, H., Li, W., Wu, M., Huang, N., Li, G., Li, X., Niu, Z., 2017. Dynamic monitoring of the largest Freshwater Lake in China using a new water index derived from high spatiotemporal resolution Sentinel-1A data. Remote Sens. 9, 521–528.

Tóth, G., Rman, N., Ágnes, R.S., Kerékgyártó, T., Szcs, T., Lapanje, A., Černák, R., Remsík, A., Schubert, G., Nádor, A., 2016. Transboundary fresh and thermal groundwater flows in the west part of the Pannonian Basin. Renewable and Sustainable Energy Reviews, 57, 439-454. https://doi.org/10.1016/j.rser.2015.12.021.

Yesou, H., Pottier, E., Mercier, G., Grizonnet, M., Haouet, S., Giros, A., Faivre, R., Huber, C., Michel, J., 2016. Synergy of Sentinel-1 and Sentinel-2 imagery for wetland monitoring information extraction from continuous flow of sentinel images applied to water bodies and vegetation mapping and monitoring. Conference: IGARSS 2016 - IEEE international geoscience and remote sensing, 1–5 doi:10.1109/IGARSS.2016.7729033

Table of Contents

List of Figures

List of Tables

1. Conceptual hydrogeological model

The assessment of the exploitation of groundwater resources in the Estonian-Latvian transboundary area is based on 3D groundwater flow modelling according to previously established conceptual understanding of the pilot area (Figure 1) (see EU-WATERRES report “Assessment of the resources of transboundary groundwater reservoirs for the 2 pilot areas” and article by Retike *et al.,* 2021). The conceptual understanding covers hydrogeological settings of the transboundary area (aquifers, aquitards), hydraulic characteristics of hydrogeological units, climate, major surface water/hydrological units (lakes, rivers) that interact with groundwater as well as major anthropogenic pressures, including groundwater intakes and mining activities.

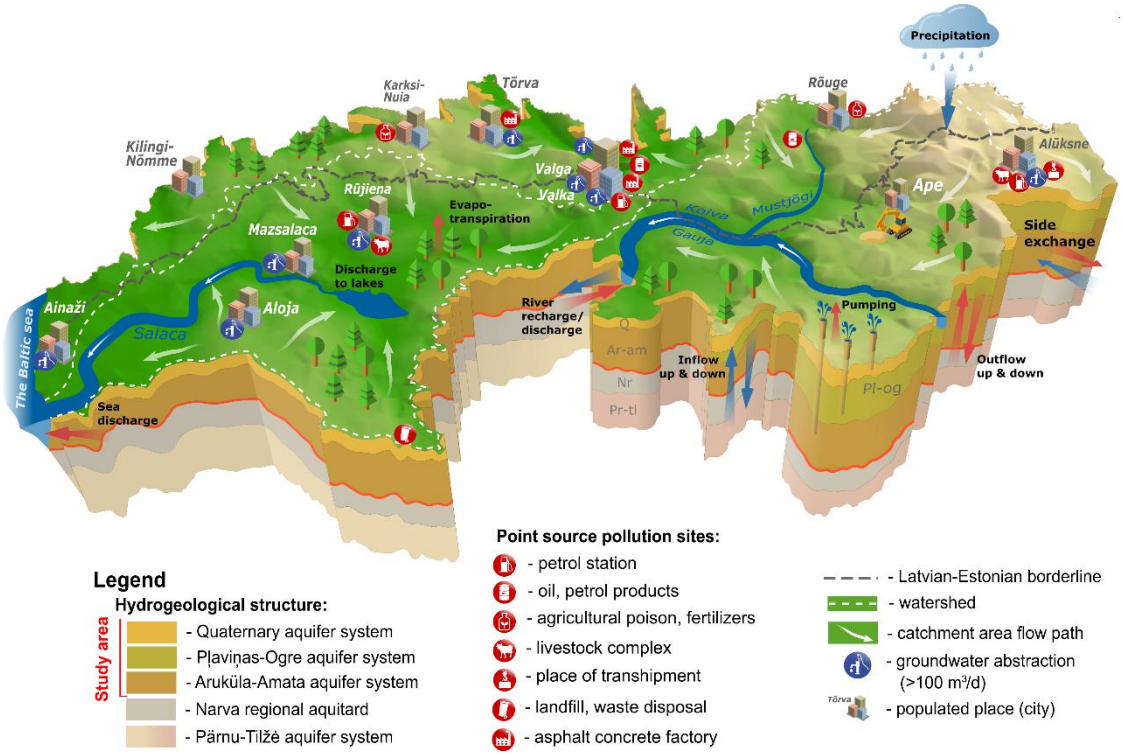

Figure 1. Conceptual model of the Latvian-Estonian transboundary aquifers

1.1 Description of Model Area

The model area is located in the North-East of Europe, on the coast of the Baltic Sea (Figure 2). The model area that covers about 45 000 km^2 is bounded to the west by the Baltic Sea and east by Lake Peipsi and Lake Pihkva. The Gauja River, which drains northeastwards into the Baltic Sea, is the dominant perennial river in the region. Ema River and Võhandu River drain westwards into Lake Peipsi.

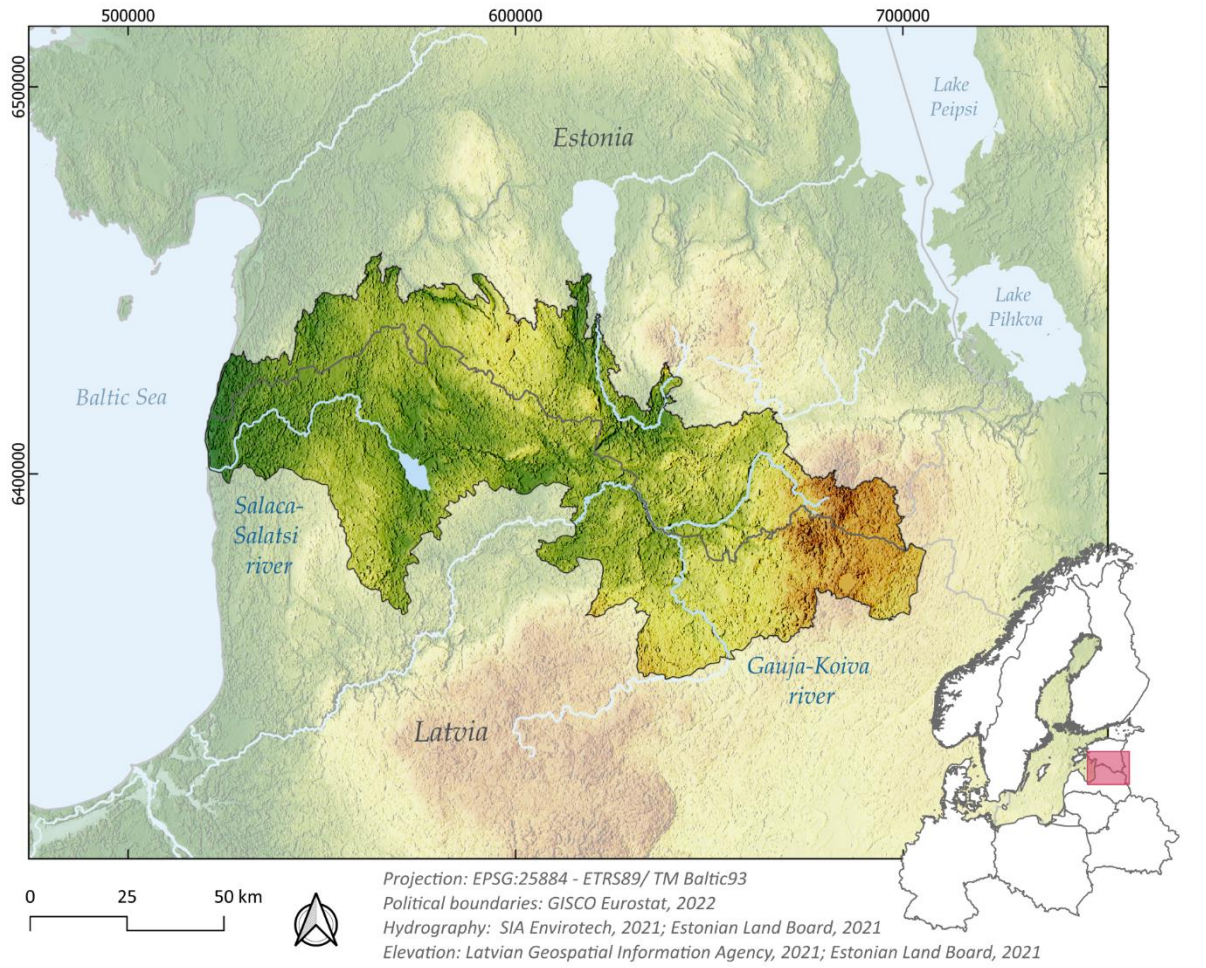

Figure 2. Location of Latvia-Estonia transboundary area. The figure encompasses the model domain

Southern Estonia and northern Latvia are located on the Great Northern European Plain. The region's topography is typically flat in coastal regions, and hilly in the inland eastern part, with the ground elevation ranging from 0 to 320 m above mean sea level (a.m.s.l).

The land use in the area is dominated by forest and semi-natural areas. Forest and woodland are usually a mixture of coniferous spruce, pine, white birch, ash, maple, and aspen, covering 58% of the study area. Forest and semi-natural areas are followed by agricultural areas, wetlands, and artificial surfaces (European Environment Agency, 2018).

The climate in the region is considered moderately cool and humid (Vallner, 2016). The long-term average annual precipitation at Valga weather station (Figure 3), in the central part of the study area, is 675 mm/yr for 1991–2020; June, August, and October are the wettest months, and March and April are the driest months. The average annual air temperature at Valga from 1991 to 2020 was 6.3°C. The maximum average monthly temperature of 23.6°C occurs in July, and the minimum average monthly temperature of -6.6°C occurs in January (Estonia Environmental Agency, 2022).

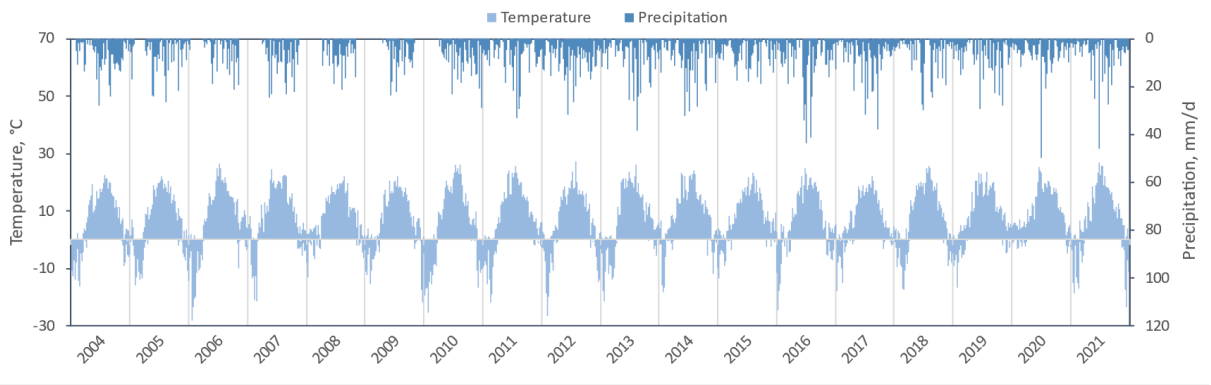

Figure 3. Daily precipitation and the average temperature at Valga weather station (Estonia Environmental Agency, 2022)

Hydrogeologic Units

The model area is underlain by Paleozoic (Cambrian, Ordovician, Silurian, and Devonian) and Proterozoic (Ediacaran) sedimentary bedrock (primarily sandstone and limestone) overlying Precambrian crystalline bedrock. Bedrock is largely flat lying, dipping regionally about 1 to 3 meters per kilometer. Unlithified glacial deposits overlie the bedrock formations over most of the model area. Since this study concentrates on transboundary groundwater bodies, only upper units (Quaternary sediments, Devonian, and upper part of Silurian formations) are included in the groundwater model.

Geologic units were grouped into hydrogeologic units based on lithologic and hydrologic (hydraulic conductivity and unit geometry) characteristics. Solovey *et al.* (2021) delineated five hydrogeologic units in the model area listed from upper to lower:

- Quaternary aquifer system (Q)
- Upper-Devonian (Pļaviņas-Ogre) aquifer system (D_3)
- Upper-Middle-Devonian (Aruküla-Amata) aquifer system ($D_{3\text{-}2}$)
- Narva regional aquitard (D_2nr)
- Lower-Middle-Devonian aquifer system ($D_{2\text{-}1}$)

The uppermost aquifer system in the model area is formed by Quaternary sediments, which mostly consist of glacial till and glaciolacustrine sandy loam. **The Quaternary aquifer** is directly affected by meteorological conditions, and most groundwater discharge flows through it to deeper aquifers (Perens and Vallner, 1997). The thickness of the Quaternary deposits varies in the model area from less than 10 m to up to 100 m in buried valleys.

In the south-eastern part of the model territory, the **Upper-Devonian (Pļaviņas-Ogre) aquifer system**, composed mainly of carbonate sediments (karstified or fissured dolomites and limestones), is embedded under Quaternary sediments. It consists of Pļaviņas, Salaspils

(Dubnik), Daugava, Katleši, and Ogre Stages. The thickness of the aquifer system range in the study area from 17–110 m, and the depth from 10 m to 100 m.

The Upper-Middle-Devonian (Aruküla-Amata) aquifer system underlies the Upper-Devonian (Pļaviņas-Ogre) aquifer system deposits in the southeast model area or directly below the Quaternary sediments elsewhere. The Upper-Middle-Devonian (Aruküla-Amata) aquifer system consists of Amata, Gauja, Burtnieki, and Aruküla Stages, and its thickness can reach up to 380 m. The aquifer system is formed by terrigenous sedimentary formations, mostly sandstones with clay and siltstone interlayers. The Middle-Devonian Narva Stage surface forms the base of the Upper-Middle-Devonian (Aruküla-Amata) aquifer system.

Narva regional aquitard, which consists of Middle-Devonian Narva Stage marl and clay sediments, separates the active water exchange zone from the slow water exchange zone in the study area. The aquitard system's total thickness ranges from less than 50 m to more than 110 m. The Narva regional aquitard extends across the southern portion of the model area and is absent to the north.

Below the Narva regional aquitard system lies **the Middle-Lower-Devonian-Silurian aquifer system**. The Middle-Lower-Devonian-Silurian aquifer system is formed by Devonian Pärnu, Rēzekne, Ķemeri, Gargždai, and Tilžė Stage, as well as Silurian Raikküla, Adavere, Jaani, and Jaagarahu Stages. The aquifer system consists mainly of sandstone, siltstone, and Silurian carbonates. As in Estonia, Silurian carbonates' upper part is heavily karstified; these formations are also considered part of the aquifer system. Deeper than 100 m from the bedrock surface, carbonates turn into the Silurian-Ordovician regional aquitard (Vallner, 2016).

Hydraulic Conductivity

Horizontal hydraulic conductivity was estimated for the hydrogeologic units using available field pumping test measurements (GSE, 2021; LEGMC, 2021). Data were compiled and analyzed for 458 wells containing hydraulic conductivity, well-construction data, and lithologic descriptions. The median values of estimated hydraulic conductivity for the aquifers (Table 1) are similar in magnitude to values compiled by Virbulis *et al.* (2013).

Table 1. Summary of measured horizontal hydraulic conductivities, by hydrogeologic unit

Hydrogeologic unit	Number of wells	Hydraulic conductivity (m/d)		
		Minimum	Median	Maximum
Quaternary (Q)	339	0.01	12.00	258.80
Upper-Devonian (D_3)	25	0.20	2.30	140.00
Upper-Middle-Devonian (D_{3-2})	49	0.06	3.60	72.70

Middle-Lower-Devonian-Silurian (D_{2-1}-S)	45	0.10	5.43	34.70

Water Budget

Previous water budget calculations are available only for the Estonian area. A groundwater budget for each groundwater body (GWB) (Marandi *et al.*, 2019) and aquifer (Vallner, 2016) is presented in table 2. In both studies, the water budget is calculated with the steady-state regional groundwater model.

Table 2. Groundwater flow of the model area

	Inflow (m^3/d)			Outflow (m^3/d)			Water exchange (m^3/d)
	Lateral	From above	From below	Lateral	Up	Down	
D_3 aquifer[a]	3 100	194 200	<100	16 600	<100	180 600	197 200
GWB nr 26[b]	33 489	188 095		185 168	36 418*		221 586
D_{3-2} aquifer[a]	77 200	2 562 100	200	464 200	1 943 400	23 900	2 639 500
GWB nr 23[b]	42 673	355 895	61 678	56 135	234 482*	169 630	460 246
GWB nr 24[b]	372 269	1 720 866	135 700	292 758	1 805 160*	130 920	2 228 835
GWB nr 25[b]	116 080	420 605		243 343	293 000*	1	536 689
D_{2-1} aquifer[a]	48 500	281 700	101 000	22 500	330 400	78 300	431 200
GWB nr 22[b]	199 376	81 096	24 845	181 447	99 098*	24 776	305 317
GWB nr 21[b]	168 860	167 010	70 101	129 373	226 150*	50 454	405 971

[a] Vallner 2012

[b] Marandi et al. 2019

* Directly to channel network

2. Numerical model of groundwater flows in transboundary aquifers

2.1 Model grid and boundary conditions

A 3D groundwater flow model was developed using open-source software MODFLOW-NWT (Niswonger *et al.*, 2011) using the user interface of the open-source software ModelMuse (Winston, 2019) developed by the U.S. Geological Survey. MODFLOW-NWT uses the finite-difference method to numerically solve the three-dimensional groundwater flow equation in a porous medium. MODFLOW-NWT's modular design allows it to represent groundwater-flow system processes, including recharge, flow, discharge, and interactions between aquifers and surface bodies. This report describes a model that simulates transient conditions. Transient groundwater flow is a dynamic system in which inflows, outflows, and groundwater storage change over time. Recharge, discharge, and other groundwater-flow system processes are simulated based on yearly variations.

2.1.1 Model Grid and Layering

MODFLOW calculates hydraulic heads and flows within the model domain using data sets describing a groundwater-flow system's hydrogeologic units, recharge, and discharge. To run the program, it is necessary to subdivide the groundwater-flow system into model cells vertically and horizontally. Each cell is assumed to have homogeneous hydraulic properties. The study area was horizontally discretized into square cells of 250 to 1000 m side length.

The model's grid comprises eleven layers with varying thicknesses, with about 200 000 cells within each layer covering an area of 45 000 km^2. In the model, the three-dimensional hydrogeologic framework and vertical layering were represented using the hydrogeologic units defined by Solovey *et al.* (2021) and Virbulis *et al.* (2013). The thickness of hydrogeologic units in the study area may vary considerably over short distances due to buried valleys, and most units are not spatially contiguous throughout the model area. Figure 4 illustrates the extent of active cells in each layer.

The geological surfaces of model layers vary spatially and correspond to the data published by Virbulis *et al.* (2013). The Quaternary sediment unit is represented by layers 1 and 2 in the model (Table 3). The bedrock unit was divided into four aquifer and aquitard units – the Upper-Devonian (Pļaviņas-Ogre) aquifer system (layers 3–6), the Upper-Middle-Devonian (Aruküla-Amata) aquifer system (layers 7–9), Narva regional aquitard (layer 10), and the Lower-Middle-Devonian-Silurian aquifer system (layer 11). Model bottom (bottom of layer 11) represents the Silurian-Ordovician aquitard surface and is defined as a no-flow boundary.

For the model to work, all layers must be present in all active cells. When hydrogeologic units constituting a model layer were absent, the layer was altered to ensure proper model operation. In that case, model layers were assigned 1-meter thicknesses, and the specified hydraulic properties were changed to reflect the Quaternary aquifer system's hydraulic conductivity. In this way, the "altered" layer is treated as if it were a part of the adjacent model layer.

Table 3. Generalized stratigraphy, hydrostratigraphy, and model layers (modified from Koit et al., 2022)

Age	Series	Stage	Regional Stage	Index	Aquifer system	Aquifer type	Groundwater bodies		Model layer
							Estonia	Latvia	
Quaternary	Holocene	Meghalayan			Quaternary (Q)	Sand, gravel and loam	Attached to the first embedded GWB		Layers 1, 2
		Northgrippian							
		Greenlandian							
	Pleistocene	Upper							
		Middle							
Devonian	Upper-Devonian	Frasnian	Ogre	D_3og	Upper-Devonian (D_3)	Fractured and karstified carbonate	26	D6, D8	Layers 3, 4
			Katleši	D_3kt					
			Daugava	D_3dg					Layers 5, 6
			Dubniki	D_3db					
			Pļaviņas	D_3pl					
	Middle-Devonian		Amata	D_3am/D_2am	Middle-Devonian (Estonia)/Upper-Middle-Devonian (Latvia) (D_{3-2})	Sandstone	23, 24, 25	A8, A10	Layers 7, 8
			Gauja	D_3gj/D_2gj					
		Givetian	Burtnieki	D_2br					Layer 9
			Aruküla	D_2ar					
		Eifelian	Narva	D_2nr	Narva regional aquitard				Layer 10
	Lower-Devonian		Pärnu	D_1pr	Lower-Middle-Devonian-Silurian (D_{2-1}-S)	Sandstone and fractured, karstified carbonate	21, 22	P	Layer 11
		Emsian	Rēzekne	D_1rz					
			Ķemeri	D_1km					
		Pragian							
		Lochkovian	Stoniškiai						
			Tilže	D_1tl					
Silurian	Wenlock		Jaagarahu	S_1jg					
	Llandovery		Jaani	S_1jn					
			Adavere	S_1ad					
			Raikküla	S_1rk					

Stress Periods

The time discretization of the model has three purposes:

- to separate the natural conditions from post-development conditions, which have been influenced by variations in pumping rates;

- to simulate changes in pumping rates on a short enough timescale to capture hydrological trends;
- to simulate groundwater extraction scenarios reflecting the maximum allowed pumping rates and potential mining impacts.

The first objective was met by constructing a combined steady-state/transient model, with the first stress period devoted to natural conditions: its water-level output is the basis for calculating drawdown and recovery in subsequent transient stress periods. To achieve the second objective, variable stress periods were assigned according to the available data (years 2000–2020). To achieve the third objective, nine time-steps were added to the model to simulate 30 years of mining and ten years of recovery (after quarries are closed).

In all, there are 30 stress periods in the model, with 29 transient stress periods extending over 64 years (Table 4). The first model stress period consists of one steady-state time step. The subsequent transient stress periods are each divided into one, five, or ten time-steps regarding the stress-period length.

Table 4. Stress period setup for model

Stress period	StartTime	EndTime	Duration	Time period
1	-1	0	Steady-state	Natural conditions
2	0	365	1 year	2000
3	365	730	1 year	2001
4	730	1095	1 year	2002
5	1095	1460	1 year	2003
6	1460	1825	1 year	2004
7	1825	2190	1 year	2005
8	2190	2555	1 year	2006
9	2555	2920	1 year	2007
10	2920	3285	1 year	2008
11	3285	3650	1 year	2009
12	3650	4015	1 year	2010
13	4015	4380	1 year	2011
14	4380	4745	1 year	2012
15	4745	5110	1 year	2013
16	5110	5475	1 year	2014
17	5475	5840	1 year	2015
18	5840	6205	1 year	2016
19	6205	6570	1 year	2017
20	6570	6935	1 year	2018
21	6935	7300	1 year	2019
22	7300	7665	1 year	2020
23	7665	11315	10 years	2020–2030
24	11315	14965	10 years	2030–2040
25	14965	18250	10 years	2040–2050

26	18250	18615	1 year	2051
27	18615	18980	1 year	2052
28	18980	20805	5 years	2052–2057
29	20805	22630	5 years	2057–2062
30	22630	22995	1 year	2062

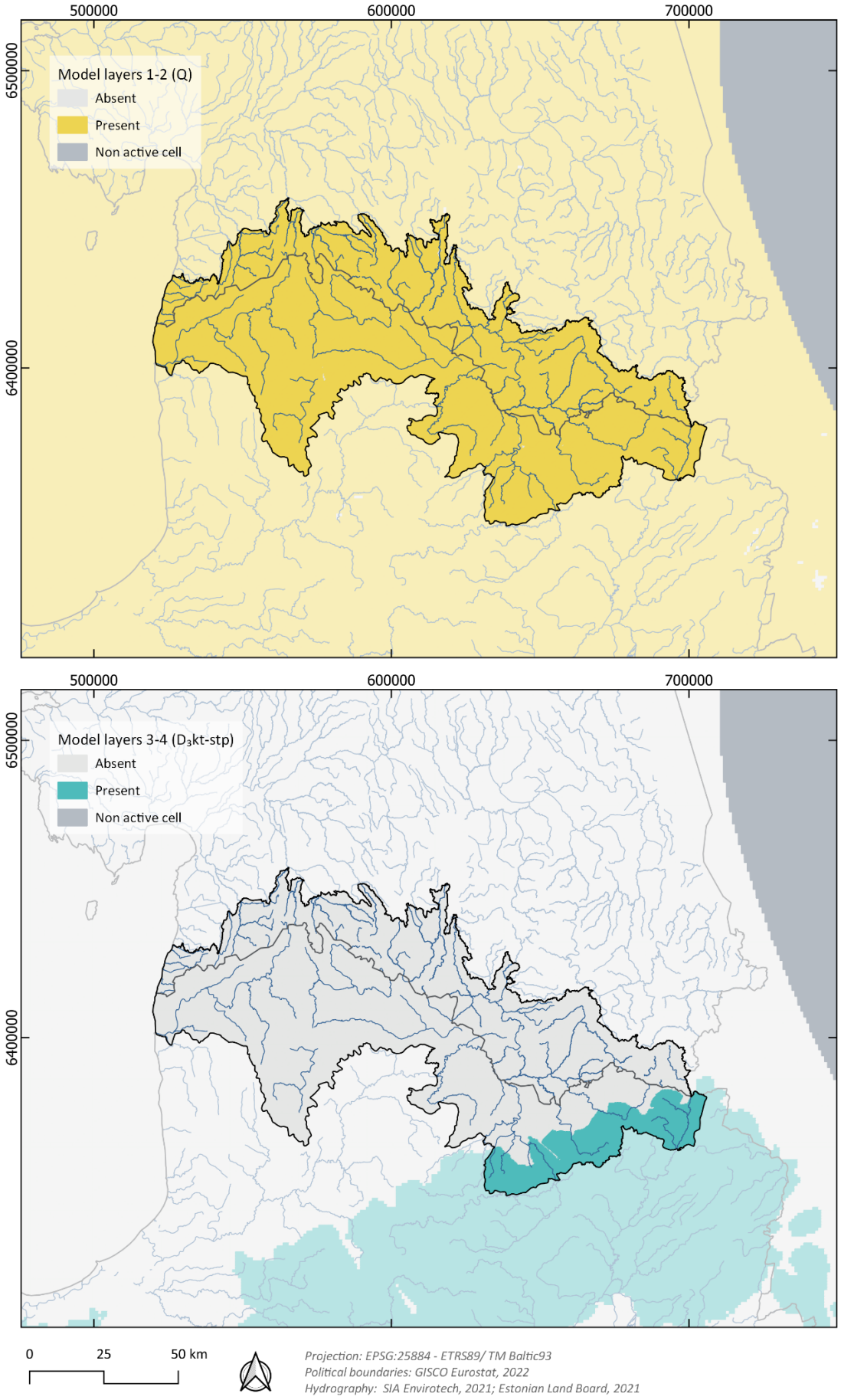

Figure 4. The areal extent of model layers

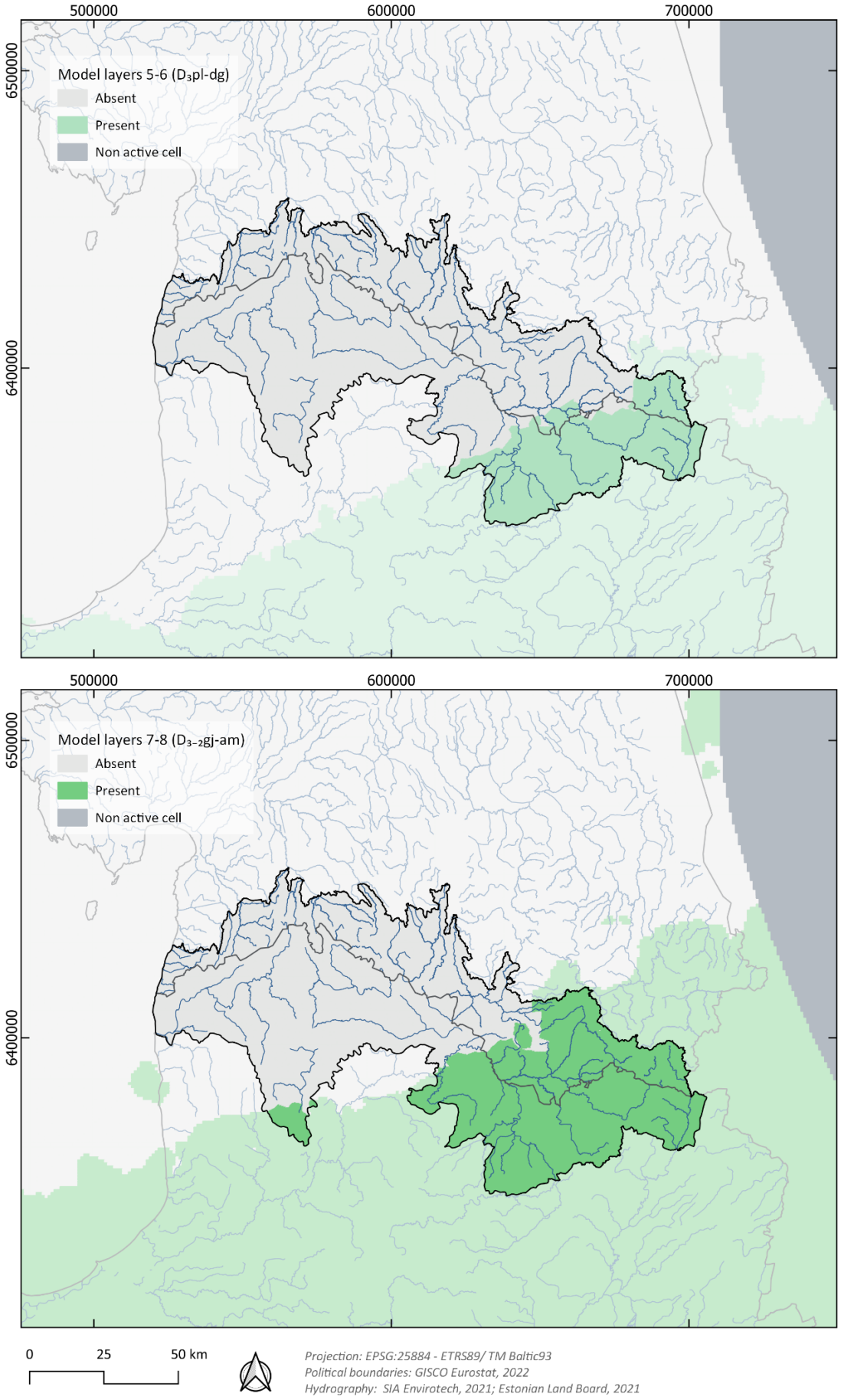

Figure 4. —Continued

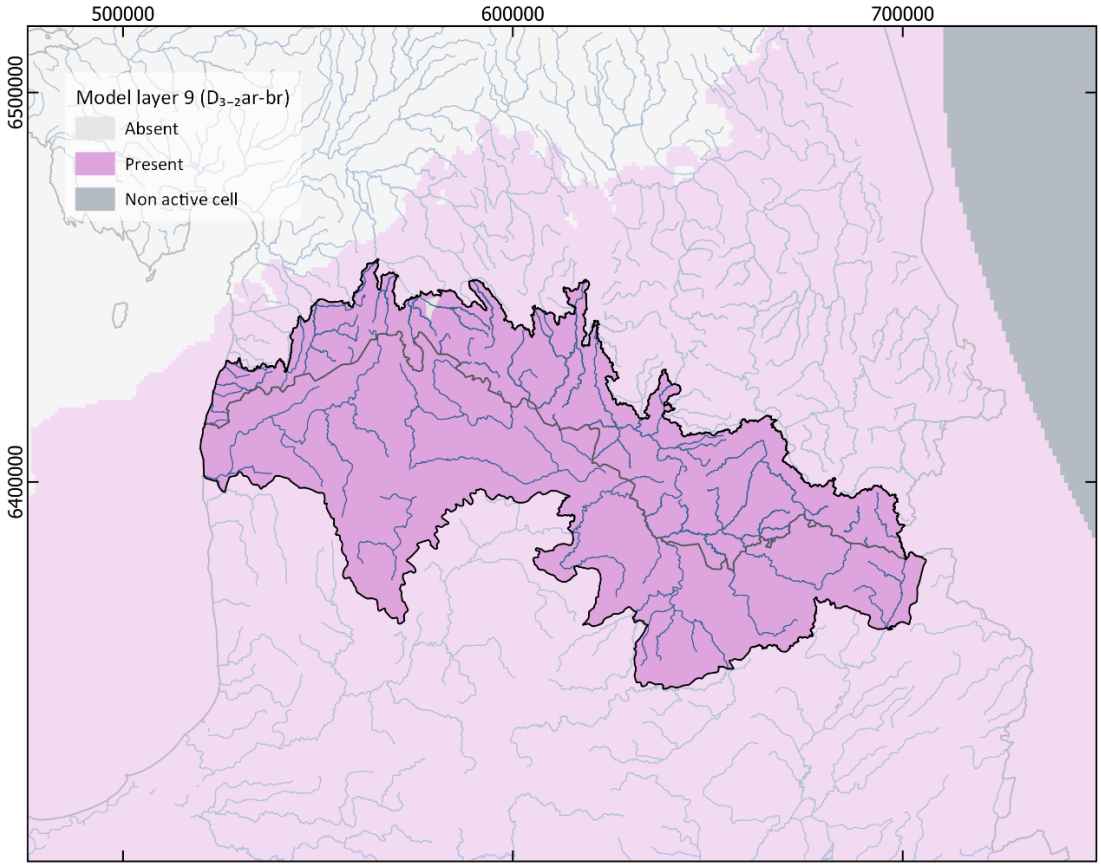

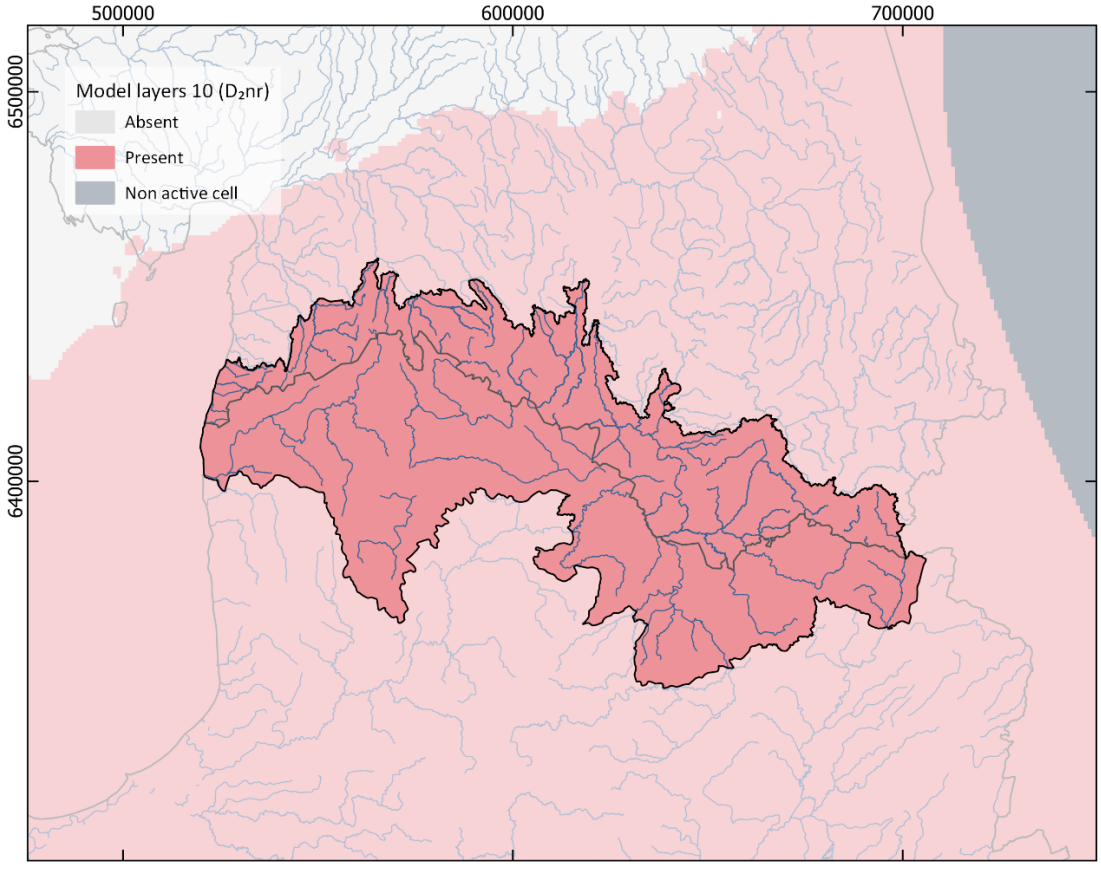

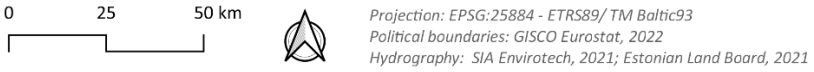

Figure 4. —Continued

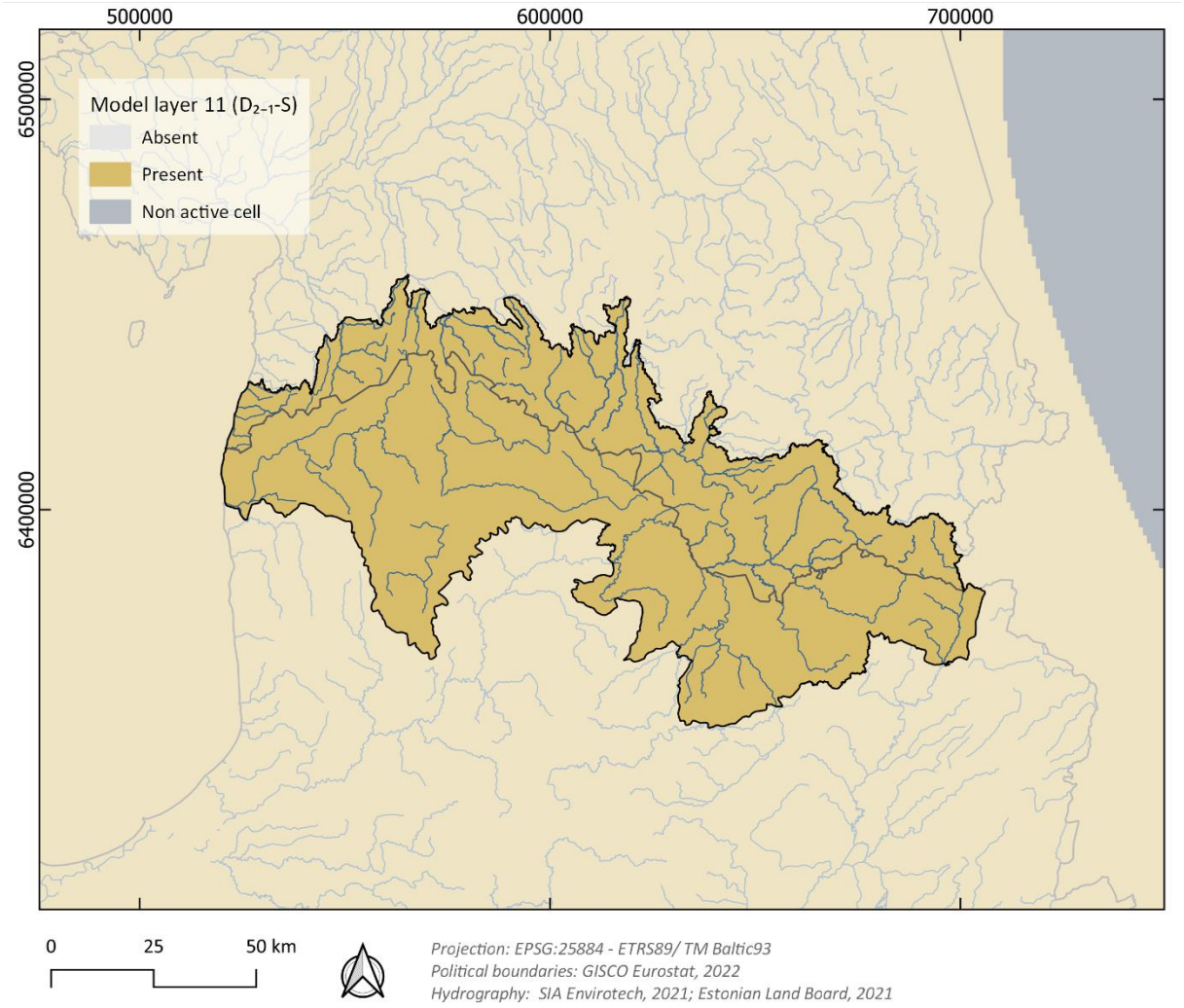

Figure 4. —Continued

2.1.2 Boundary Conditions

No-Flow

No-flow boundary conditions exist on the model's northern, eastern, southern, and western borders. Even though this boundary condition does not reflect the actual groundwater conditions at these locations, its effect on simulated conditions in the model nearfield is minimal because (1) there is a significant distance between the model sides and the model nearfield, and (2) other model boundary conditions limit its influence. A no-flow boundary also defines the bottom of the model (at the interface with the Silurian-Ordovician aquitard).

Constant Head

A large part of the model represents the Baltic Sea, Lake Peipsi, Lake Pihkva, Lake Võrtsjärv, and Lake Burtnieki (Figure 5). These areas are defined in the model by the Constant Head Boundary (CHB) package.

Each object is assigned a constant stage (meter above mean sea level):

- Baltic Sea = 0.00
- Lake Peipsi = 30.0
- Lake Pihkva = 30.0
- Lake Võrtsjärv = 28.0
- Lake Burtnieki = 39.0

The stages for four lakes were derived from a 10-m digital elevation model (Latvia Geospatial Information Agency, 2021; Estonia Land Board, 2021) using the minimum elevation within the lake area. Constant-head cells in the model are held constant through all stress periods.

General-Head Conditions

The General-Head (GHB) Boundary Package is a head-dependent boundary condition, whereby the flow rate into or out of the cell is calculated according to the head calculated in the boundary cell, the head outside the boundary cell, and the conductance term. To simulate the connectivity between the model domain and the wider BAB, GHBs were assigned to cells along the southern extent of the model. The heads associated with this boundary were ascribed to the topographic surface elevation at each model cell. This involved model layer 11 of the LL-EE model. GHB conductance values were then calibrated to accommodate groundwater heads observed in wells near the boundary.

Surface-Water Network

Stream is represented as River (RIV) Boundary Conditions cells in the model. According to RIV boundary definitions, groundwater can discharge into streams as base flow when the stream stage is below the simulated water table. Meanwhile, stream water can discharge into groundwater if the stage is above the simulated water table.

River locations were based on the stream network described in the Latvia SIA Envirotech (2021) and Estonia Land Board (2021) databases (Figure 5). River stages were calculated based on the minimum elevation (Latvian Geospatial Information Agency, 2021; Estonia Land Board, 2021) within each model cell that the river overlapped. The elevations were smoothed to eliminate rises in the downstream direction. Two meters from the river stage were subtracted to get the value of the river bottom. The initial riverbed hydraulic conductivity for each river cell was set to 1 m^2/d.

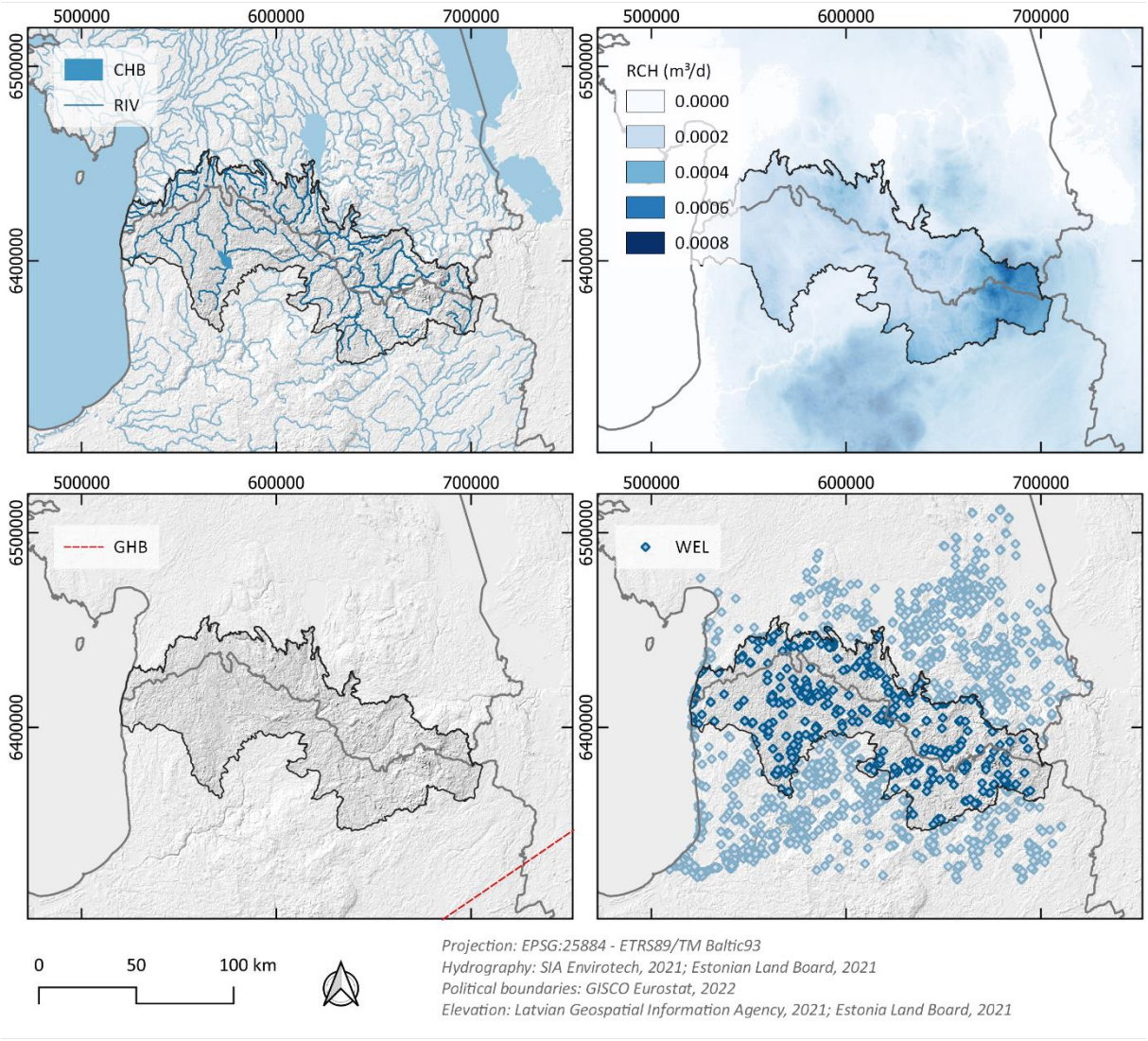

Figure 5. Model boundary conditionsFigure 5. Model boundary conditions

Recharge

The Recharge Package (RCH) was used to simulate groundwater recharge from precipitation. Recharge is affected by the permeability of surface hydrogeologic units, relief, precipitation variations, and land cover characteristics in the study area. The initial values of recharge were obtained from previous studies (Vallner, 2016) and applied to the model's uppermost layer. In the study area, recharge values range from 0 m/d to 0.00081 m/d. Recharge values are constant through all stress periods.

Groundwater withdrawals

The Well Package (WELL) simulates a specified-flux boundary in each model cell to which a well is assigned based on the withdrawal rate for each well or group of pumping wells in the cell. A simulation of groundwater withdrawal from pumping wells was done using the WELL package. The daily pumping rates (cubic meters per day) were specified for each well for

each stress period. Locations and pumping rates of wells were obtained from the Latvian Environment, Geology and Meteorology Centre (2021), and Estonia Environmental Agency (2021) (Figure 5).

Horizontal and Vertical Hydraulic Conductivity

Initial values of horizontal hydraulic conductivity (K_h) for the hydrogeologic units were based on the available field pumping test measurements and previous studies (Virbulis *et al.,* 2013). A horizontal isotropy assumption was made ($K_x = K_y$) since there is no evidence that hydraulic conductivity varies with direction. Initial values of horizontal hydraulic conductivity in aquifer units ranged from 0.8 m/d in the Upper-Middle-Devonian (Aruküla-Amata) aquifer system to 100 m/d in the Upper-Devonian (Pļaviņas-Ogre) aquifer system. The initial value of horizontal hydraulic conductivity in the Narva regional aquitard unit was set to $2*10^{-9}$ m/d and the Quaternary aquifer unit – 10 m/d.

For every hydrogeological unit, vertical hydraulic conductivity (K_v) was assigned as a ratio of horizontal to vertical hydraulic conductivity (vertical anisotropy). The vertical hydraulic conductivity values were initially set relative to the horizontal hydraulic conductivity during calibration using the anisotropy of 10 ($K_v = K_h/10$).

Storage Properties

Specific storage values were assigned to model layers to reflect changes in groundwater storage caused by changes in water levels in confined aquifers. According to Vallner (2016), specific storage in sandstones, limestones and dolomites ranges from $1.0*10^{-5}$ to $1.0*10^{-3}$ m^{-1}. An initial specific storage value of $1.0*10^{-6}$ m^{-1} to all aquifer units and $1.0*10^{-5}$ m^{-1} to all aquitard units was assigned.

2.2 Model calibration

In model calibration, parameters are adjusted within reasonable limits to minimize differences (residuals) between measured and simulated groundwater levels and stream baseflows.

Calibration was carried out using the trial-and-error adjustment. After each model run, simulated groundwater levels and stream baseflows were compared to measured values. Model runs continued until the correlation coefficient between simulated and measured values heads exceeded 0.9.

Calibration Data

Water level and stream baseflow measurements were used to calibrate the model. 44 water-level measurements were used from 40 wells from January 2010–December 2021. The Upper-Devonian (Pļaviņas-Ogre) aquifer system was represented by 16 wells, the Upper-

Middle-Devonian (Aruküla-Amata) aquifer system – by 18 wells, and the Lower-Middle-Devonian-Silurian aquifer system – by five wells. Streamflow was measured at 43 locations (LEGMC, 2021; KAUR, 2021). The hydrograph separation from the time series of daily flows using the nonlinear reservoir algorithm (ArciniegaEsparza et al., 2017) estimated the baseflow portion of the discharge measurement.

Assessment of Model Fit

By comparing measured and simulated groundwater levels and streamflow values graphically and descriptively, we gain a deeper understanding of model fit and complement the statistical measures. It is possible to assess the model's ability to replicate a flow system through such a comparison. In the groundwater-flow system, it is critical that the model accurately simulates the regional direction and flow amounts.

To evaluate the calibration results, statistical parameters (mean, standard deviation, and root-mean-square error (RMSE) were also examined. The meaning of residuals represents the difference between simulated and measured values (residues), and the bias indicates whether it is over- or under-predicting. Variations between residual values greater and less than the mean are measured by standard deviation. A low standard deviation indicates that residuals are close to the mean, while a high standard deviation indicates that residuals are spread over a wide range of values. The RMSE of residuals provides a measure of variation that considers measurement accuracy. A minimum RMSE should be less than 10% between simulated and measured hydraulic heads in observation wells, divided by the total range of water levels in the groundwater system.

Table 5 shows calibration statistics for groundwater levels (by hydrogeologic unit) and stream baseflow. Calibration statistics were used to evaluate the model's ability to simulate measured values (fit). According to the RMSE, the best fit occurred in Quaternary (Q) and Lower-Middle-Devonian-Silurian ($D_{2\text{-}1}$-S) aquifer systems; the worst fit occurred in Aruküla-Amata ($D_{3\text{-}2}$) aquifer system. The lowest mean residual values were found in Quaternary (Q) and Aruküla-Amata ($D_{3\text{-}2}$) aquifer systems, indicating that simulated groundwater levels in these units were the most accurate.

Table 5. Calibration statistics for numerical flow model

Calibration statistic	Q	D_3	$D_{3\text{-}2}$	$D_{2\text{-}1}$-S	All head measurements, m	All baseflow measurements, m^3/s
Number of observations	5	16	18	5	44	43
Mean residual	-0.7	-1.3	-0.1	0.6	-0.4	-0.1
Standard deviation of residuals	0.7	4.6	4.9	0.5	4.5	0.6
Range of observations	0.4	164.4	90.5	22.2	172	45.9

Root mean-square error	0.9	4.6	4.8	0.6	4.5	0.6

Based on the final calibration, the RMSE is 4.5 m for all water levels and 0.6 m^3/s for stream baseflows. With an average groundwater level range of 172 m, RMSE of 4.5 m constitutes about 2.6 percent of the total. Also, the average stream baseflow measurements range is 45.9 m^3/s, and the RMSE of 0.6 m^3/s represents 1.3 percent of the total range. Based on the groundwater level and baseflow measurements, the RMSE divided by the total range of values is less than 10%.

The plot of measured and simulated groundwater-level altitudes can be used to assess model calibration (Figure 6-A). Values measured and simulated should be plotted close to a line with a slope of 1.0 and an intercept of zero. Because the diagonal line represents the perfect agreement between measured and simulated values (the line of equal measured and simulated values), the magnitude of the residual is shown by how far the value is above or below the line. As shown in Figure 6-A, the measured and simulated groundwater level values are usually along the line of equal measured and simulated values; however, groundwater level altitudes in the 30–60 meters range are often underestimated.

A comparison of the measured and simulated groundwater discharge to streams (baseflow) in the model area was based on calculated streams' baseflow. Calculated baseflow values from 43 measurement sites were compared to simulated groundwater discharge to streams at a given stream watershed (Figure 6-B). As shown by the line of equal measured and simulated values, the calibration was reasonably accurate at simulating the baseflow.

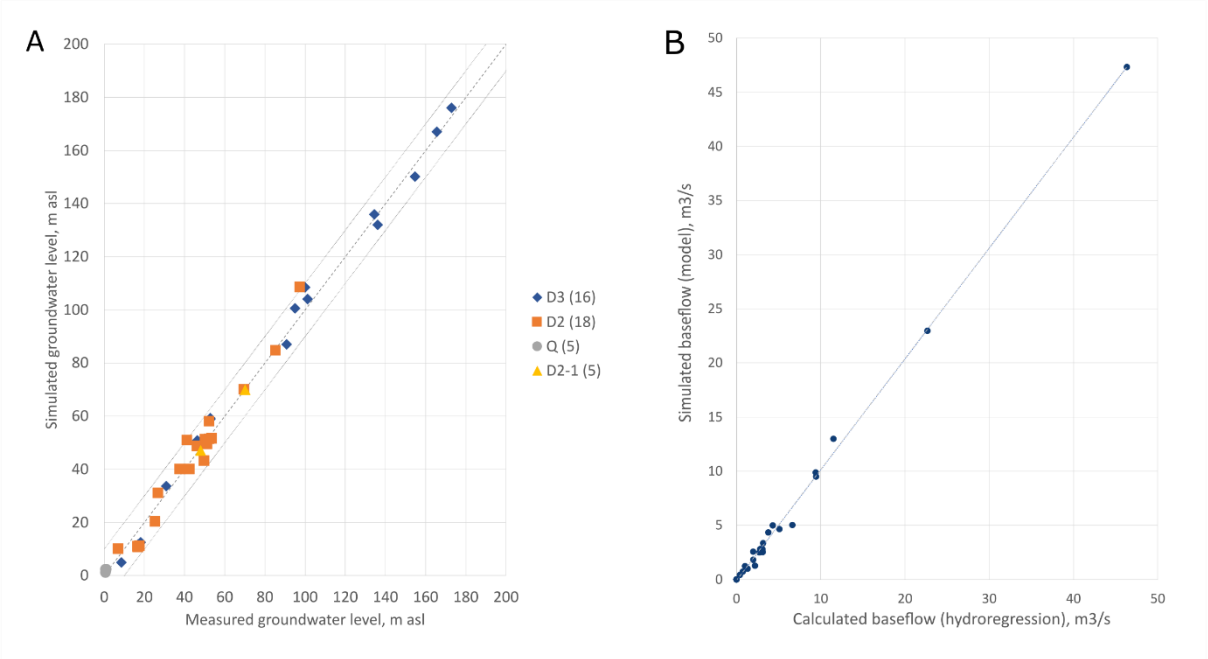

Figure 6. A- Simulated and measured water-level altitudes, B- Simulated and measured baseflows

2.3 Model limitations

A groundwater-flow model describes the flow of groundwater in a complex, natural system through mathematical equations. Various approximations, assumptions, and simplifications must be made within the model, introducing error and uncertainty. There are typically three causes of errors in hydrologic models: (1) input data, (2) model grid spacing, and (3) model time stepping. Below are three examples of model errors and how they limit the model's application:

Data gaps- Input data on thicknesses of hydrogeologic units, water levels, and hydraulic properties represent only approximations of actual values. There are parts of the model domain that are poorly characterized. It is possible that hydrogeologic properties or depths of contacts in areas without lithologic well logs may be out of range of values in better-characterized areas and that errors associated with this variability would not be represented. In regions of the model with sparse observations, conclusions should be limited to general flow directions and relative magnitudes. Due to the lack of information about streambed hydraulic conductivity values, groundwater/surface-water exchanges may be limited.

Grid spacing- The model grid spacing of 1000 meters (250 meters in the small study area) and the 11 layers used to accommodate multiple aquifer systems yield a model with more than 2 million cells and approximately 200 000 cells per layer. With the tools employed, a more finely discretized model would produce too many cells for efficient input and output

management. Calibration targets in shallow flow systems are limited in their value in estimating parameters by the coarse spacing, and the partitioning of discharge among surface-water sinks is also distorted. Furthermore, it limits the accuracy with which point features (especially pumping wells) can be located and prevents the model from simulating flow paths shorter than 1000 meters.

Time stepping- The model's temporal resolution also affects the system's dynamics and the spectrum of results. In MODFLOW-NWT simulations, each stress period has its own imposed conditions. During a stress period, the conditions are updated at the beginning and remain constant; they do not change continuously over time. As these conditions progress, the modeled system responds first by changing water levels, reflected in the storage term, and then by changing fluxes between the groundwater system and external features, such as surface water. As a result of the stepwise changes in stress imposed in the first time-step, the rate of removal (or addition) of water from storage is greatest immediately after the first time-step. In the final time-step, after water levels have stabilized and external inflows and outflows have reacted, the rate of water removal (or addition) is lowest. Similarly, at the end of the stress period, the accumulated response to variations in pumping or recharge is at its maximum value. This report presents results for the last step in the stress period for all sources and sinks.

The effects of simplifications and other potential errors can be limited by appropriately using the regional groundwater-flow model. However, the model's results can be significantly affected if generalizations and assumptions are made beyond their design limits. Due to the model's scale and level of detail, it is most suitable for analyzing groundwater problems at the regional scale. This study's regional-scale groundwater flow model does not represent local-scale heterogeneity in hydrologic properties, recharge, and discharge.

3. Simulation of groundwater extraction scenarios

Coordinated management of transboundary groundwater resources is important to minimize adverse transboundary impacts. Although previously no intensive anthropogenic pressure was identified in the Estonian-Latvian transboundary area, which could affect the quantity of transboundary groundwater aquifers (no significant groundwater intakes and no regions with active quarries were identified that could affect the hydrogeological regime at the regional scale), potential areas were identified for further research on transboundary groundwater resources. These include the transboundary Gauja-Koiva river basin district, where the most intensive groundwater flow between national borders has been identified, as well as the Valka-Valga region, where the most intensive groundwater abstraction has been identified (Demidko *et al.*, 2021).

To assess the changes in groundwater levels in these areas, as well as in the entire Estonian-Latvian transboundary area, groundwater flow model was used to simulate potential effects on water levels caused by changes in well withdrawals. Three scenarios were developed and simulated using the model to demonstrate how the calibrated model can be used to investigate water resource issues. Model results were compared to “base case scenario” results representing natural conditions. The changes in water budget components and water level altitude were evaluated as a result. For the Quaternary, Upper-Devonian (Pļaviņas-Ogre) and Upper-Middle-Devonian (Aruküla-Amata) aquifer systems, results are presented. The following conditions were simulated using a model:

Table 6. Detailed description of the simulated scenarios

	Scenario I (base case scenario)	Scenario II	Scenario III
Duration	Steady state	20 years	30 years
Time period		2000-2020	2021-2051
Transboundary area			
Pumping rate (m^3/d)	0	4712-7284	8733
Draining from quarries (m^3/d)	0	0-4274	27647
Whole model area			
Pumping rate (m^3/d)	0	32417-50658	123460
Draining from quarries (m^3/d)	0	0-4274	27647
Description	Natural conditions, without any abstraction volume	Current state	Maximum allowed pumping rate, four potential quarries

Simulation 1 is steady-state simulation that reflects natural conditions, where there is no abstraction in the study area (base case scenario, BC). All wells and quarries were removed from the model. Simulated groundwater tables are shown in Figure 7.

Simulated water level altitudes in the Quaternary aquifer system indicate regional groundwater flow moving from highlands and uplands to river valleys or the western study area – to the Baltic Sea. The Quaternary aquifer system intermediated flow rises from Vidzeme, Alūksne and Haanja highlands, as well as Karula upland, where the groundwater table is 100-180 m above the sea level, while in plateaus, its height mostly ranges from 40 to 80 m above sea level.

In the Upper-Devonian (Pļaviņas-Ogre) aquifer system (model layers 3–6), the direction of the groundwater flow is determined by Vidzeme and Alūksne highlands, as well as Haanja highland. From the highlands, groundwater flows down to lower areas like the Gauja River valley. Groundwater table ranges from 70 m to 190 m above sea level.

Simulated water level altitudes in the Upper-Middle-Devonian (Aruküla-Amata) aquifer system (model layers 7–9) indicate flow moving from Sakala and Karula uplands, as well as Haanja and Idumeja highlands toward Mustjõgi and Salaca river valleys and the Baltic Sea. In general, groundwater levels range from 0 m to 160 meters above sea level.

A further description of groundwater heads and the groundwater flow behavior is presented in Figures 9–10 to illustrate the difference in groundwater levels of each scenario of the discharge from wells compared to the BC.

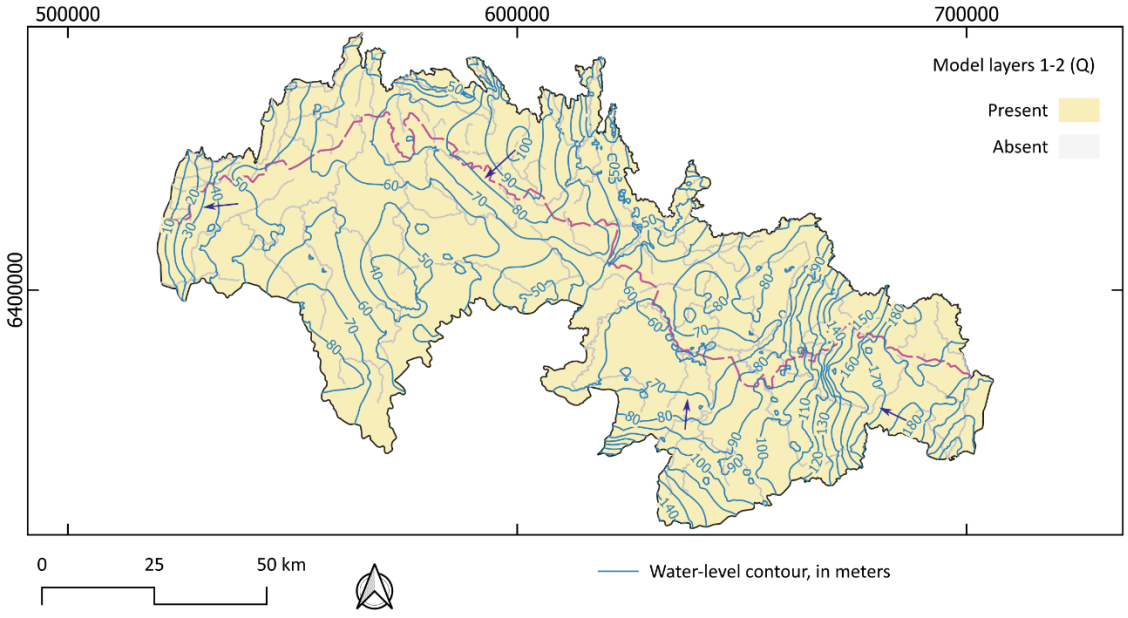

Figure 7. Simulated water-level altitudes in natural conditions (scenario 1)

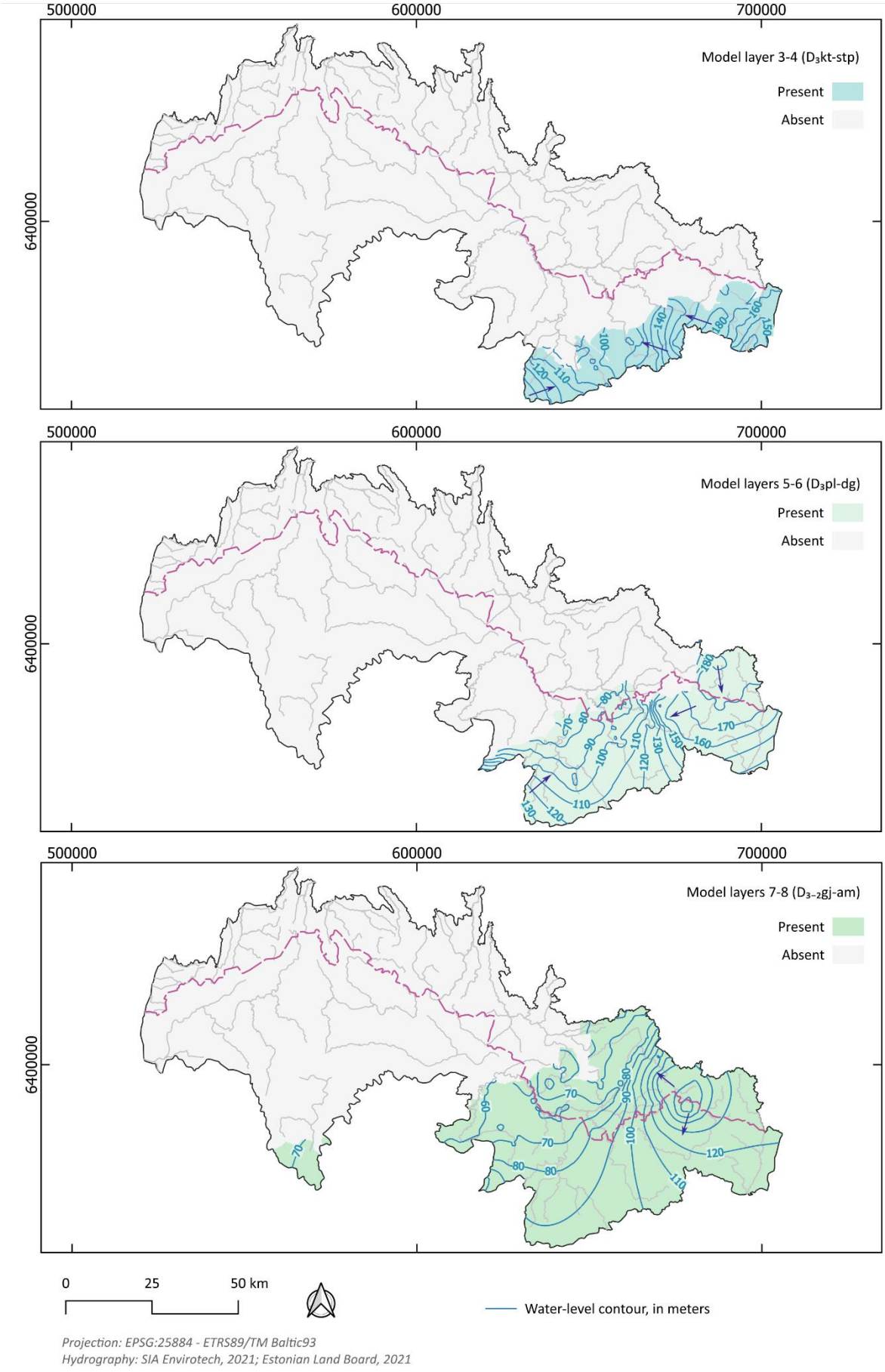

Figure 7. —Continued

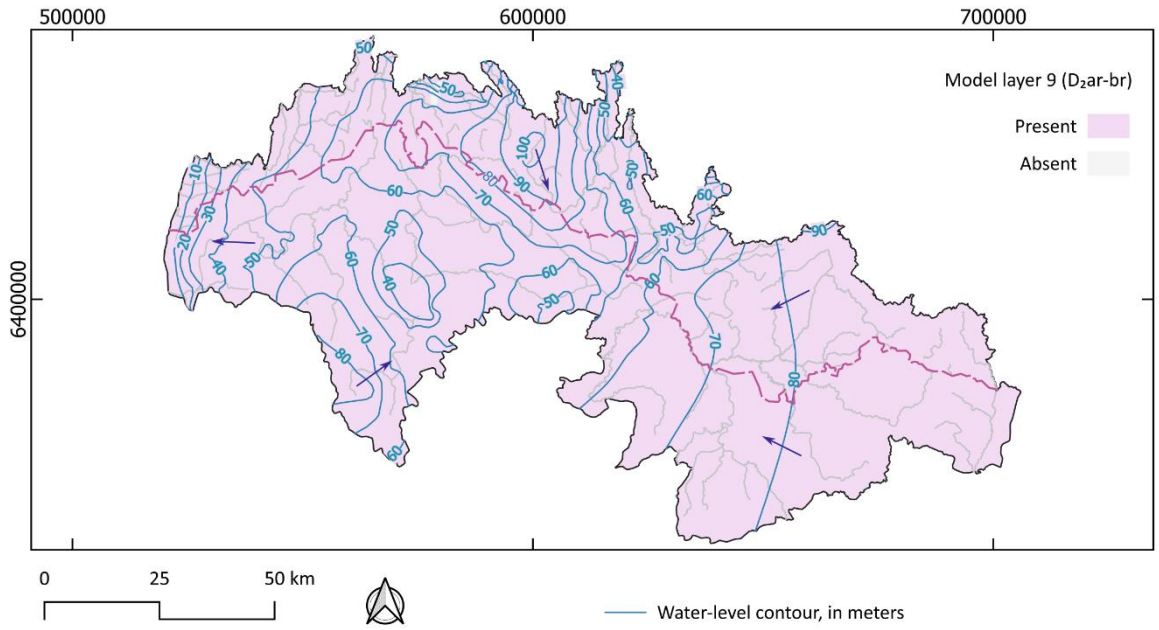

Projection: EPSG:25884 - ETRS89/TM Baltic93
Hydrography: SIA Envirotech, 2021; Estonian Land Board, 2021

Figure 7. —Continued

Simulation 2 represents the current situation (2000–2020) in the Estonian-Latvian transboundary area. All wells with registered pumping rates and active dolomite quarry "Ape" on the Latvia side were inserted into the model. This was done to assess the effects of the current amount of water abstractions. Dolomite quarry "Ape" was inserted into the model as a drain boundary (DRN) condition, the elevation of the Upper-Devonian (Pļaviņas-Ogre) aquifer system, for the period of 2009–2020. Pumping volumes were calibrated based on annual pumping volumes (Figure 8).

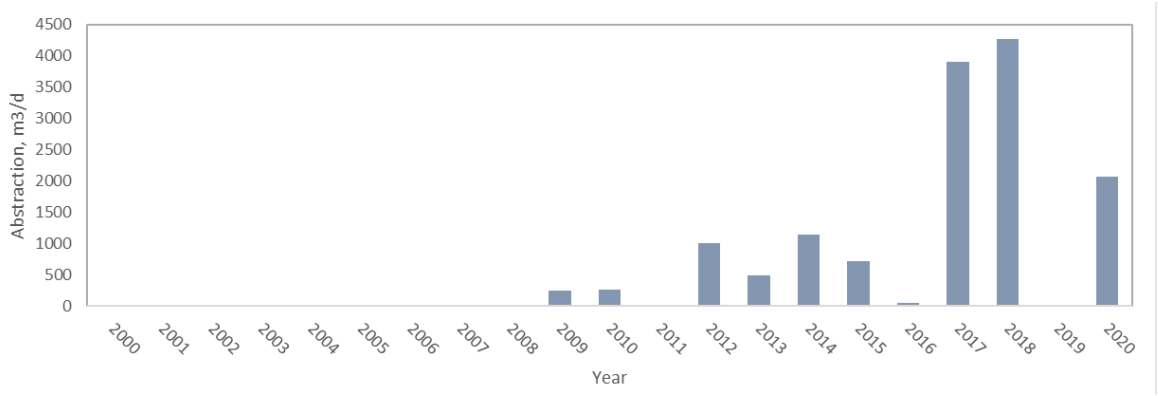

Figure 8. "Ape" quarry abstraction

The given scenario is divided into 20 time-steps, each representing one year (20 years in total) for 2000-2020. Figure 9 shows the difference between the base case scenario and 2020 water levels. As shown in Figure 9, the impact of current groundwater abstraction is insignificant. Most of the area's groundwater drawdown is 0.0 m or between 0.2–1.2 m. Only

in remote locations in the Quaternary (Q) and Upper-Devonian (Pļaviņas-Ogre) aquifer systems groundwater level is more than 2 m lower in the quarries area.

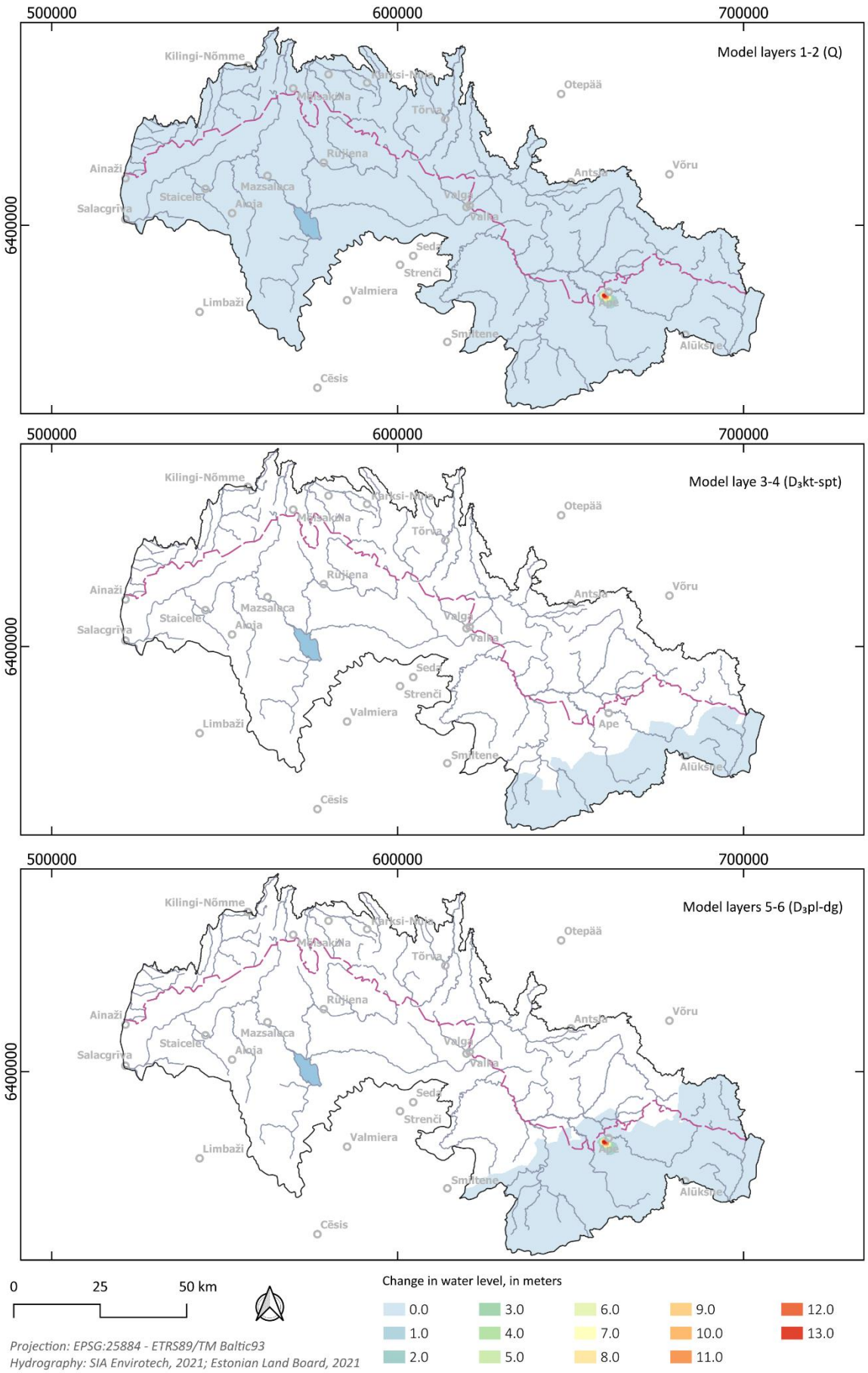

Projection: EPSG:25884 - ETRS89/TM Baltic93
Hydrography: SIA Envirotech, 2021; Estonian Land Board, 2021

Figure 9. Water-level altitude changes between the current conditions' simulation and base case scenario

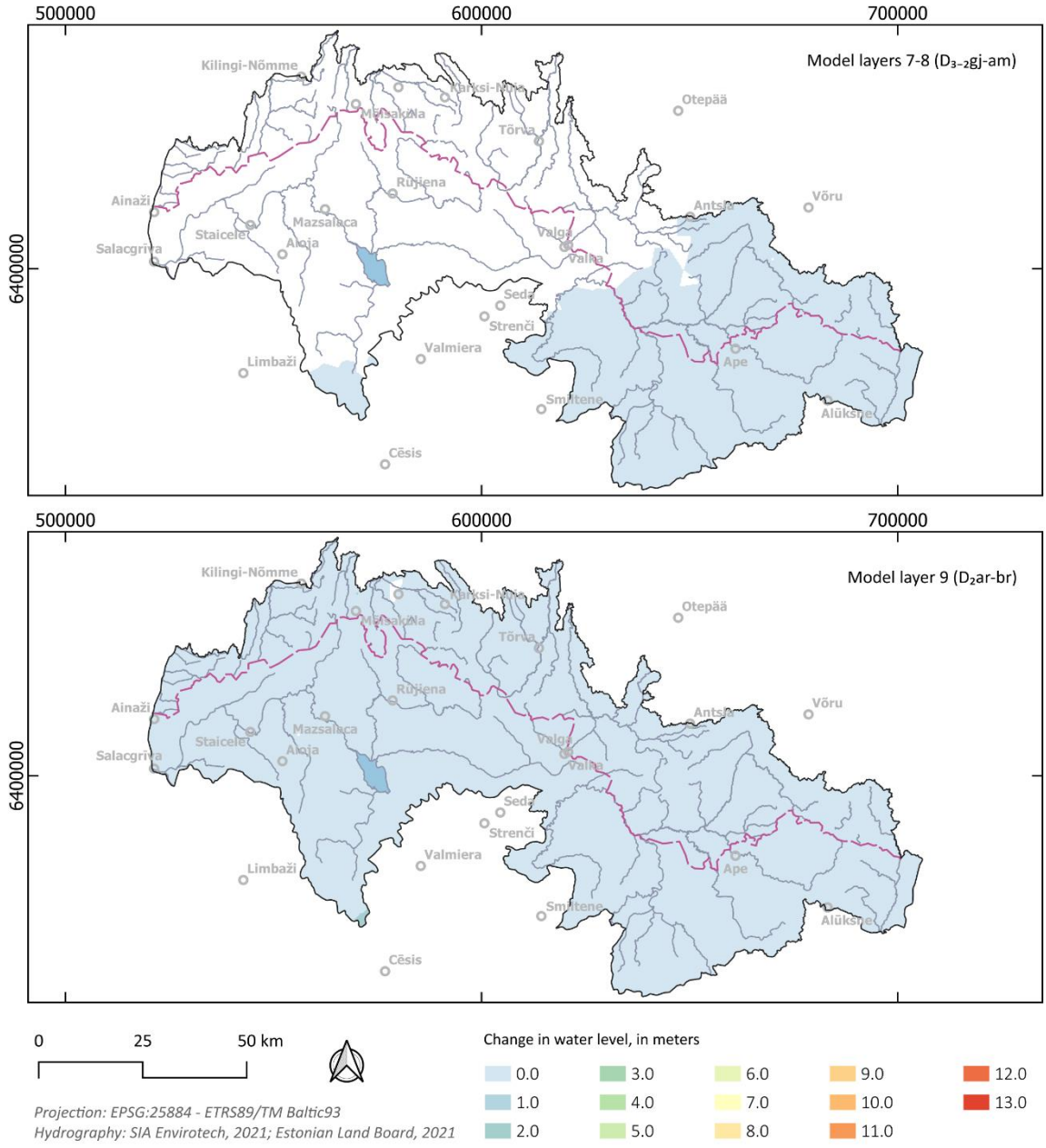

Figure 9. —Continued

In **Simulation 3**, all pumping was increased, according to maximum allowed rates, and four quarries (one active – "Ape", and three potential- "Naha", "Kalkahju", and "Dārzciems-2") were inserted into the model.

All four quarries modeled in the third scenario are on the Upper-Devonian (Pļaviņas-Ogre) aquifer complex outcrop, where it is recharged by precipitation. In the case of the model calculation, the maximum abstraction has been considered, which was previously calculated during the assessment of the impact of the quarries (Geological Survey of Estonia, 2013; Engineering Bureau Steiger, 2013; SIA "Zemes Puse, 2015; SIA "Firma L4", 2006). The

quarries are entered into the model as a drain boundary (DRN) condition, the elevation of the Upper Devonian aquifer.

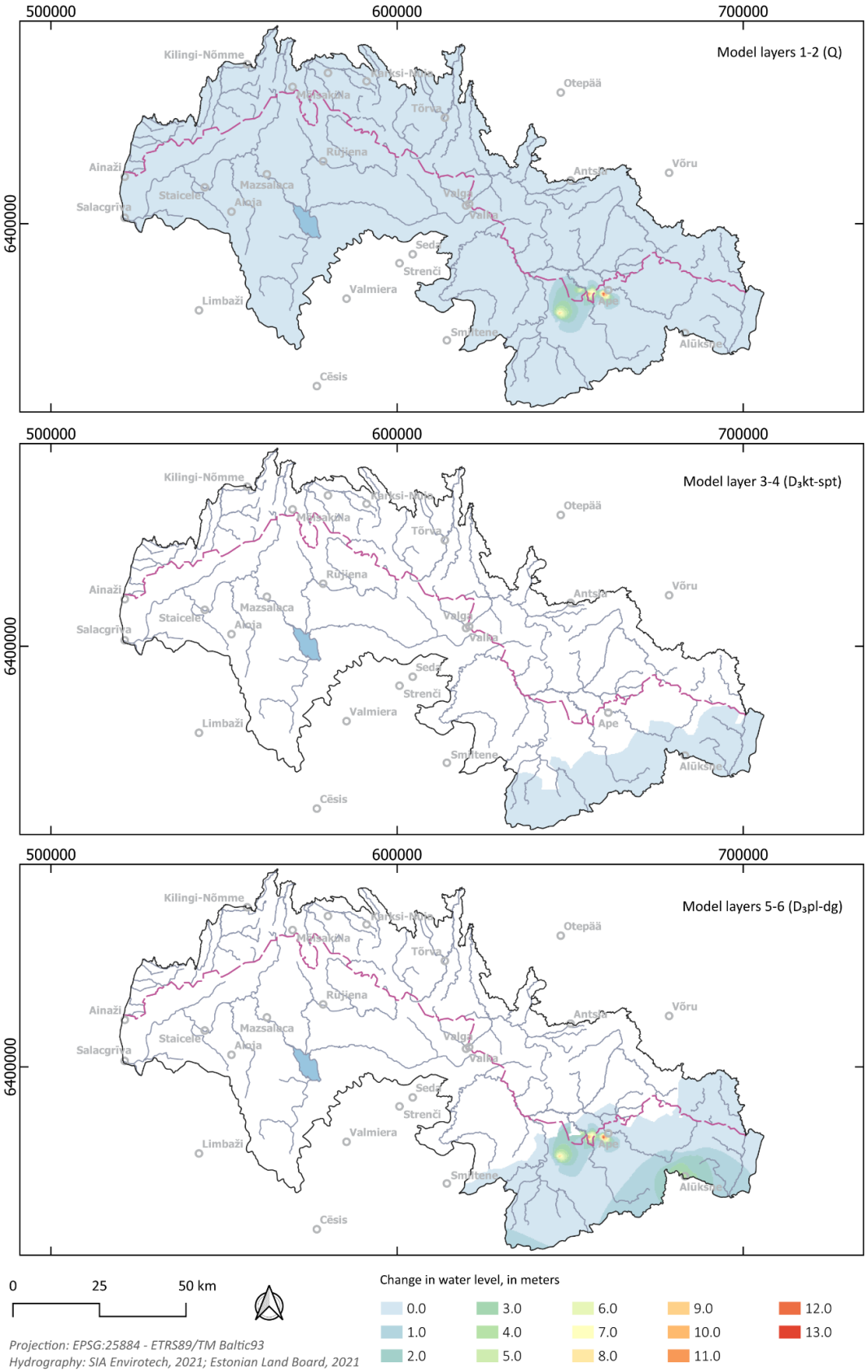
500000
600000
700000
6400000
Model layers 1-2 (Q)
Model layer 3-4 (D₃kt-spt)
Model layers 5-6 (D₃pl-dg)
Kilingi-Nõmme
Türi
Otepää
Tõrva
Rūjiena
Ainaži
Mazsalaca
Staicele
Alūksne
Salacgrīva
Aloja
Valga
Võru
Valka
Antsla
Sēda
Strenči
Valmiera
Limbaži
Smiltene
Ape
Cēsis
0
25
50 km
Change in water level, in meters
0.0
1.0
2.0
3.0
4.0
5.0
6.0
7.0
8.0
9.0
10.0
11.0
12.0
13.0
Projection: EPSG:25884 - ETRS89/TM Baltic93
Hydrography: SIA Envirotech, 2021; Estonian Land Board, 2021

Figure 10. Simulated water-level altitude changes between the base case scenario and increased pumping simulation

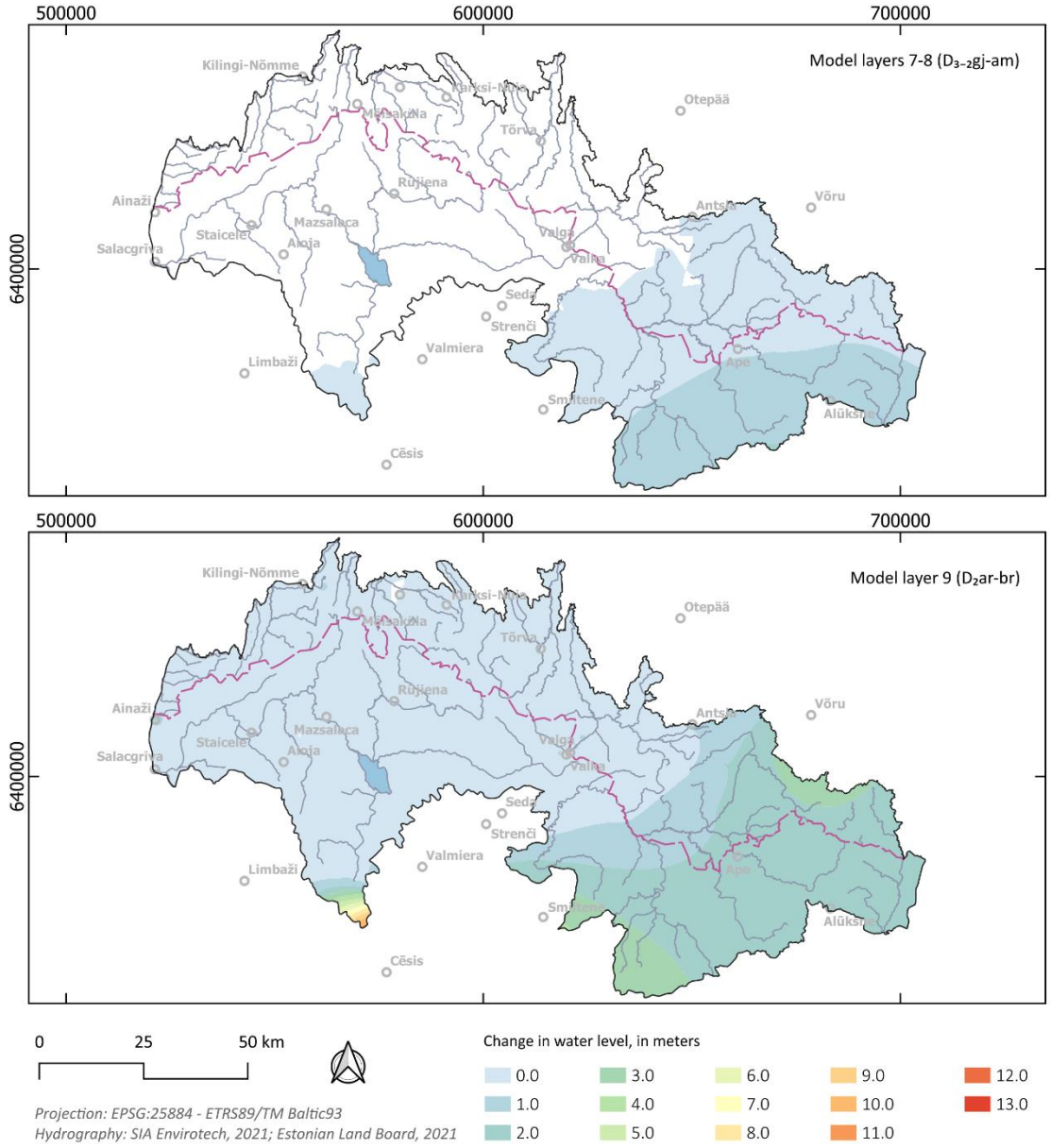

Figure 10. —Continued

This model does not contain spatial figures for the progress of mining activity by year; the total areas of the potential quarry have been entered into the model. To model the third scenario, the drain boundary for all four quarries was entered for 30 years from 2021. To analyze the depression cone, the difference between the base scenario and the water levels after quarries have worked for 30 years has been calculated. Detailed quarry data is given in table 7.

For this simulation, water-level altitudes in the Quaternary (Q) aquifer system would decline between 0 m to 1 m due to increased pumping with localized areas between 7.0–13.0 m due to quarries activity. In the Upper-Devonian (Pļaviņas-Ogre) aquifer system, water level altitudes decline between 0 m and 2 m, and near quarries – up to 13 m. Most Upper-Middle-

Devonian (Aruküla-Amata) aquifer system water levels would decline by 0–3 m. Localized areas would have slightly greater declines.

Table 7. Description of the quarries (Geological Survey of Estonia, 2013; Engineering Bureau Steiger, 2013; SIA "Zemes Puse, 2015; SIA "Firma L4", 2006)

Quarry	Country	Status	Area, ha	Pumping rate, m^3/d	Depth, m
Ape	Latvia	Working	16.34	10170	17.3
Dārzciems-2	Latvia	Working (currently above the groundwater level)	40.65	4800	16.8
Naha	Estonia	Non active	73.93	10766	11.2
Kalkahju	Estonia	Non active	77.56	1911	8.5

Impact of quarries on transboundary groundwater

As already mentioned in the previous chapter, the most significant changes in the Estonian-Latvian study area are related to the water pumping to lower the groundwater level in the quarry working area. In Simulation 2 (current groundwater abstraction), there is only one working quarry – quarry "Ape". Dolomite quarry "Ape" is an open-pit quarry and is located about 2 km from the Latvian-Estonian border. Dolomite rocks of the Pļaviņas stage (Pļaviņas-Ogre aquifer system) are mined here. As the extracted material lies deeper than the groundwater level, groundwater lowering is performed.

In the simulation of the current situation, pumping data for the year 2020 were used. According to monitoring data, in 2020, about 2067 m^3/d was pumped out of the quarrying site. It should be noted that the amount of pumped water depends on the intensity of quarry development (seasonal character). For example, in 2019, no groundwater pumping was performed.

Figure 11 shows that in the simulation of the current situation (A), the operation of the quarry affects the groundwater water on a local scale, however, significant changes in the transboundary groundwater flow pattern are not observed, according to the simulation.

In Simulation 3, the situation was modeled with the maximum allowed groundwater abstraction rates (see Table 7). For this simulation, information about three more additional quarries (one in Latvia - "Dārzciems -2" and two prospective dolomite quarries on the Estonian side - "Kalkahju" and "Naha") were inserted into the model.

All the above-mentioned quarries are located relatively close to each other, so Figure 11 shows that in the scenario of maximum water abstraction, the modeled drawdowns interact with each other.

Similar to Simulation 2 (current water abstraction), changes are mainly observed near the quarries (Figure 10, 11), however, no significant changes in transboundary flow pattern are observed. The modeling results confirm that even with maximum water abstraction, there is no significant impact on transboundary groundwater resources.

The current hydrogeological model represents a regional scale (entire Estonian-Latvian study area), and therefore, it is impossible to accurately reflect local groundwater changes. For this, it is recommended to develop a local hydrogeological model for a more accurate assessment of the impact of these quarries.

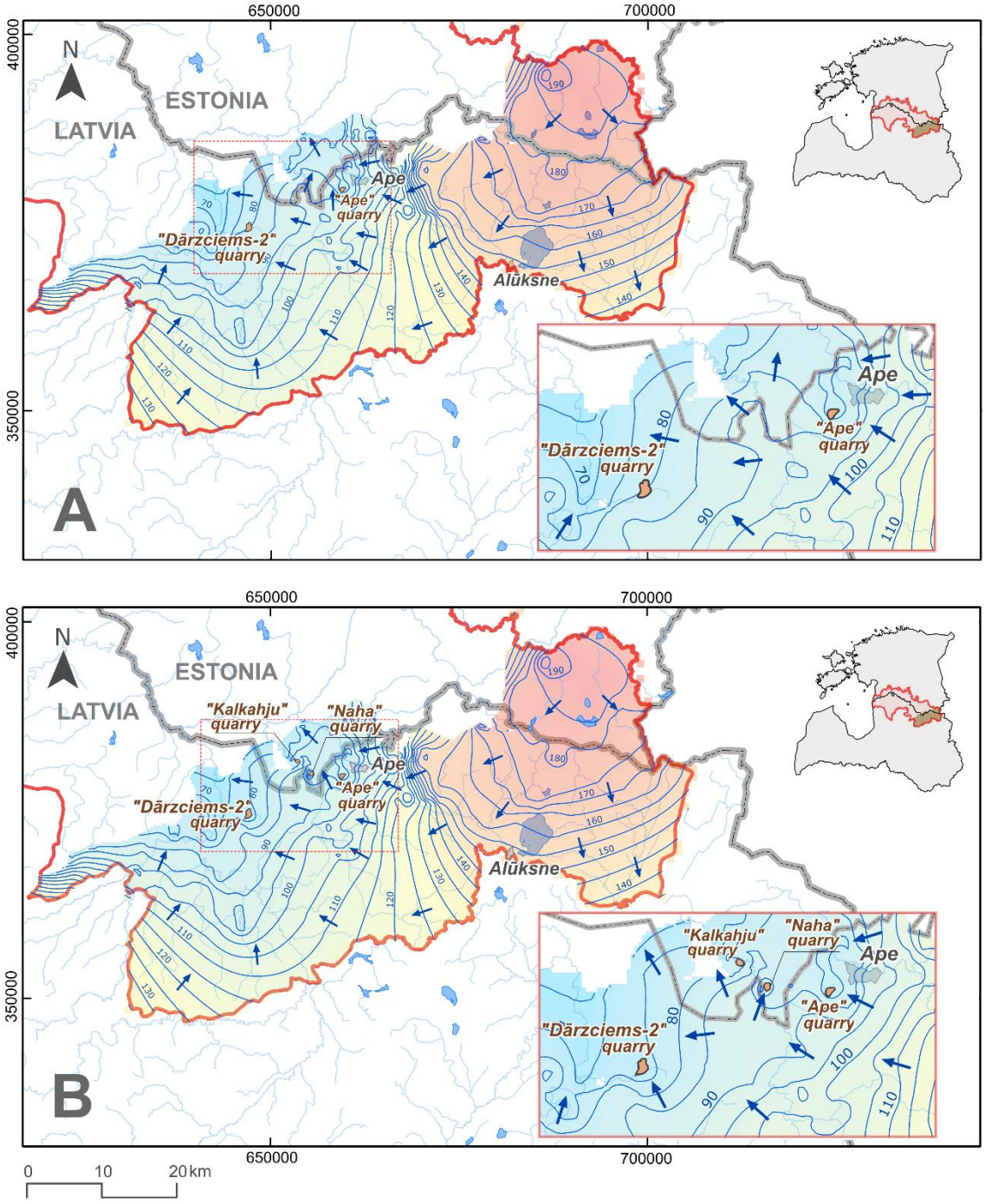

Figure 11. Groundwater flow changes between the A) current conditions simulation and B) maximum scenario in the quarry area

4. Water balance and change in storage

A calibrated model is an appropriate tool for estimating the groundwater budget of the Estonian-Latvian transboundary area and its response to future pumping conditions. As discussed in the "Model Limitations" section, these applications carry forward the uncertainties associated with the model.

For the study area, equation 1 represents the approximate average groundwater budget for the years 2010–2020:

$R + S_{in} = D + S_{out}$

where:

R is recharge,
S_{in} is groundwater coming in from storage,
D is discharge, and
S_{out} is groundwater going out to storage

The groundwater system in the study area is recharged primarily through precipitation and seepage from streams. Water can be discharged from the system through seepage into streams, lakes, and seepage faces, evaporation from soil and transpiration by plants, and submarine seepage into the Baltic Sea. Detailed groundwater budgets are shown in the following equation:

$R_{ppt} + R_{st} + R_{lat} + S_{in} = D_{st} + D_{sea} + D_{lake} + D_{et} + D_{pump} + D_{lat} + S_{out}$

where:

R_{ppt} is recharge from precipitation,
R_{st} is recharge from streams,
R_{lat} is lateral inflow from neighboring areas,
S_{in} is amount coming from storage,
D_{st} is discharge to streams,
D_{sea} is discharge to Baltic Sea,
D_{lake} is discharge to lakes,
D_{et} is discharge by evapotranspiration,
D_{pump} is pumping amount from wells,
D_{lat} is lateral outflow to neighboring areas,
S_{out} is amount going out to storage.

Based on the calibrated model, all water budget components can be quantified except for evapotranspiration. The model assumes evaporation from groundwater is insignificant ($D_{et} = 0$) and is not explicitly represented. The components of the water balance are shown in Figure 12 and listed in Table 8.

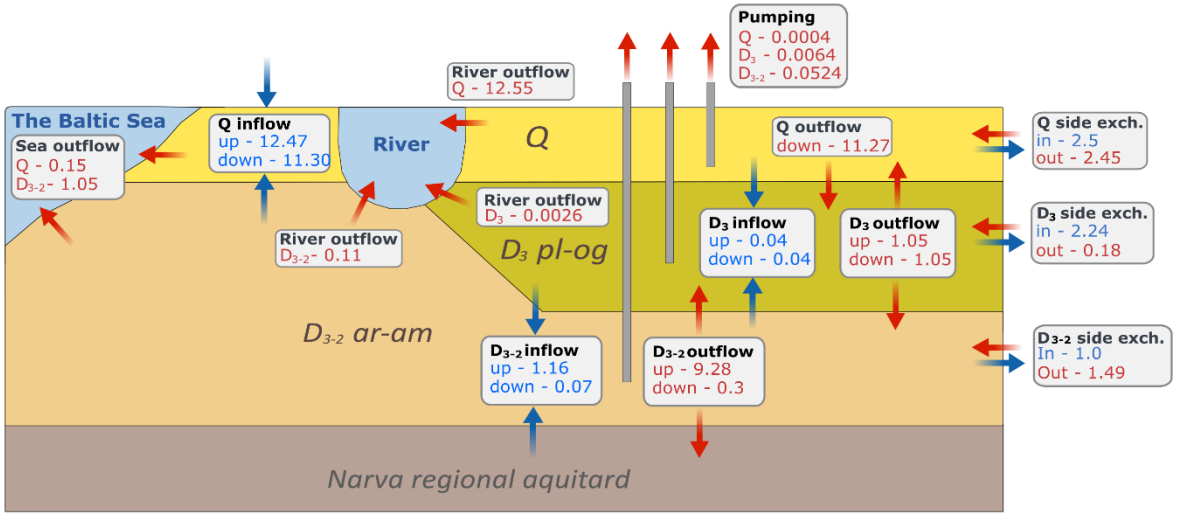

*Figure 12. Schematic representation of components of groundwater budget (*105 m^3/d)*

Some general observations can be made of the groundwater system using the calibrated-model groundwater budget. For example, for 2010–2012, total flow through the groundwater system of the study area averaged more than 39*10^5 m^3/day (Table 8).

Table 8. Water budget of Estonia-Latvia transboundary area in period 2010-2020 (10^5 m^3/d)*

		Quaternary (Q) aquifer	Upper-Devonian (Pļaviņas-Ogre) aquifer	Upper-Middle-Devonian (Aruküla-Amata) aquifer
Inflow	Side exchange	2.50	0.24	1.00
	From below	11.30	0.04	0.07
	From above	12.47	1.16	11.20
Outflow	Side exchange	2.45	0.18	1.49
	Down	11.27	0.06	0.30
	Up		1.05	9.28
	To sea	0.15		1.05
	Pumping	0.0004	0.0064	0.0524
	River	12.55	0.0026	0.11
	Water exchange	26	1	12

The primary form of groundwater recharge is precipitation. Primary forms of groundwater discharge were streams (13*10^5 m^3/day) and groundwater outflow to marine waters (1*10^5 m^3/day). Total groundwater withdrawals averaged about 0.15 percent (5925 m^3/day) of the total flow, excluding changes in storage.

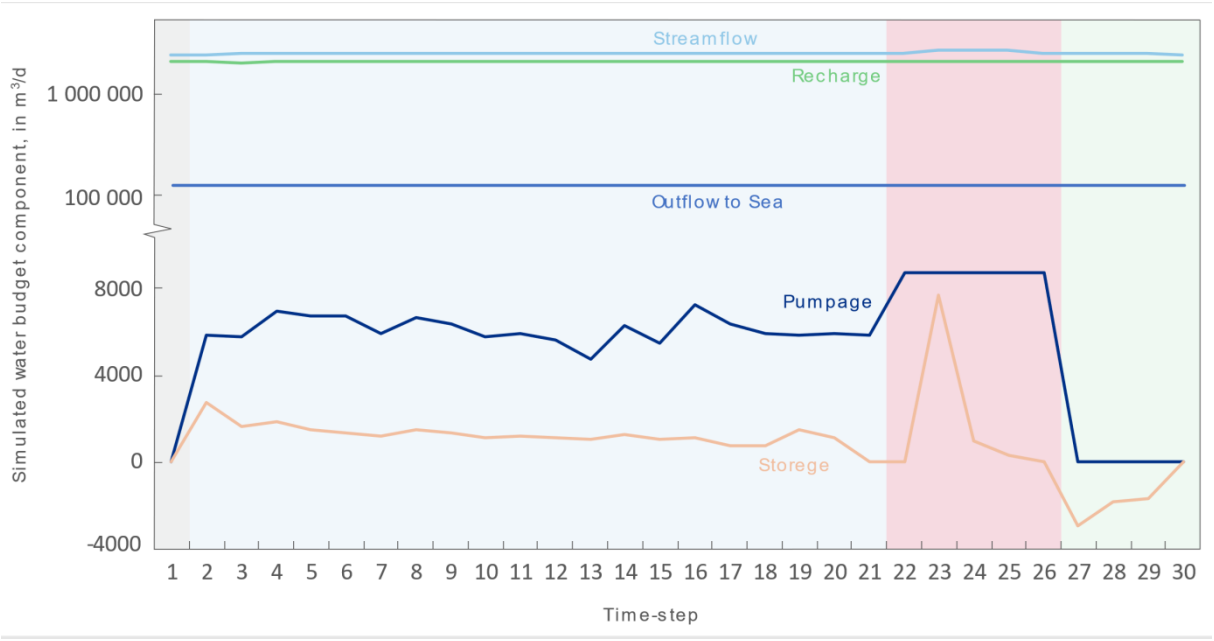

Figure 13. Simulated water budget (gray background - scenario 1; blue background - scenario 2; red background - scenario 3; green background - recovery period)

Based on the variation of storage values during 2000–2020 (Figure 13), the groundwater budget indicates that the system was not in a steady state. The net amount being added to storage 1500 m^3/d. In the years 2000 to 2020, the amount moving into and out of storage in the groundwater system shows no significant variation from year to year. Since recharge from precipitation is constant throughout all stress periods, the variation in storage reflects mostly the variation in pumping rates.

In stress periods 23–25, when scenario two is modeled, storage into the groundwater system increases rapidly (up to 8000 m^3/d) but then recovers to the initial level. And in the recovery period (stress periods 27–29), when all wells and quarries are closed, water is withdrawn from storage, which is indicated by negative storage numbers.

In addition, in order to assess the impact of water abstraction on transboundary groundwater resources, the calculation of the groundwater budget at the groundwater body-level was also carried out. Figure 14 shows the groundwater budget between cross-border groundwater bodies (GWBs) in the study area.

According to the model results, in Simulation 1 (basic scenario) and Simulation 2 (current water extraction), the groundwater balance between groundwater bodies is the same, which shows that the existing water extraction in the territory practically does not affect the transboundary groundwater overflow. In Simulation 3 (maximum allowed abstraction rates), small changes are observed mostly in the Upper Devonian groundwater bodies. However,

even with the maximum possible water abstraction, significant changes in cross-border groundwater flow pattern are not expected.

Detailed water balance separately for each groundwater body in the study area is given in tables 9–15.

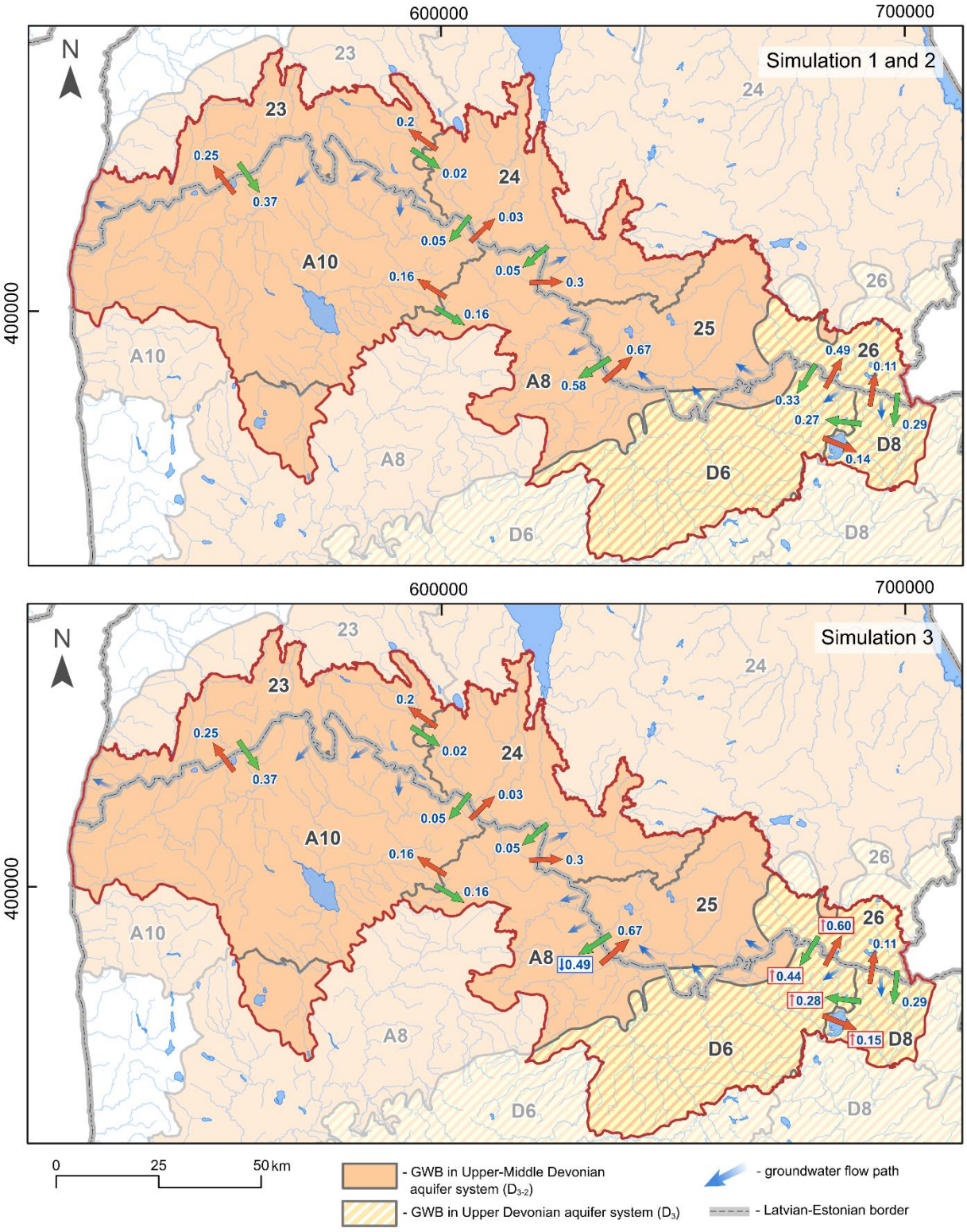

*Figure 14. Groundwater budget between groundwater bodies in Estonian-Latvian transboundary area (*105 m^3/d)*

*Table 9. Detailed water budget of groundwater body nr 26 (Estonia) (*10^5 m^3/d)*

	Scenario I	Scenario II		Scenario III	
GWB nr 26					
Inflow					
Side exchange					
Outside study area	0.38	0.38	0.00%	0.38	0.03%
GWB nr D6	0.49	0.49	0.30%	0.60	21.44%
GWB nr D8	0.11	0.11	0.00%	0.11	-0.02%
From above	0.67	0.67	0.00%	0.67	0.00%
From below	0.30	0.30	-0.07%	0.30	-0.80%
Outflow					
Side exchange					
Outside study area	1.58	1.58	0.00%	1.58	0.02%
GWB nr D6	0.33	0.33	1.31%	0.44	33.17%
GWB nr D8	0.29	0.29	0.04%	0.29	0.31%
Down	0.90	0.91	0.10%	0.89	-1.93%
Up	-	-		-	
To sea	-	-		-	
Pumping	0.000	0.000		0.001	
River	0.01	0.01	0.00%	0.01	0.00%

*Table 7. Detailed water budget of groundwater body nr D6 (Latvia) (*10^5 m^3/d)*

	Scenario I	Scenario II		Scenario III	
GWB nr D6					
Inflow					
Side exchange					
Outside study area	0.71	0.71	-0.33%	0.70	-0.83%
GWB nr 26	0.33	0.33	1.31%	0.44	33.17%
GWB nr D8	0.27	0.27	0.16%	0.28	0.49%
From above	2.95	2.95	0.00%	2.95	0.00%
From below	0.05	0.05	-0.67%	0.05	-3.45%
Outflow					
Side exchange					
Outside study area	0.25	0.26	0.87%	0.26	1.94%
GWB nr 26	0.49	0.49	0.30%	0.60	21.44%
GWB nr D8	0.14	0.14	1.15%	0.15	9.22%
Down	0.90	0.91	0.10%	0.89	-1.93%
Up	-	-		-	
To sea	-	-		-	
Pumping	0.000	0.003		0.000	
River	2.15	2.15		2.15	

Table 8. Detailed water budget of groundwater body nr D8 (Latvia) (10^5 m^3/d)*

	Scenario I	Scenario II		Scenario III	
GWB nr D8					
Inflow					
Side exchange					
Outside study area	0.28	0.29	1.84%	0.28	-1.36%
GWB nr 26	0.29	0.29	0.04%	0.29	0.31%
GWB nr D6	0.14	0.14	1.15%	0.15	9.22%
From above	0.19	0.19	0.00%	0.19	0.00%
From below	<0.01	<0.01	0.00%	<0.01	0.00%
Outflow					
Side exchange					
Outside study area	0.34	0.35	0.64%	0.35	1.46%
GWB nr 26	0.11	0.11	0.00%	0.11	-0.02%
GWB nr D6	0.27	0.27	0.16%	0.28	0.49%
Down	<0.01	<0.01	0.14%	<0.01	-0.04%
Up	-	-		-	
To sea	-	-		-	
Pumping	0.000	0.004		0.007	
River	0.18	0.18		0.18	

Table 9. Detailed water budget of groundwater body nr A8 (Latvia) (10^5 m^3/d)*

	Scenario I	Scenario II		Scenario III	
GWB nr A8					
Inflow					
Side exchange					
Outside study area	0.79	0.78	-0.29%	0.78	-0.47%
GWB nr 24	0.05	0.05	0.02%	0.05	-0.10%
GWB nr 25	0.58	0.58	0.08%	0.49	-15.04%
GWB nr A10	0.16	0.16	0.12%	0.16	0.42%
From above	2.57	2.57	0.00%	2.57	0.00%
From below	<0.01	<0.01	-0.26%	<0.01	-29.05%
Outflow					
Side exchange					
Outside study area	0.72	0.72	1.10%	0.75	5.26%
GWB nr 24	0.30	0.30	0.27%	0.30	0.45%
GWB nr 25	0.67	0.67	-0.25%	0.67	-0.05%
GWB nr A10	0.16	0.16	0.01%	0.16	-0.29%
Down	<0.01	<0.01	-0.11%	<0.01	-2.85%
Up	0.28	0.28	0.53%	0.28	0.53%
To sea	-	-		-	
Pumping	0.000	0.016		0.019	
River	2.50	2.50		2.50	

Table 10. Detailed water budget of groundwater body nr A10 (Latvia) (10^5 m^3/d)*

	Scenario I	Scenario II		Scenario III	
GWB nr A10					
Inflow					
Side exchange					
Outside study area	0.27	0.27	0.03%	0.27	0.75%
GWB nr 23	0.37	0.37	0.01%	0.37	0.03%
GWB nr 24	0.05	0.05	0.00%	0.05	0.00%
GWB nr A8	0.16	0.16	0.03%	0.16	-0.29%
From above	3.42	3.42	0.00%	3.42	0.00%
From below	<0.01	<0.01	0.48%	<0.01	-30.52%
Outflow					
Side exchange					
Outside study area	0.29	0.29	0.14%	0.29	-0.56%
GWB nr 23	0.25	0.25	0.12%	0.25	0.30%
GWB nr 24	0.03	0.03	0.01%	0.03	0.01%
GWB nr A8	0.16	0.16	0.12%	0.16	0.42%
Down	<0.01	<0.01	-0.09%	<0.01	16.27%
Up	-	-		-	
To sea	1.17	1.17		1.17	
Pumping	0.000	0.015		0.011	
River	3.40	3.40		3.40	

Table 11. Detailed water budget of groundwater body nr 23 (Estonia) (10^5 m^3/d)*

	Scenario I	Scenario II		Scenario III	
GWB nr 23					
Inflow					
Side exchange					
Outside study area	0.42	0.42	0.03%	0.42	0.02%
GWB nr A10	0.25	0.25	0.12%	0.25	0.30%
GWB nr 24	0.22	0.22	0.00%	0.22	0.00%
From above	1.40	1.40	0.00%	1.40	0.00%
From below	0.23	0.23	-0.76%	0.22	-2.34%
Outflow					
Side exchange					
Outside study area	0.48	0.48	-0.02%	0.48	-0.15%
GWB nr A10	0.37	0.37	0.01%	0.37	0.03%
GWB nr 24	0.02	0.02	0.04%	0.02	0.07%
Down	0.46	0.47	0.66%	0.47	2.54%
Up	-	-		-	
To sea	0.02	0.02		0.02	
Pumping	0.000	0.003		0.004	
River	0.91	0.91		0.91	

Table 12. Detailed water budget of groundwater body nr 24 (Estonia) (10^5 m^3/d)*

	Scenario I	Scenario II		Scenario III	
GWB nr 24					
Inflow					
Side exchange					
Outside study area	1.05	1.05	-0.10%	1.05	-0.06%
GWB nr 23	0.02	0.02	0.04%	0.02	0.07%
GWB nr 25	0.25	0.25	0.06%	0.25	-0.24%
GWB nr A8	0.30	0.30	0.27%	0.30	0.45%
GWB nr A10	0.03	0.03	0.01%	0.03	0.01%
From above	1.77	1.77	0.00%	1.77	0.00%
From below	<0.01	<0.01	0.18%	<0.01	-10.08%
Outflow					
Side exchange					
Outside study area	0.58	0.58	0.02%	0.58	0.09%
GWB nr 23	0.22	0.22	0.00%	0.22	0.00%
GWB nr 25	0.06	0.06	0.00%	0.06	0.88%
GWB nr A8	0.05	0.05	0.02%	0.05	-0.10%
GWB nr A10	0.05	0.05	0.00%	0.05	0.00%
Down	0.02	0.02	2.36%	0.02	6.37%
Up	-	-		-	
To sea	-	-		-	
Pumping	0.000	0.020		0.045	
River	2.08	2.08		2.08	

5. Recommendations for sustainable exploitation of transboundary resources

The transboundary area between Estonia and Latvia is in the northeastern part of the BAB. For this report, a 3D hydrogeological model was created to assess the water level changes of the groundwater aquifers in the cross-border area. In the Estonia and Latvia transboundary area, the Quaternary aquifer, Upper-Devonian aquifer, and Upper-Middle-Devonian aquifer are delineated. The Quaternary aquifer consists of glaciogenic sediments (mostly moraine) and sand and gravel sediments. The Upper-Devonian aquifer is mostly formed of karstified limestone and dolomite. The Upper-Middle-Devonian aquifer, which underlies the Upper-Devonian aquifer in the southeastern part of the study area or directly under the Quaternary sediments in the rest of the area, consists of sandstone. The horizontal water conductivity of the given aquifers ranges between 0.2–100 m/d.

The total water balance of the transboundary area is $39*10^5$ m^3/d, of which the Quaternary aquifer water exchange is $26*10^5$ m^3/d, the Upper-Devonian aquifer water exchange $1*10^5$ m^3/d and the Upper-Middle-Devonian aquifer water exchange $12*10^5$ m^3/d. Aquifers are recharged by precipitation and discharged through river runoff or groundwater flow to the sea. The regional water flow of all aquifers in the study area is from east to west. The direction of local groundwater flow is determined by highlands to river valleys.

Using the calibrated model, three different scenarios were simulated - the natural state, the current state, and a state where all wells were working at the maximum allowed rate, and four potential dolomite mines were working at the same time. The effects of maximum groundwater abstraction in the cross-border area are localized, and the biggest drawdown in water level compared to the base case scenario remained at 13 m in the Upper-Devonian and Quaternary aquifers near the quarries. Mostly, however, the water levels decline remained in the range of 0–3 m.

The aquifers' recharge areas are located within both countries. Therefore, both countries' cooperation and an effective cross-border quantitative monitoring network are necessary to assess the cross-border groundwater flow and quantitative status. More specifically, the recommended location of the monitoring network is described in the EU-WATERRES project report on WP3 “Program of cross-border groundwater monitoring for Polish-Ukrainian and Estonian-Latvian transboundary areas” and WaterAct project joint report on WP2 activities AT.2.2 “Assessment of the status of transboundary groundwater bodies according to harmonized principles”, AT.2.3 “Development of transboundary monitoring strategy” and AT.2.4 “Spring monitoring optimization and watershed modeling”.

Although there was no significant impact on the change in water levels even when pumping was at maximum, it is important to assess the impact of abstraction on cross-border flow changes when planning large groundwater intakes or quarries near the border.

References

Arciniega-Esparza, S., Breña-Naranjo, J. A., Pedrozo-Acuña, A., Appendini, C. M., (2017). HYDRORECESSION: A Matlab toolbox for streamflow recession analysis, Computers & Geosciences, Volume 98, pp 87-92, https://doi.org/10.1016/j.cageo.2016.10.005.

Borozdins, D., Demidko, J., Bikše, J., et al., (2022). WaterAct joint report on WP2 activities AT.2.2 “Assessment of the status of transboundary groundwater bodies according to harmonized principles”, AT.2.3 “Development of transboundary monitoring strategy” and AT.2.4 “Spring monitoring optimization and watershed modeling”

Demidko, J., Borozdins, D., Valters, K., et al., (2021). Integrated groundwater observation network in Latvian-Estonian transboundary area

Engineering Bureau Steiger, (2013). Kalkahju dolomite mineral deposit Kalkahju research area study report. https://fond.egt.ee/fond/egf/8411

Estonia Environmental Agency (KAUR), (2021). EELIS Database [Dataset] https://veka.keskkonnainfo.ee/veka.aspx

Estonia Environmental Agency (KAUR), (2022). Climate and hydrology database [Dataset] https://www.ilmateenistus.ee/?lang=en

Estonia Land Board, (2021). Elevation data 2017-2020 [Dataset] https://geoportaal.maaamet.ee/eng/Spatial-Data/Elevation-Data-p308.html

Estonia Land Board, (2021). Estonian Topographic Database [Dataset] https://geoportaal.maaamet.ee/eng/Spatial-Data/Estonian-Topographic-Database-p305.html

European Environment Agency, (2018). Corine Land Cover (CLC) [Dataset] https://land.copernicus.eu/pan-european/corine-land-cover

Geological Survey of Estonia, (2013). Geological study of the Naha research area dolomites in Võrumaa. https://fond.egt.ee/fond/egf/8462

Koit, O., Retiķe, I., Bikše J., et al., (2022). Hydrochemical signatures of springs as a tool for unveiling transboundary hydrogeology. Unpublished manuscript.

Latvia Geospatial Information Agency, (2021). Elevation data [Dataset] https://www.lgia.gov.lv/lv/digitalais-augstuma-modelis-0

Latvia SIA Envirotech, (2021). Latvia Topographic Database [Dataset]

Latvian Environment, Geology and Meteorology Centre (LEGMC), (2021). [Dataset]

Marandi, A., Osjamets, M., Polikarpus, M., et al., (2019) Põhjaveekogumite piiride kirjeldamine, koormusallikate hindamine ja hüdrogeoloogiliste kontseptuaalsete mudelite koostamine (Characterization of the borders of the groundwater bodies, evaluation of pressures and compilation of hydrogeological conceptual models). Geologic Survay of Estonia, Rakvere, Estonia

Niswonger, RG., Panday, S., Ibaraki, M. (2011). MODFLOW-NWT, A Newton Formulation for MODFLOW-2005. In: U.S. Geological Survey Techniques and Methods 6. U.S. Geological Survey, Virginia, p 44

Perens, R., Vallner, L. (1997). Water-bearing formation. In: Geology and Mineral Resources of Estonia. Estonia Academy Publishers, Tallinn, Estonia, pp 137–145

Retike, I., Männik, M., Marandi, A., et al., (2021). Conceptual Model Development for the Assessment of Transboundary Groundwater Resources in Cross-border Area (Estonia- Latvia). UNESCO, Paris, France

SIA “Firma L4”, (2006). Izstrādes un rekultivācijas tehniskais projekts "Dolomīta ieguve atradnē "Ape” (Quarrying and recultivation technical project "Dolomite mining at the “Ape” quarry"). SIA “Firma L4”, Riga, 2006. State Geological Fund archive inventory No.16452

SIA “Zemes Puse, (2015). Pārskats par atlikuši dolomītu krājumu aprēķinu atradnē “Ape-1966.g.”, ieguves licences Nr.8/291 laukumā (Overview of the calculation of the remaining dolomite reserves in the quarry "Ape-1966", mining license No.8/291 area). SIA “Zemes Puse”, Riga, 2015. State Geological Fund archive inventory No.24633

Solovey, T., Janica, R., Przygodzka, M., et al., (2021), Assessment of the resources of transboundary groundwater reservoirs for the 2 pilot areas

The Geological Survey of Estonia (GSE), (2021). [Dataset]

Vallner, L., Porman, A., (2016). Groundwater flow and transport model of the Estonian Artesian Basin and its hydrological developments. Hydrology Research 47:814–834. https://doi.org/10.2166/nh.2016.104

Virbulis, J., Bethers, U., Saks, T., et al., (2013). Hydrogeological model of the Baltic Artesian Basin. Hydrogeol J 21:845–862. https://doi.org/10.1007/s10040-013-0970-7

Winston, RB., (2019). ModelMuse Version 4: A graphical user interface for MODFLOW 6. Reston, VA